Evaluation of the Effectiveness of Deep Polymer Impregnation as a Corrosion Abatement Technique for Overlaid Bridge Decks

by

Tapas Dutta

Thesis submitted to the Faculty of the
Virginia Polytechnic Institute and State University
in partial fulfillment of the requirements for the degree of
Master of Science
in
Civil Engineering

APPROVED:

Richard E. Weyers, Chairman

Donald R. Drew

Richard D. Walker

Imad L. Al-Qadi

April 12, 1991

Blacksburg, Virginia

Evaluation of the Effectiveness of Deep Polymer Impregnation as a Corrosion Abatement Technique for Overlaid Bridge Decks

by

Tapas Dutta

Richard E. Weyers, Chairman

Civil Engineering

(ABSTRACT)

The focus of this research was primarily on corrosion of the reinforcing steel (rebars) in bridge decks. It has been estimated that over $20 billion is required to repair or rehabilitate corrosion induced deficient bridge decks and that the cost is rising at the rate of $0.5 billion annually.

Corrosion occurs when there is a sufficiently high concentration of chloride ions at the top rebar mat. The principal source of chloride ions is from the deicing salts applied on the decks during winter. More than 9 million tons of deicing salts are consumed each year in the U.S.A. As corrosion products have a larger volume than steel, corrosion causes cracking and spalling of the deck.

Concrete laboratory specimens with rebars were cast and subjected to a chloride environment. The corrosion potential and rate were monitored with Cu-$CuSO_4$ half-cell and the 3LP device, respectively. When active corrosion had been initiated, the specimens were treated in six ways, one being

the 'control'. Two overlay types and polymer impregnation were used in all combinations as treatment methods. The specimens which were impregnated were grooved and dried to 230 °F prior to impregnation and polymerization. The post-treatment corrosion rates were appreciably reduced.

Mortar cubes were made, dried to different temperatures between room temperature and 600 °F, impregnated and polymerized. The cubes were then vacuum saturated and their resistivity obtained. They were then cut, dried to 220 °F and the effects of drying temperature was evaluated using a Mercury Porosimeter and a Scanning Electron Microscope. The cubes were subjected to a chloride environment and subsequent chloride content was determined. The results suggested that a lower drying temperature was sufficient for effective impregnation.

Other laboratory specimens were dried to 150 °F and 180 °F and impregnated as before. The post treatment corrosion rates supported the conclusions determined in the cube study.

ACKNOWLEDGEMENTS

This study was sponsored by Strategic Highway Research Program (SHRP).

I would like to thank Dr. Richard E. Weyers for his substantial help throughout the course of the study, Dr. Imad L. Al-Qadi for his assistance at the latter stages of the study, Dr. Donald R. Drew and Dr. Richard D. Walker for being on my committee, Dr. Tawei Sun for doing the porosimeter testing, and Frank Cromer for doing the SEM testing. I would also like to acknowledge the students in the Civil Engineering Structures and Materials Research Laboratory, especially Mark B. Henry, J. Eric Peterson, William D. Collins, N. Lalith Galagedera, Brian D. Prowell and Erin Larsen who helped in various ways in the eighteen months it took to complete this research work.

I am grateful to Dennis Huffman, Clark Brown and Brett Farmer for their technical assistance.

TABLE OF CONTENTS

LIST OF TABLES

LIST OF FIGURES

1.0 INTRODUCTION

1.1 Description of the problem

Premature deterioration of reinforced concrete bridge decks was first recognized by highway agencies in the latter part of the 1950's and early 1960's. An initial study determined that the principal cause was spalling which resulted from corrosion of the reinforcing steel caused by the high chloride content of the concrete [1,2]. The major source of chlorides is the deicing salts applied to the roadways during winter. In 1950, about 1 million tons of salt were used in the U.S. In 1970 it was over 9 million tons [3]. A second source of chlorides is the spray from sea water on bridge components in marine environment.

By the 70's, highway agencies had begun to identify the enormous cost involved in the repair/rehabilitation of deficient bridges. The rehabilitation costs the agencies were faced with kept spiralling alarmingly. As the number of bridges that became deficient each year far exceeded the actual number of bridges that were repaired in the same time frame, an increasingly large backlog of deficient bridges were created with each passing year. In the 1986 final report of SHRP Research Plan, the cost of rehabilitation of deficient

bridges related to corrosion alone was estimated at $20 billion with an annual increase of $0.5 billion [4].

1.2 Present Rehabilitation Techniques

An early response to the bridge deck deterioration problem was to modify the design parameters. The cover depth was increased up to 3 inches which prolonged the time it took the chloride ions from reaching the top mat of rebars. By reducing the water to cement ratio to between 0.40 and 0.45, the chloride permeability of concrete was reduced and hence the rate of diffusion of the chloride ions was diminished. However, these methods did not arrest or stop the corrosion process. They merely extended the time to initiate the corrosion of the rebars.

Rigid overlay systems on bridge decks had been used for some time as a rehabilitation technique. The most commonly used rigid overlays are Latex Modified Concrete (LMC), Low Slump Dense Concrete (LSDC) and Polymer Concrete (PC). These overlay systems were also applied to new bridge decks as corrosion protection means. On existing chloride contaminated bridge decks, the spalled and delaminated areas are first repaired and then the relevant overlay is placed.

Electrochemical chloride removal in conjunction with the injection of materials such as penetrating sealants and corrosion inhibitors has been recently used. Corrosion inhibitors such as calcium nitrite when injected into the concrete encapsulates the steel and acts as a barrier to

chloride ions.

Protective methods which are only applicable to new bridge decks include coating the steel rebars with materials such as epoxy and stainless steel. Galvanized rebars were also once used. Of the coating materials, the most popular at the present time is epoxy. In fact the use of epoxy coated rebars has been extended to include the parapet, substructure and superstructure components of bridges. However, this method has not proved completely successful over long periods of time in severe environments such as the Florida Keys. One possible reason might be the loss of adhesion of the epoxy coating by the formation of $Fe(OH)_2$ under the coating. This can occur without the presence of oxygen in a sufficiently high acidic medium.

The application of waterproofing membranes along with an asphaltic concrete wearing surface has also been in use as a protection technique. Preformed thermoplastics and polyurethane are used as membrane materials.

Impressed current systems and galvanic cathodic protection systems have demonstrated their capability of arresting corrosion of steel in concrete. In cathodic protection, a current is applied to the corrosion cell. Its value is such as to reduce the anodic (corroding) current of the rebar to zero. Consequently, there is no anodic reaction and corrosion stops. The cathode (non-corroding site) still acts as a normal cell

cathode but with an increased reaction rate [5].

Deep impregnation (to depths > 3.0 inches) of monomer into concrete and subsequent in situ polymerization abates corrosion where it has started and prevents corrosion from initiating in the steel. A deep grooving method of the concrete which was developed [6,7] resulted in the feasibility of polymer impregnating entire bridge decks. The monomer which was used is methyl methacrylate (MMA). The polymer encapsulates the concrete around the reinforcing steel and fills most of the void spaces, thereby stopping the flow of current and consequently prevents the onset or continuation of any corrosion activity.

This is the only non-electrochemical method of stopping corrosion of steel in concrete bridge decks.

1.3 Scope

The objective of this study is to evaluate the effectiveness of polymer impregnation as a possible cost effective method for arresting corrosion in sound but salt contaminated rigid overlaid bridge decks.

To achieve this, bridge decks conditions were simulated in the laboratory with scaled down concrete specimens which were made and tested in a controlled environment. The laboratory specimens were first exposed to a deicer salt solution until corrosion had been initiated. Although the focus was on the impregnation of overlaid decks, several combinations of corrosion abatement treatment methods were applied to the specimens for comparison of the variability both between and within each group. The overlay systems used were LMC and LSDC. For impregnation, the deep grooving technique was employed. There were also non-treated control specimens. In all, five treatments were used. They were LMC overlay, LSDC overlay, polymer impregnation, impregnation of specimens overlaid by LMC and impregnation of specimens overlaid by LSDC.

This study compared the corrosion arresting capability of each treatment method.

The other objective of this study was ascertaining an optimum drying temperature of the concrete prior to impregnation. In order to accomplish this task, mortar cubes were made and

impregnated after being dried at different temperatures. The results indicated that a lower drying temperature than what was used in previous studies [9] might be sufficient for impregnation to the desired depth. To validate this hypothesis, several specimens, with actively corroding rebars, were impregnated after being dried at the lower temperatures. The post impregnation corrosion activity levels were used to evaluate the results.

The cubes were further observed under the Scanning Electron Microscope (SEM) and the Mercury Porosimeter. The former indicated the nature and distribution of the impregnated polymer molecules in the concrete as well as the amount of each element present in them, while the latter revealed the pore size distribution of both impregnated and normal concrete. Several cubes were subjected to chloride environment and their chloride contents were obtained which gave a measure of the resistance offered by impregnated concrete to the ingress of chloride ions.

2.0 REVIEW OF POLYMERS

2.1 General Description of Polymers

A polymer is an organic chemical made up of large molecules which consist of carbon and one or more elements, with repeat units which are linked together by covalent bonds. The basic unit is termed as monomer, and the combination of this repeat unit comprises a polymer.

Polymeric materials which are used in industry can be broadly divided into two categories: plastics and elastomers. Of the two, plastics form the largest category by production volume [8]. Plastics are further subdivided into thermoplastics and thermosets. Thermoplastics melt on heating and may be processed by several molding and extrusion techniques. Examples are polyvinyl chloride (PVC) and polyethylene (PE). The monomer used in this study - MMA - or rather its polymeric form PMMA (poly methyl methacrylate) is also a thermoplastic. PMMA was first produced on a commercial basis in the UK in 1934 [8].

Thermosets, on the other hand, cannot be melted and remelted and thus its set is irreversible. Examples are epoxy (EP) and polyurethane (PUR). Examples of elastomers are natural rubber (NR), polybutadiene (BR) and silicon rubber.

The rubber industry was well established before the advent of the modern plastic industry. At that time it was not known that rubbers were polymeric substances. At present synthetic rubber is widely used alongside natural rubber and as such a clear distinction between plastics and rubbers is hard to define.

As mentioned earlier, monomer is the basic repeating unit. A large number of monomers link together to form a polymer. The basic property of a monomer is its functionality which is defined as the number of sites that a monomer can link with other monomer molecules to form a long chain. The linking process is termed polymerization. The minimum value of functionality is 2. For example, vinyl chloride - a monomer - has functionality of 2. It is a colorless gas with a chemical formula C_2H_3Cl. The carbons have a double bond giving it a functionality of 2.

During polymerization of the monomer to form poly vinyl chloride (PVC), the double bond breaks into a single one and results in two sites where other monomer molecules can link. MMA which has a chemical formula of $C_5H_8O_2$ also has a functionality of 2 (see Figure 1).

Primary bonds hold the individual atoms together and make the polymer molecule. Secondary bond is the attraction between the molecules. A third type of force called the Van-der-Waal's force exists between all molecules.

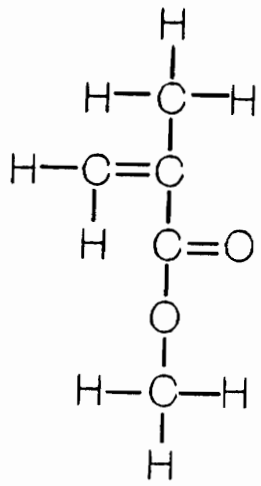

Figure 1 Chemical Structure of MMA

Bond length is the distance between the individual carbon atoms. Bond energy is the external energy required to break the bonds between carbon atoms, expressed as the amount of energy per molecule. Both these quantities are constant for a particular type of bond. As an illustration, a double bond has a bond length of 1.32×10^{-10} meter and possess a bond energy of 607 kJ/mol. As can be expected, a triple bond has a shorter bond length and a larger bond energy. Another parameter of the structure is the bond angle, which is the angle between individual carbon atoms. This quantity is also constant for a specified type of bond. A single bond molecule is free to rotate about the C-C bond while the double and triple bond molecules can experience no rotation.

A polymer can form in linear chains of monomer or it can be a branched chain. A third possibility arises when there are two or more kinds of repeating units. This type of polymer is called a copolymer. Depending on the relative position of its constituting repeating units, a copolymer can be further divided into alternating copolymer, random copolymer and the block copolymer.

A polymer can also consist of two and three dimensional networks of chemical bonds. Graphite has a two dimensional network while diamond is three dimensional. The networks are interconnected through primary chemical bonds and are called cross linked polymers. Cross linking increases the mechanical

strength of a polymer.

Converting the monomer into polymer, that is the process of polymerization can occur in three ways depending upon the monomer involved. They are chain polymerization, stepwise polymerization and thermoset polymerization. In chain polymerization a single monomer continues to link with the same repeating unit until a stable configuration is reached. There are very few intermediate polymers formed. In stepwise polymerization, the polymerization occurs in a number of steps with intermediate polymers formed at each stage of its formation. Thermoset polymerization occurs when there are more than two functional groups in a step polymerization reaction. The reaction leads to branched structures which intercombine to random three-dimensional networks which finally extends through the whole mass to form a single giant molecule. The degree of polymerization is defined as the weight of a typical polymer molecule divided by the weight of the repeating unit.

2.2 Polymers in Bridge Deck

The main reasons for the growing use of polymers in bridge deck repair and rehabilitation are its properties of rapid cure and low permeability as well as the flexibility of many possible formulations. It has been estimated that about 90% of the voids in concrete is filled up by the process of polymer impregnation.

The factors which control the selection of an appropriate monomer system are familiarity with its physical, chemical, fire hazard and health hazard properties. In an earlier study on the use of polymers in highways [9], the monomer system chosen was one for which all of the aforementioned properties were known in detail. The system was as follows:

90% Methyl Methacrylate (MMA)

10% Trimethylolpropene trimethacrylate (TMPTMA)

0.5% of the above monomer mix of Azobisiobutyronitrile (Azo)

All the above proportions are by weight. TMPTMA is the cross linking agent. The Azo acts as the initiator to the polymerization reactions.

In the present study, the same monomer system was employed. Other monomer system can conceivably be used once detailed knowledge of its properties is available.

The specific advantages of this monomer system are mainly its properties of low viscosity and its rapid auto accelerating

polymerization reaction.

However, this monomer system has several disadvantages, most of which can be virtually eliminated by adhering to good safety practices. They are flammability (due to its low flash point at 70° F and high vapor pressure), high cost, toxicity and its irritating odor.

Standard precautionary measures employed during the handling of the monomer were as follows:

(1) The three components of the monomer system were stored separately in adequately ventilated areas with explosion proof electrical facilities.

(2) Mixing was done under the fume hood at a temperature not exceeding 70° F. Over this temperature, the components may react spontaneously giving rise to an exothermic reaction.

(3) Care was taken not to subject the Azo to strong physical shocks.

(4) The Azo was refrigerated when not in use due to flammability at high temperatures.

(5) The maximum volume of monomer mixed in one batch was allowed not to exceed 55 gallons.

(6) All unused monomer mixture was kept under refrigeration and later disposed of safely by burning.

(7) Monomer loading was initiated only after the concrete had cooled to a temperature below 100° F.

(8) Class B fire extinguishers were kept available.

(9) During impregnation all persons in the immediate vicinity wore protective gloves, masks and goggles.

3.0 REVIEW OF CORROSION

3.1 Mechanism of Corrosion

The process of corrosion involves the conversion of metal into non-metallic corrosion products. When the metal involved is iron or its products like steel, the phenomenon is called rusting and the non-metallic end product is called rust [10]. Although the only metal considered in this study is steel (the reinforcing bars in concrete bridge decks), the more general term "corrosion" will be used throughout. Pore water in reinforced concrete is alkaline in nature with a pH value between 12.5 and 13.5 [11,12]. A layer of gamma iron oxide (Fe_2O_3) is formed around the steel in this alkaline environment which renders it passive thus preventing the onset of any corrosion activity. Thus, the breaking down of this passive layer by any external agent will cause corrosion to initiate. The passive layer can be degraded primarily by two mechanisms. One is by leaching of water or a reaction with carbon dioxide or other acidic material which causes partial neutralization of the passive layer. Depassivation will occur if the pH value drops below approximately 10-11 [13]. The second mechanism is by electrochemical reactions involving chloride ions in the presence of oxygen. Relative to corrosion in bridge decks, the

latter is by far the predominant method in which the passive layer is destroyed.

As mentioned earlier, the major source of chlorides on bridge decks is from the deicing salts - mainly sodium and calcium chloride - used during the winter season. Splashes and sprays from sea water on concrete bridge components in marine environment is a second source. Chlorides may also be present in the mixing water, in admixtures (if used) or in aggregates in the concrete mix.

Chlorides penetrate into the concrete mainly by the process of diffusion. Another mode is through cracks on the deck which may have been formed due to shrinkage or other means. When the chloride ion concentration at the rebar level reaches the threshold level, the corrosion reactions start. From previous studies, the level is taken as 1.2 lb of chloride ions per cubic yard of concrete [14].

The chloride ions which first react with iron are then released for reuse; thus an accumulation of chloride ions are maintained. The corrosion product, rust has a larger volume than steel. The generated pressure causes a rupture in the concrete above the surface of the rebar. The cracks which are formed allows an increased penetration of chloride and oxygen which in turn accelerates the corrosion rate.

The electrochemical reactions in chloride contaminated concrete are as follows.

Anode Reactions:

$$Fe + 2Cl^- \rightarrow Fe^{2+} + Cl^- + 2e^-$$

$$Fe^{2+}Cl_2 + 2H_2O \rightarrow Fe(OH)_2 + 2H^+ + 2Cl^-$$

In the presence of oxygen:

$$6(Fe^{2+} + 2Cl^-) + O_2 + 6H_2O \rightarrow 2Fe_3O_4 + 12H^+ + 12Cl^-$$

Cathode Reaction:

$$\tfrac{1}{2}O_2 + H_2O + 2e^- \rightarrow 2OH^-$$

A corrosion cell consists of two electrodes, the anode and the cathode, which are electrically connected so that electrons can flow. In concrete the reinforcing steel is the electrodes and the medium through which the current is propagated is the pore water.

The Electromotive force (EMF) of a cell is the algebraic sum of the two electrode potentials. As a reminder, electrical potentials are normally stated in comparison to the potential of the hydrogen electrode. As the electrode with the lower potential value will undergo corrosion, the EMF of a cell is always negative. It follows that the more negative the EMF is, the greater the corrosion activity. If there is no difference

in potential between the cathode and anode, the EMF of the cell is zero and there is no flow of current and no corrosion activity.

In the corrosion reactions, the anode undergoes oxidation and is the electron donor as has already been illustrated in the reactions listed in page 18. The cathode undergoes reduction and is the electron acceptor. Thus, the corroding site is the anode.

Faradays' first and second law govern the rate of corrosion. The first law states that the rate of corrosion is directly proportional to the corrosion current. In mathematical terms:

$$\text{weight of metal reacting/time } \alpha \quad I_{corr}$$

$$\text{or} \quad R = k\, I_{corr} \qquad (1)$$

where,

R = rate of corrosion in grams/second,

k = electrochemical equivalent in grams/Coulomb, and

I_{corr} = corrosion current in Ampere.

The second law of Faraday states that the rate of reaction at the anode is equal to the rate of reaction at the cathode.

For bridge decks, cracking is a secondary mode of entry of chloride ions, the primary mode being diffusion. Cracks may occur due to load deflection during concrete placement operation, plastic shrinkage, drying shrinkage or by subsidence cracking. Subsidence cracking occurs due to the

differential settlement of concrete. If t_s is the tensile stress due to the differential settlement of concrete and t_c is the tensile strength of the fresh concrete, subsidence cracking will take place if

$$t_s > t_c$$

A possible third mode of chloride penetration was thought to be by capillary action. However this has been discarded as being extremely doubtful [14]. Capillary action is thought to be prevalent to a depth of about 0.5 inch or 1.27 cm from the top surface of the bridge deck.

The process of diffusion of chlorides through concrete obeys Fick's second law.

$$\delta C/\delta t = D_c \ (\delta^2 C/\delta X^2) \qquad (2)$$

where,

C = chloride ion concentration in %,

X = distance or depth in cm,

t = time in years, and

D_c = diffusion constant in cm^2/year.

A solution to the above second order differential equation is:

$C(X,t) = C_o [1 - erf\{X/(2 \sqrt{(D_c t)})\}]$

where,

C_o = integration constant in %, and

erf is a probability function based on random variable. Desired values are available from standard tables.

As the chlorides penetrates into the deck from the top surface, the top mat of rebars which it would encounter first will be the corroding site and act as the anode.

There are two types of corrosion cells. Micro-cell corrosion occurs when the cathode and anode are close to each other as on the same rebar in a bridge deck. In macro-cell corrosion, the cathode and anode are separated by some distance. In a bridge deck, the anode will be located in the top mat of rebars while the cathode will be in the bottom mat of rebars. It has been estimated that 90% of bridge deck corrosion is micro-cell in nature.

3.2 Factors Influencing Corrosion

Corrosion of steel is influenced by various factors like cover depth, type of cement, relative humidity, nature of ions present, concrete permeability or its indicator water/cement (w/c) ratio and degree of consolidation.

The presence of oxygen is an important factor in initiating the corrosion reaction. However, in most cases oxygen is readily available for diffusion into the concrete. A far more important factor is the water content of the concrete. At a low water content there is very little ionic conduction and the corrosion rate is low. At very high water contents there is less available oxygen and the corrosion rate is low. Thus, there is an optimum water content at which corrosion is least inhibited [15]. As with lower permeabilities, larger cover depths increase the time to initiate corrosion. Whereas a lower permeability decreases the rate of chloride diffusion, larger cover depths increase chloride diffusion path length.

4.0 EXPERIMENTAL DESIGN

4.1 Overview of Experimental Design

Simulation of bridge deck conditions was achieved in the laboratory by casting small reinforced concrete specimens. Previous studies had indicated that scaling down test specimens from bridge deck size to laboratory size has no substantial effect on the validity of results obtained and results and conclusions from one apply equally to the other. Eighteen specimens of approximately one foot-square were made with two triad of rebars in each specimen. The specimens were then subjected to alternate wet and dry cycles with salt solution until corrosion had been initiated. The 3LP device manufactured by Kenneth C. Clear, Inc. as well as standard copper-copper sulfate half cell (CSE) were used to determine the degree of corrosion activity in the specimens. These measurements were further validated by determining the chloride ion concentration of the concrete. Once it was evident that there was active corrosion in the rebars, the specimens were subjected to five different corrosion abating treatments. Treatments included LMC and LSDC overlays and impregnation with the chosen monomer system. Control specimens were not treated. A comparison of pre and post treatment

corrosion activity for each treatment method indicated the effectiveness of the treatment procedures as a means of arresting corrosion in bridge decks.

In the study just outlined, the concrete was dried prior to impregnation such that the temperature at half inch below the top rebar was about 230 °F. This is the drying criterion used in previous polymer impregnation studies [9]. However, if a lower drying temperature was to be equally acceptable for effective impregnation, it would represent a large saving of time, energy and consequently cost. In order to investigate that possibility, a number of mortar cubes were made. They were divided into several sets and each set was dried to a different temperature ranging from room temperature to 600 °F. The cubes were then polymer impregnated. Cut pieces of the cubes were evaluated using a mercury porosimeter and a scanning electron microscope. The cubes were also exposed to saline environment and chloride content tests were run to obtain the resistance of polymer impregnation following different degrees of drying to the ingress of chloride ions. Results obtained from these studies indicated that a lower drying temperature was sufficient for the purpose of impregnation.

To validate the above conclusion, several other laboratory specimens were dried to 150 °F and 180 °F (temperature at half inch below the top rebar level) and then polymer impregnated

as before.

4.2 Impregnation of Rigid Overlay Systems

In the past, deep polymer impregnation (impregnation to a depth of 3" to 4") had been used as a rehabilitation technique for salt contaminated but sound bridges. With the development of the grooving procedure, [6,7] deep polymer impregnation became feasible under other conditions such as decks with rigid overlays where the sound but chloride contaminated concrete had been left in place.

The objective of this study was to evaluate polymer impregnation of overlaid bridge decks as an effective means of abating corrosion. As a means for comparison, several treatment methods were employed other than impregnation through rigid overlays.

Eighteen laboratory concrete specimens were cast. They were 12" long and 10 ⅜" wide. Each specimen had two triad of rebars, see Figure 2. Each triad consisted of one rebar at the top and two rebars equidistant from the top rebar at the bottom, thus forming an isosceles triangle. The bottom rebars were 1 ¼" from the bottom of the specimens. The rebars were placed along the width of the specimens. The rebars were approximately 11 ⅞" long such that they extended about ¾" each beyond the two ends of the specimens. The rebars used were #4 (ASTM specifications A 615) with nominal diameter of ½". The overall height of the specimens was 4". The cover depth was

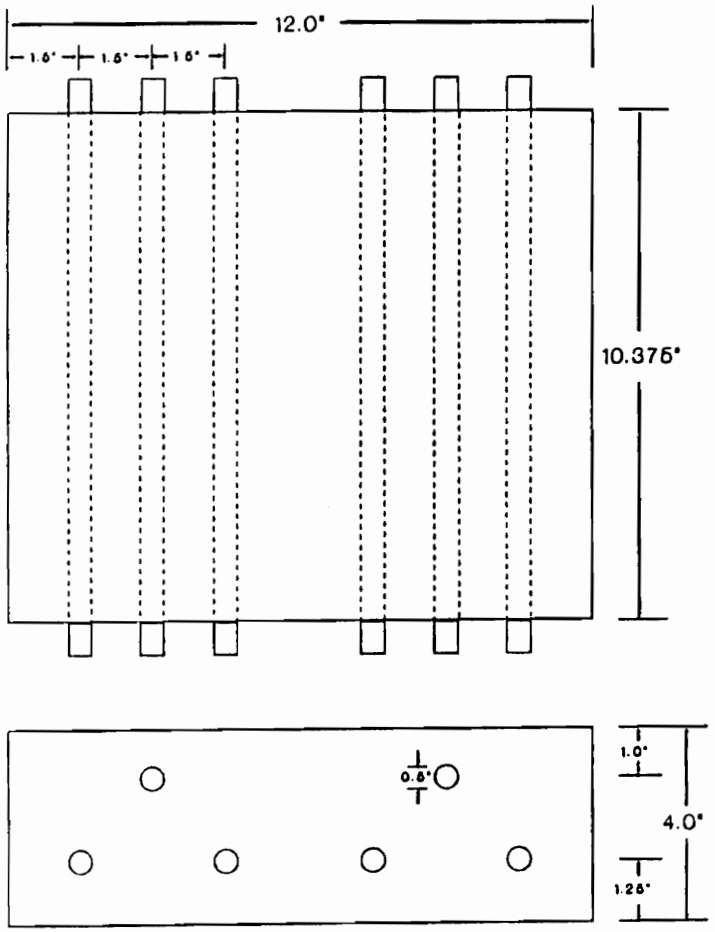

Figure 2 Plan and Elevation of Specimens

1".

The forms for the specimens were made of ¾" plywood A-C exterior grade and fastened by 2" #8 dry wall screws. Spacers of dimensions ¾" × ¼" made of plexiglass were used on one side of the forms (two spacers per form) so that the thermocouple (TC) wire could be accommodated. For adequate clearance, holes that were drilled in the form for the rebars were ⅝" in diameter.

The rebars were cut to size, drilled and tapped at one end to a depth of ⅝" to accommodate screws of diameter ⅛". In order to minimize the effects of manufacturing oil and existing rust on the rebars, the rebars were cleaned by soaking in a solution of hexane for about 20 minutes and then wiped clean. The rebars were then dried in an oven at 240 °F for 10 minutes. Hexane is a suitable cleanser as it leaves no residual ions on the rebars and thus eliminates contamination from the cleaning process. To prevent corrosion from taking place at the exposed ends, the two ends were covered by electroplating tape such that the uncovered length of each rebar was 6.5". Thus the exact surface area exposed for corrosion was known and hence corrosion rates could be normalized to a square foot of surface area of the rebar. The wooden forms were painted with two coats of form oil with overnight drying between coats. This was done to prevent the concrete from adhering to the forms.

Thermocouple (TC) junction was taped at the center of each top right rebar of the specimens. Type T plugs were attached to the other ends. The TC was thus designed to indicate temperature at the top rebar, i.e. the anode of each specimen. A notch was filed at the bottom of the hole in the forms which would contain the TC attached rebar to facilitate pulling out of the TC wire out of the hole after the specimens were cast. The rebars along with the TC wire and spacers were assembled in each form in an inverted configuration to minimize consolidation (subsidence) cracking. Care was taken to ensure that the drilled and tapped holes in all rebars were on the same side. The forms were then codified with a permanent marker according to the treatment process each specimen would undergo. Five treatment methods were used and one set of specimens acted as controls which were not subjected to any treatment. Thus there were six sets of three specimens each. The two letter code assigned to each set was as follows:

- CO: Specimens which acted as controls and were not treated,
- LM: Specimens which were overlaid with LMC,
- LS: Specimens which were overlaid with LSDC,
- PC: Specimens which were polymer impregnated,
- PM: Specimens which were overlaid with LMC and polymer impregnated, and
- PS: Specimens which were overlaid with LSDC and polymer impregnated.

To distinguish between the three specimens in each group, numbers 1, 2 and 3 were used after the two letter code. For instance, the three specimens which were polymer impregnated were named PC1, PC2 and PC3.

Concrete was then placed in the forms. For mix designs, properties and compressive strengths see Appendix A. The specimens were removed from their forms after 24 hours of moist curing. Being cast inverted, the top surface of the specimens were in contact with the wooden form. There was a possibility of the surface being contaminated with form oil. To eliminate this, the surfaces were cleaned with muriatic acid (dilute hydrochloric acid).

In bridge decks, there is no ingress of salt from the sides. To incorporate this factor into the laboratory specimens the sides were coated with epoxy. Two kinds of epoxy were used for this purpose. The first was EP-5. This epoxy consists of two components, A and B which were mixed in equal proportions for three minutes with a paddle attached to a hand drill. The other type of epoxy was Epon 828 resin. 100 parts of the resin was mixed to 10 parts of DETA (the curing agent) by weight. These epoxies have relatively short curing time and small batches were mixed at one time to prevent premature hardening. Care was taken to ensure that no epoxy spilled on the top surface or seeped to the bottom surface.

Plexiglass dikes 1" high and 5/16" thick were fixed on top of

each specimen with silicon rubber. Glass covers were used on the specimens to minimize moisture loss during wet cycles. Electrical connections were fitted on the rebars with screws of diameter ⅛". A resistor of 100 Ω was connected between the top rebar and bottom right rebar of each triad. A jumper cable was fitted between the two bottom rebars of each triad.

Prior to the first wet cycle, potential and temperature readings were taken in order to establish base readings. Temperature readings were with a digital Type T TC meter. Potential readings were taken with a CSE half cell according to the procedure outlined in ASTM C-876 [16]. For each top rebar, three readings were taken one in the front, one in the middle and one in the rear of the specimen. The three readings for each rebar did not show appreciable variation and the mean of the three readings was recorded. The interpretation of the potential values are also given in ASTM C-876 and are:

- If the potential is more positive than -200 mV CSE, there is a probability of more than 90% that there is no active corrosion present.
- If the potential is between -200 mV CSE and -350 mV CSE, corrosion activity is in the uncertain region.
- If the potential is more negative than -350 mV CSE, there is a probability of more than 90% that there is active corrosion present.

Thus, the interpretation of the potential values from the copper-copper sulfate half cell is based on a probability function.

Five days after the concrete was placed, the first wet cycle was started. As the permeability of concrete decreases with age, the first wet cycle was started as soon as practicable to introduce chloride ions into the concrete at the earliest. A 6% solution of sodium chloride by weight was used as the source of chloride ions for the concrete. 500 ml of the solution was used for ponding each specimen. The wet cycle extended for a period of three days. At the end of the period, the solution was taken off the specimens with a 2.25 peak HP, 16 gallon wet-dry shop vacuum. During the dry cycle the ambient temperature was raised to 120 °F by using several infra red lamps. The maximum temperature that the concrete attained at the top rebar level was in general somewhat higher than the highest ambient temperature. The high temperature dried the concrete and made it moisture hungry so that the penetration of salt solution during the next wet cycle was at a higher rate. The duration of the dry cycle was four days. Ponding with salt solution was continued and measurements were taken periodically.

Another instrument, the three electrode linear polarization device (3LP device) manufactured by Kenneth C. Clear, Inc. was used to monitor the corrosion current. As mentioned in the

previous chapter, the corrosion rate of metal is directly proportional to the corrosion current. The 3LP devise impresses a current in the reverse direction and polarizes the corrosion current. Knowing the impressed current and the corresponding value of the potential, the corrosion current is obtained by using the Stern-Geary equation. A description of the test procedure is outlined in Appendix B. Interpretation of the corrosion current (I_{corr}) values obtained is given in the 3LP manual [17] as:

- I_{corr} < 0.2 mA/sq ft → no corrosion damage expected.
- I_{corr} between 0.2 and 1.0 mA/sq ft → corrosion damage possible in 10 to 15 years.
- I_{corr} between 1.0 and 10 mA/sq ft → corrosion damage expected in 2 to 10 years.
- I_{corr} > 10 mA/sq ft → corrosion damage expected in 2 years or less.

During the ponding period, chloride contents of some selected specimens were determined at different depths using the specific ion probe test method developed by James Instruments, Inc. [18]. Description of the method can be found in Appendix B. Earlier work by Herald [19] correlated the results obtained by the specific ion probe method and the standard AASHTO test method, T-260-78.

In the available literature, several different values of chloride ion concentration have been suggested as a threshold

value for the initiation of corrosion. The author has used the value of 1.2 lb of chloride ions per cubic yard of concrete as concluded from research done by the Federal Highway Administration (FHWA) [20,21].

The alternate wet and dry cycles were continued and corrosion activity was monitored at regular intervals.

Treatment activities were started when it was determined that there were active corrosion in most of the rebars. At that point in time, all the potentials were more negative than 350 mV, the mean corrosion current was 4.2 mA/sq ft with most of the values being over 2 mA/sq ft and the chloride content at the rebar level of selected test specimens were greater than 1.2 lb/cubic yard. The treatments took about a month to be completed from the time the last pre-treatment measurements were taken. Several sets of readings prior to treatments indicated accelerating rates of corrosion in the rebars. Thus, it is likely that the corrosion levels were higher when the treatments were applied than were indicated in the last pre-treatment readings.

During the treatment processes, the application of periodic salt solution on all the eighteen specimens were suspended.

As a reminder, the specimens of the LM and LS series were overlaid by LMC and LSDC, respectively. The PC series was polymer impregnated. The PM series was overlaid with LMC and polymer impregnated while the PS series was overlaid with

LSDC and polymer impregnated. The CO series were left untreated. Thus, there were twelve overlayed specimens, nine impregnated specimens and three untreated specimens.

Twelve forms with height measuring about 6" were made to accommodate the overlays which were 2" high. As before, two coats of form oil were applied to the forms. The specimens of the LM, LS, PM and PS series were placed in the form. The inner periphery between the edge of the specimens and the form was covered by duct tape to prevent the overlay concrete from dripping along the sides of the existing concrete. The surfaces of the specimens were wetted with plain water and covered with plastic sheets twelve hours prior to the application of the overlays.

LMC overlays were applied to the LM and PM series, while the LS and PS series were overlaid with LSDC. Mix designs for LMC and LSDC, properties of the aggregates and compressive strengths of the overlays are given in Appendix A.

The specimens with LMC overlays were kept moist for 48 hours while the specimens with LSDC overlays were kept moist for a period of 14 days. This was done by placing moist burlap covered by plastic sheets on the specimens and keeping the burlap wet during the period of moist curing. After the curing period, the specimens were freed of the forms. The sides of the overlays were coated with epoxy like the original concrete layer.

The seven and fourteen day compressive strengths of the overlays were satisfactorily high for the next step of the treatment procedures for the overlayed specimens to be initiated.

The specimens of the PC, PM and PS series had to be grooved as the first stage in the polymer impregnation treatment process. In an earlier study [7], an empirical formula was developed to determine the grooving parameters: groove spacing, groove depth and groove width for optimum polymer impregnation. The objective in deep polymer impregnation is to encapsulate the steel by impregnating the concrete to about a depth of ½" below the top rebar level. A greater depth is not desired as impregnating the concrete further is redundant and the larger volume of monomer required becomes an unnecessary expense. Encapsulation of the top rebar results in isolating the anode and thus forcing electrical discontinuity between the cathode and anode. Consequently, the corrosion current decreases.

In this study the grooving parameters were roughly determined by assuming a 10% polymer loading of concrete by volume as determined in the earlier study [6,7]. The depth of impregnation is ½" below the top rebar.

There were two values of depth of impregnation involved. The specimens of the PC series had the original cover depth of 1" and the final depth of polymer penetration was 2". For these specimens, the depth of groove was ½". For all the specimens,

the groove width was ¾" and the edge to edge distance between grooves was 2 ¼". The overlay specimens (PM and PS series) had a cover depth of 3" and the final depth of polymer penetration was to be 4". The groove depth for the overlaid specimens was 2 ½". With the above groove parameters, the number of grooves on each specimen was three (see Figure 3).

The groove lines were marked on each specimen with a permanent ink marker. A masonry saw was used to cut along the groove lines. Concrete between the cut lines were then chipped out with a mason's chisel.

The next stage in treatment for the three impregnated series (PC, PM, PS) was drying. Prior to monomer impregnation, the concrete has to be sufficiently dry so that the monomer can diffuse into the concrete and fill the void spaces. Thus, it would seem that the concrete had to be dried to above the boiling point of water at the depth of impregnation which is ½" below the top rebar level. The drying temperature used at this depth in a former study on polymer impregnation of concrete [9] was 230° F. The same value was used in the treatment of the current specimens. Later studies investigated the possibility of using lower drying temperatures without lower corrosion abatement effectiveness (see section 4.3).

Because concrete bridge decks have to be dried from their top surface, oven drying was not appropriate. Thus, propane fired infra-red heaters were used to dry the specimens. Three

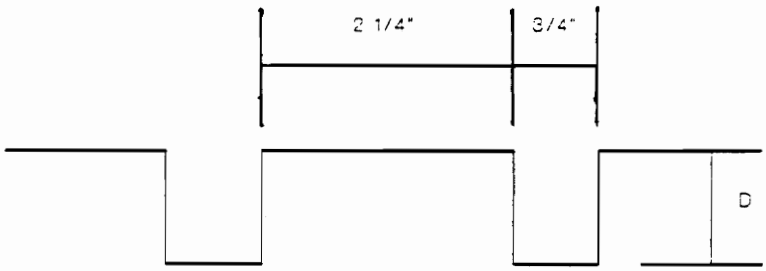

D = 1/2" for PC
D = 2 1/2" for PM and PS

Figure 3 Groove Dimensions

heaters were placed side by side suspended by chains from a metal framework so that the height of heaters from the top of the specimens could be adjusted as necessary. A partial enclosure was made around the heaters to a height of 3 feet from ground level with sheet metal. The pressure of the gas was adjusted to 3 psi.

In order to monitor the temperature at a depth of ½" below the top rebar level high temperature TC wires were encased in ceramic tubing and inserted into a hole made in the bottom of the specimens to a depth such that the TC junction was ½" below the top rebar. A ¼" carbide drill bit was used to drill the TC holes. The TC wire inside the concrete was kept secure in the concrete by duct tape. The TC wire used was about five feet in length so that the other end could be brought out of the drying enclosure.

The nine specimens were set up below the heaters. For uniformity, all the specimens were placed so that their top surfaces were at the same level and thus all the specimens were at the same distance from the heaters. Fiberglass insulation (3½" thick) was wrapped around the specimens. The fiberglass was supported by a layer of sand and gravel. The TC wires leading outside the enclosure were covered with sand and gravel. Insulating the specimens thus, prevented the entry of heat from the sides. The TC wires were insulated so that the TC junction would measure the temperature at the proper

location. A metal sheet with rectangular holes cut in it was placed over the specimens so that only the top of the specimens was exposed to the heaters. This ensured that the concrete was heated only from the top surface.

Along with the nine specimens, three 4 × 8 cylinders made from the same concrete mix design as the impregnated specimens were also dried. The cylinders were used to determine the rate of monomer impregnation of the concrete.

A tag was attached to each TC wire to identify each specimen when the temperatures were taken during the heating and the subsequent cooling. A probe was fixed to record the shaded ambient temperature outside the heating enclosure. A second probe was placed on the top surface of the specimen at the center of the drying area in order to record the surface temperature.

The heaters were then lowered so that the distance between the edge of the heaters and the top surface of the specimens was 9".

Initial temperatures were taken of all locations before the heaters were turned on. The locations were internal temperatures at ½" below the top rebar level, surface and ambient temperature.

The heaters were then turned on with a self-igniting propane fired torch. Temperatures at all locations were recorded at regular intervals.

After 70 minutes of heating, the internal temperatures of two specimens, PC1 and PC3 reached 230° F. As the internal temperatures of the other specimens were substantially lower, the heaters could not be turned off. To remedy the situation, the two specimens were covered with a metal sheet to prevent further heating of these specimens.

At 150 minutes, most of the specimens had internal temperatures which were nearly the requisite value. Therefore, the heaters were turned off. Because concrete acts as a heat sink, the internal temperatures of all the specimens continued to rise even after the heaters were turned off until a thermal equilibrium was established. Thus, the maximum internal temperatures of all but two specimens were in the vicinity of 230 °F.

Temperatures at all the previous locations were taken at regular intervals after the heaters were turned off. Temperature readings were taken for about five hours after the heaters were turned off. The specimens were then covered with a layer of fiberglass insulation and left to cool for about 12 hours before impregnation was started.

The ends of the grooves in the nine specimens were sealed with epoxy putty which does not dissolve in MMA. Like most epoxies, epoxy putty has two components which were mixed in equal quantities by kneading vigorously by hand. After application, the epoxy putty was allowed to cure for about two hours. The

putty was also used to make dikes about one inch high on the three cylinders. The specimens and the cylinders were covered with plastic sheet cut to size and taped around the edges with duct tape. A slit was made in the middle of the plastic of each. The slits were covered by pieces of duct tape. This arrangement ensured little loss of the monomer by evaporation during the monomer loading period.

The monomer was mixed carefully under the fume hood. 90 % of MMA was mixed with 10 % of TMPTMA, by weight. 0.5 % of the above mixture of Azo, by weight, was added.

The monomer was ponded on the top surface of the specimens and cylinders using a 20 ml pipette and placed through the slit in the plastic. The slit was kept covered after monomer was placed on the specimens.

The three cylinders which were marked as 3E, 6E and 7E had impregnation times of 6 hours, 14 hours and 23 hours, respectively. During this period more monomer was added as required when all existing monomer had diffused into the concrete. The same was done in the case of the specimens during their impregnation period. After the designated impregnation time for each cylinder, the residual monomer was drawn off with the pipette. Volume of monomer placed on each cylinder as well as the volume of the remaining monomer at the end of the impregnation periods were recorded.

The cylinders were then placed in a hot water bath at 185 °F

for polymerization of the monomer. They were kept in the bath for four hours. The cylinders were taken out of the bath and cut longitudinally in half using a masonry saw. The cut cylinders were then etched with muriatic acid. The acid etches all portions of the concrete except the area of impregnation. Thus, the depth of impregnation of the cylinders could be visually distinguished. A previous study [9] demonstrated that the rate of monomer impregnation of concrete is a function of the square root of time of impregnation.

Using this relation a graph of depth in inches versus square root of time in hours was plotted from the data obtained from the acid etching of the three cylinders. A fourth data point was the origin of the graph. The resulting graph was a straight line (see Appendix C). Thus, the rate of impregnation for the particular concrete was ascertained. As the bottom of the grooves in the specimens were ½" above the top rebar level and the desired depth of impregnation was ½" below the top rebar level, the distance monomer had to diffuse in the specimens was 1½". Since the monomer loading is approximately 10 % by volume, the actual depth of impregnation was 1.5 ÷ 0.9 = 1.67". From the graph, the time corresponding to this depth is 16 hours.

Accordingly, the specimens were allowed to be impregnated for a period of 16 hours. At the end of this period, the residual monomer was drawn of with a pipette and the specimens were

polymerized in a water bath at 185 °F for 24 hours. During this period the specimens also absorb water.

At the end of 24 hours, the heaters were turned off and the specimens taken out. The grooves in the PM and PS series of specimens were filled with latex modified mortar (LMM). For mix proportions of the LMM, see Appendix A.

Application of salt solution was resumed with the same wet and dry cycles used before treatments.

Post treatment potential and corrosion current measurements were taken periodically.

Potential and I_{corr} readings were also taken with different cathode to anode surface areas (C/A). In the standard electrical connection on the specimens, the C/A surface area ratio was 2. C/A ratios of 1, 3 and 4 were achieved by isolating the left anode, and connecting jumper cables such that the right anode was connected to 1, 3 and 4 cathodes (bottom rebars), respectively. As the left anode had been isolated, micro-cell corrosion readings were taken on this rebar.

This study was done to investigate the effect of C/A surface area ratio on the corrosion rates and to compare micro-cell corrosion to macro-cell and mixed-cell (combination of micro and macro) corrosion rates.

Along with the mixed-cell corrosion readings, the macro-cell corrosion readings were also taken. This was done by

connecting a volt meter across the resistor and recording the potential drop in mV. Since the value of the resistor was 100 Ω in each case, the corresponding macro-cell current was obtained in mA using Ohms Law. (Current = Potential/Resistance)

4.3 Optimizing the Drying Temperature for Corrosion Abatement

4.3.1 Effects of Drying Temperature on Corrosion Properties

As mentioned in the preceding section, the drying temperature of the concrete at a depth of ½" below the top rebar level prior to monomer loading was 230 °F. This value was used in a previous study [9] on polymer impregnation of concrete. The objective of this study was to investigate the possibility of using a lower drying temperature which would reduce drying time and substantially reduce impregnation costs. Specially, for a long bridge deck this would translate into a considerable reduction of time and money.

It was decided that the influence of the drying temperature on the corrosion properties would be studied for a wide range of temperatures.

Forty-two 2" mortar cubes were made for this experiment. For mix proportions, and other properties, see Appendix A. The cubes were made in accordance with ASTM C-109-90. The cubes were divided into 14 sets each set containing three cubes.

The cubes were taken out of their molds after 24 hours and inscribed with codes with a permanent ink marker. The codes used for the sets were the numbers 1 through 13 and the letters 'CON', standing for control specimens. The cubes in each set were marked with letters A, B and C. The cubes were

then moist cured for thirty days.

After curing the cubes were air dried. The cubes in set 1, that is cubes 1A, 1B and 1C were tested for compressive strength. The results are presented in Appendix A.

The cubes in set 2 were air dried at room temperature (75° F). The cubes in set 3 through 13 were oven dried to the following temperatures: 100 °F, 125 °F, 150 °F, 175 °F, 200 °F, 225 °F, 250 °F, 300 °F, 400 °F, 500 °F and 600 °F.

The cubes were weighed once in each 24 hour period to the nearest 1/10th of a gram using a digital scale. The weights of the cubes before the drying stage were approximately in the range 270 g to 290 g. Each set of cubes were taken to be fully dried to its designated drying temperature, when the decrease in the weight of each cube was less than 0.1 % of its weight in a 24 hour period, that is the difference in weight was roughly less than 0.3 g in each 24 hour period. All the cubes were placed in the oven at one time and the oven set to the lowest drying temperature: 100 °F. When the cubes of set 3 were completely dry at this temperature, they were taken out and placed in a desiccator to prevent any absorption of moisture before the cubes could be impregnated. The oven was then set at the next higher temperature, 125 °F and so on until all the cubes were dried.

At lower temperatures, the cubes required a relatively longer time to be dry. As the drying temperature at this point was

less than the boiling point of water, the molecules of water took a long time to evaporate from the cubes. For the cubes that were dried at temperatures below 225 °F, it took between 7 to 11 days to dry. In the case of cubes over this temperature it progressively required a shorter time as the drying temperature was increased. For the last set of cubes, it took 48 hours from the time the penultimate set of cubes were removed and the oven temperature raised to 600 °F.

As mentioned before, the dried cubes were placed in a desiccator before impregnation could be initiated. The drying agent used was anhydrous $CaSO_4$ which is a deliquescent material and absorbs water vapor from the atmosphere. Two kinds of $CaSO_4$ granules were used: a non-indicating and relatively cheap white colored type and an indicating but more expensive blue colored type. A handful of the blue type was mixed with a larger quantity of the white type in the desiccator. On absorbing water molecules, the blue granules turn to a purple color.

The desiccator lid was sealed using vacuum grease.

Monomer was mixed in a similar way as in the case of the specimens described in the preceding section. The cubes were again weighed and then impregnated by submerging them in monomer inside a metal box for a period of five days. During the impregnation period, care was taken so that the cubes were completely submerged at all times.

After the impregnation period, the cubes were taken out of the box and allowed to be air dried. Another set of weights were then taken.

The cubes of set 2, that is the cubes which were dried to ambient temperature, showed random cracks all over the surfaces. One cube had a small piece which had completely broken off. The other cubes which were dried to higher temperatures did not appear to be cracked. An earlier experiment performed on mortar cubes by the author resulted in the cubes dried to ambient temperature cracking during the impregnating stage. Repeatability of this phenomenon precluded faulty mix design as being a possible cause of the cracks. This matter is discussed further in Chapter 5.

Each cube was individually wrapped in aluminum foil and each set of cubes were placed in water proof plastic bags and immersed in a water bath at 185 °F for 24 hours. The aluminum foil and plastic bag were used to prevent the cubes from absorbing water during polymerization, so that when they were vacuum saturated the moisture content would be due to water uptake during the vacuum saturation *only*.

After polymerization, the cubes were removed from the bath, allowed to cool to ambient temperature and another set of weights were taken.

The cubes were then vacuum saturated, and the moisture content of the cubes were determined as follows:

$$\text{Moisture Content} = \{(W_w/W_s) \times 100\}\ \%$$

where,

W_w = weight of water absorbed in vacuum saturation in g, and

W_s = weight of the cube before vacuum saturation in g.

The resistivity of the cubes were obtained by using a Nilsson Soil Resistance Meter [22]. For the purpose, the instrument was modified slightly. See Appendix B for a description of the testing procedure.

Three resistivity values were taken across each pair of opposite sides of the cubes for total of nine values from each set of three cubes. The mean value of the nine resistivity readings was used for analysis.

The suggested criteria used for interpreting the resistivity values is presented below [23,24].

- If resistivity exceeds 12,000 Ω-cm, corrosion is unlikely.
- If resistivity is between 5,000 Ω-cm and 12,000 Ω-cm, corrosion is probable.
- If resistivity is less than 5,000 Ω-cm, corrosion is almost certain.

A separate study on marine structures in California indicated that at resistivity values over 60,000 Ω-cm no corrosion occurred but corrosion was detected below 60,000 Ω-cm [25]. Other work [26] suggested that corrosion was unlikely above

20,000 Ω-cm and active corrosion would occur at resistivities between 5,000 to 10,000 Ω-cm.

A masonry saw was used to cut sections from the "C" cube of the impregnated cube sets 3 through 13 and the non-impregnated set CON (see Figure 4).

The remaining pore size characteristics after impregnation were determined for one section using a mercury porosimeter and the chemical composition was determined for another section using a scanning electron microscope - energy dispersive x-ray spectroscope system (SEM-EDS system). The sections were approximately 2" × 1" × 1" as this is the maximum size which can be accommodated in the mercury porosimeter. The mortar sections were dried in the oven at 220° F until the weight loss in a 24 hour period were less than 0.1 % of their original weight. As the original weights were in the order of a few grams, a precision balance was used for weighing, which has a least count of 1/1000 g.

It took nine days for the concrete pieces to be dried to the requisite level. The mortar sections were then placed in the mercury porosimeter.

Mercury has a high surface tension and is non-wetting to all materials with a few exceptions. This causes mercury to occupy the minimum surface area and largest radius of curvature possible at a given pressure. In the porosimeter, mercury is forced into the pores of the sample by increasing the pressure

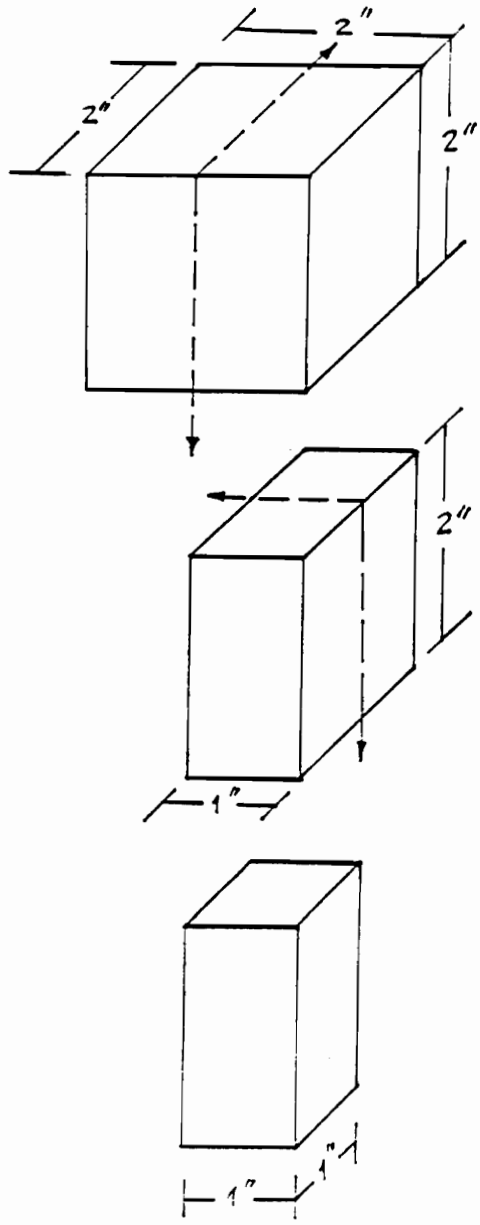

Figure 4 Cube Sections for Porosimeter & SEM Tests

in steps. The pressure is then reduced and the mercury extrudes from the sample. The parameters of pore sizes in the sample is determined on the basis of the capillary law governing liquid penetration into small pores which relate the pore diameter to the applied pressure, surface tension and contact angle [27].

In the SEM, the mortar sample was bombarded by a stream of electrons which were absorbed inelastically by the sample. Each element present in the sample possesses a characteristic excitation potential and the subsequent X ray radiation consists of these characteristic frequencies which were identified by the SEM [28,29]. The relative intensity of the radiation gave a measure of the quantity of the particular element present in the sample. The element Gold (Au) was present due to the samples being sprayed with gold powder prior to the SEM experiment in order to increase the conductivity of the specimens.

Cube A of each Set of cubes was submerged in a 6 % (by weight) NaCl solution in cycles of three days wet followed by air drying for four days. This alternate wet and dry cycle was continued for a period of 100 days. After that, the resistivity values of the cubes were taken with the cubes in a surface dry condition. The cubes were then cut in half with a masonry saw. From one half of each cut cube, powdered sample was extracted with a ¼" diameter carbide drill from a square

strip of width ¼". The beginning edge of the strip was ¼" from the edge of the cubes (see Figure 5). The sampling depth was ½".

The samples were tested for chloride content using the specific ion probe from James Instruments, Inc as discussed in the preceding section.

The other half of the cubes were etched with muriatic acid. The acid was applied to a strip of width 1" in the center of the cube section, while the rest of the surface was covered by pieces of duct tape (see Figure 5). The acid was introduced on the cubes with a glass dropper under the fume hood.

One cube which had not been impregnated nor subjected to salt solution was also acid etched. The results are discussed in Chapter 5.

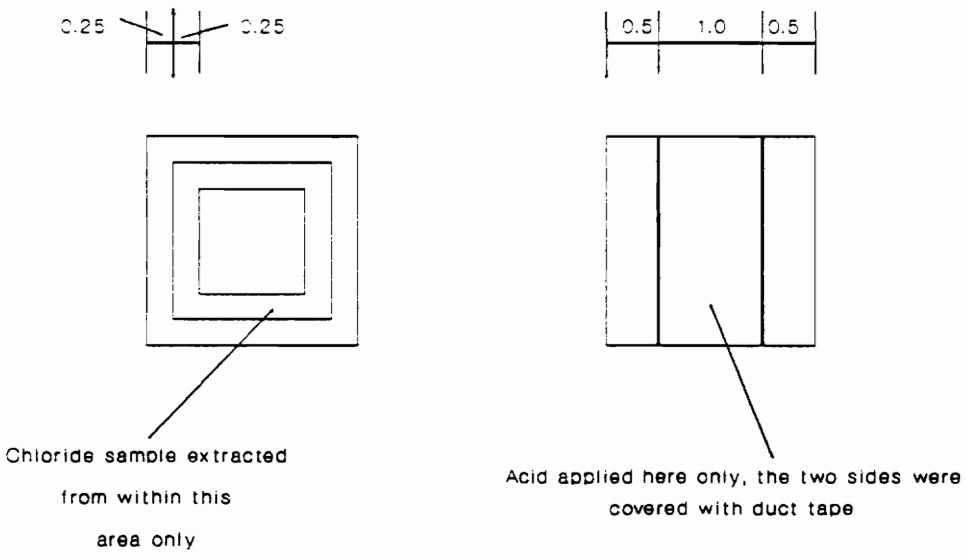

Figure 5 Cube Sections for Acid Etching & Chloride Tests

4.3.2 Effects of Drying Temperature on Corrosion Rates

From the results obtained in the section 4.3.1, it was evident that a lower drying temperature should be sufficient for effective polymer impregnation of concrete. This hypothesis is discussed in detail in Chapter 5.

To validate the above statement, eight laboratory specimens of the same dimensions and rebar configuration of the experiment described in Section 4.2 (except for cover depths), were dried using lower drying temperature criteria, polymer impregnated and polymerized as before.

Four specimens had cover depth of 2" while the other four had cover depth of ¾". Four specimens (two of each cover depth) were dried to 150 °F at ½" below the top rebar level while the other four were similarly dried to a temperature of 180 °F. Four other specimens (two of each cover depth) acted as controls and were not impregnated.

All the steps in the polymer impregnation process were as described in Section 4.2 except as noted below.

Grooves were not cut on the specimens. The impregnation was accomplished from the top surface of the specimens. The time of impregnation was estimated from the graph plotted previously. For the specimens with 2" cover, the time was 50 hours while the corresponding time for the specimens with ¾" cover was 17 hours.

In addition to recording ambient, surface and temperatures at ½" below top rebar level, temperatures at the rebar levels were also recorded at regular intervals during the heating and the subsequent cooling stages. The existing TC wire was lengthened by attaching a piece of another TC wire. The wire was insulated during the drying stage by wrapping aluminum foil around it.

Wooden dikes were made, painted with a mixture of 90 % Epon 828 resin and 10 % of DETA (by weight) in order to make them water tight and adhered on to the top of the specimens with silicon rubber. The monomer mixture was ponded on the top of the specimens.

After polymerization, potential and 3LP (corrosion rate) readings were taken as in the case of the first series of specimens.

5.0 ANALYSIS OF RESULTS

5.1 Rigid Overlay Specimens

After a number of potential and 3LP readings were taken, it was observed that the ambient temperature at the time of measurement had a marked effect on the resultant readings. The higher the temperature, the higher the 3LP reading and more negative the potential value.

In order that all the data could be analyzed without developing a temperature correction factor, all readings were taken at room temperature which was 72 °F.

The potential values and the corresponding 3LP values both before and after treatments indicated that post-treatment potential values did not reflect very accurately the corrosion activity in the specimens. While the I_{corr} values in the treated specimens showed very little active corrosion, the corresponding potential values for most specimens were well into the 90 % active corrosion region, that is more negative than -350 mV. Therefore, it would seem that once corrosion had been initiated and then abated by some treatment method, the potential values were no longer reliable indicators of the corrosion activity.

The I_{corr} value being a more direct measure of corrosion rate

(Since corrosion current is proportional to corrosion rate, according to Faraday's 1st Law, equation 1) than the potential value which is based on a probability function. A relation was attempted between I_{corr} and potential with potential as the independent variable. The objective was to try and predict 3LP values from the potential values.

Pairs of potential and the corresponding I_{corr} values were used in a simple linear regression model (SLR) from the data on the 1" cover depth specimens. SLR was performed on a IBM 3090 mainframe computer using the Statistical Analysis System (SAS) software. There were 323 pairs of data in the analysis.

The SLR analysis resulted in a F-observed value of 219.845 and a p value of 0.001. Thus, at the 5 % significant level, relationship was significant with the F-observed value well into the rejection region. Thus, there is a relationship between Potential and I_{corr}.

A good measure of the strength of this relationship is R^2 (the coefficient of determination) which was 0.4065. This meant that about 40 % of the variation in I_{corr} could be predicted from the potential in the given sample data. The adjusted R^2 which was 0.4046 was the proportion of the I_{corr} variation which could be predicted from potential values in the population. These values suggest that the relationship between potential and I_{corr} was not very strong. This conclusion was further borne out by the Pearson Correlation Coefficient

between potential and I_{corr} which was 0.64. The correlation coefficient values will be between +1.0 and -1.0 with negative value indicating negative correlation between the two factors. The closer the positive correlation value is to ±1.0, the stronger is the relationship between the two factors.

The low values of R^2 and the correlation coefficient indicated that the relationship between potential and I_{corr} was not very strong and it was not possible to predict I_{corr} values from potential values with a high degree of certainty.

In view of the above results, only I_{corr} values were used for comparative analyses.

For convenient display of information, the data was transformed into graphs and divided into three treatment groups.

The controls (CO), LMC overlaids (LM) and LMC overlaid-polymer-impregnated specimens (PM) were compared as one treatment group. The controls, LSDC overlaids (LS) and LSDC overlaid-polymer-impregnated specimens (PS) were compared as the second group. Controls polymer impregnated specimens (PC) were the third treatment group. The treated specimens in the three groups will be referred to from now on as the latex group, low slump group and polymer impregnated group, respectively.

In graphs and tables, the cover depth(s) in inches and the drying temperature(s) in °F of the specimens discussed therein

have been indicated in parenthesis following the caption. The mean measurement is the average of six readings obtained from each series of specimens, each time readings were taken. The individual readings are presented in Appendix C.

The pre-treatment potential values started with values ranging from about -225 mV to -260 mV which is more or less in the 90 % no-corrosion region. During the course of the next fifty days the values became less negative or the steel became more noble with respect to corrosion activity. See Figures 6A, 6B and 6C. This phenomenon was due to the formation of a passive layer of gamma iron oxide around the steel which protects the rebar from further corrosion activity.

After 50 days, the chlorides in the vicinity of the rebar progressively destroyed the passive layer resulting in more negative potential values. At day 214, all the specimens had potential values more negative than -350 mV, that is in the 90 % active-corrosion region.

Chloride contents were taken on selected specimens on day 71 and again on day 190. At day 190 the chloride content at a depth of 1 to 1½" (rebar level) for all the tested specimens were well over the accepted threshold level for corrosion initiation, viz. 1.2 lb/yd^3. See Appendix C.

The third method for monitoring degree of corrosion was the I_{corr} values obtained from the 3LP device. As with the

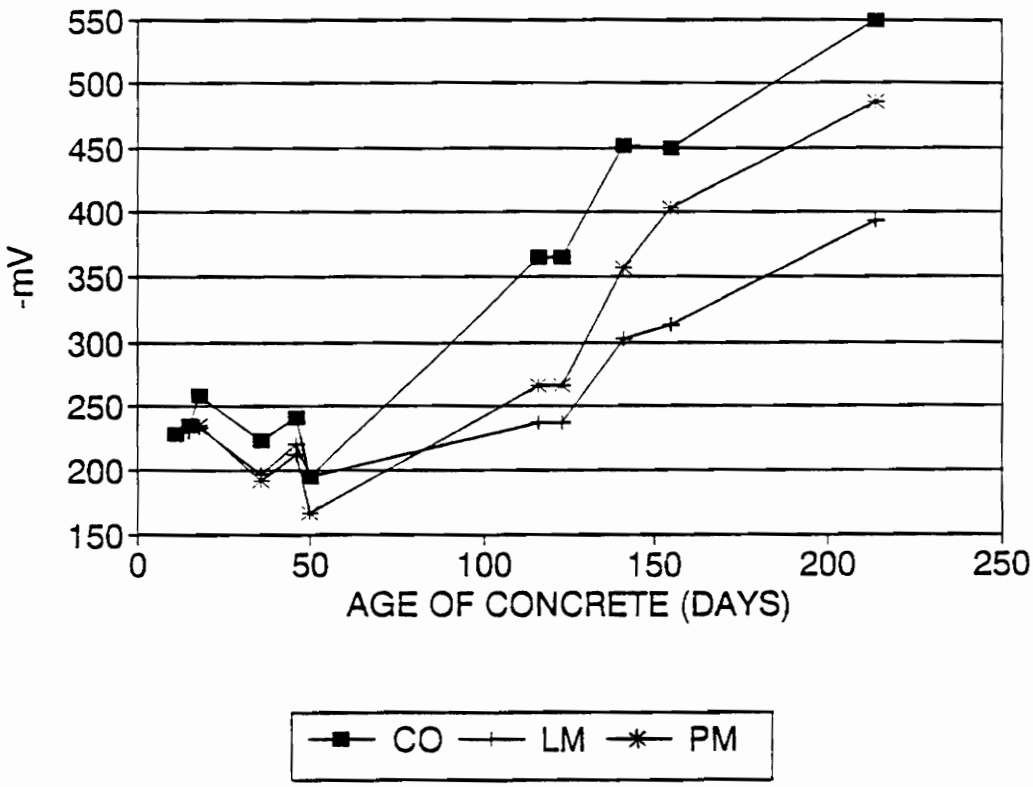

Figure 6A Pre-Treatment Mean Potential (1", 230 °F)

Latex Group

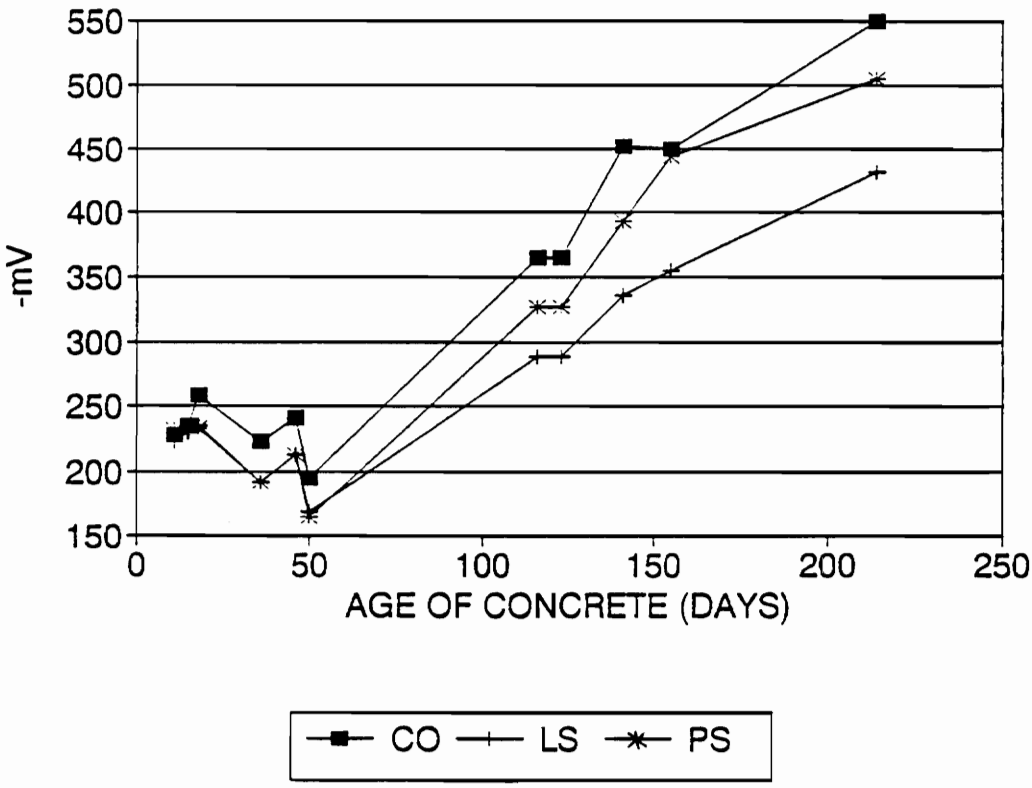

Figure 6B Pre-Treatment Mean Potential (1", 230 °F)

Low Slump Group

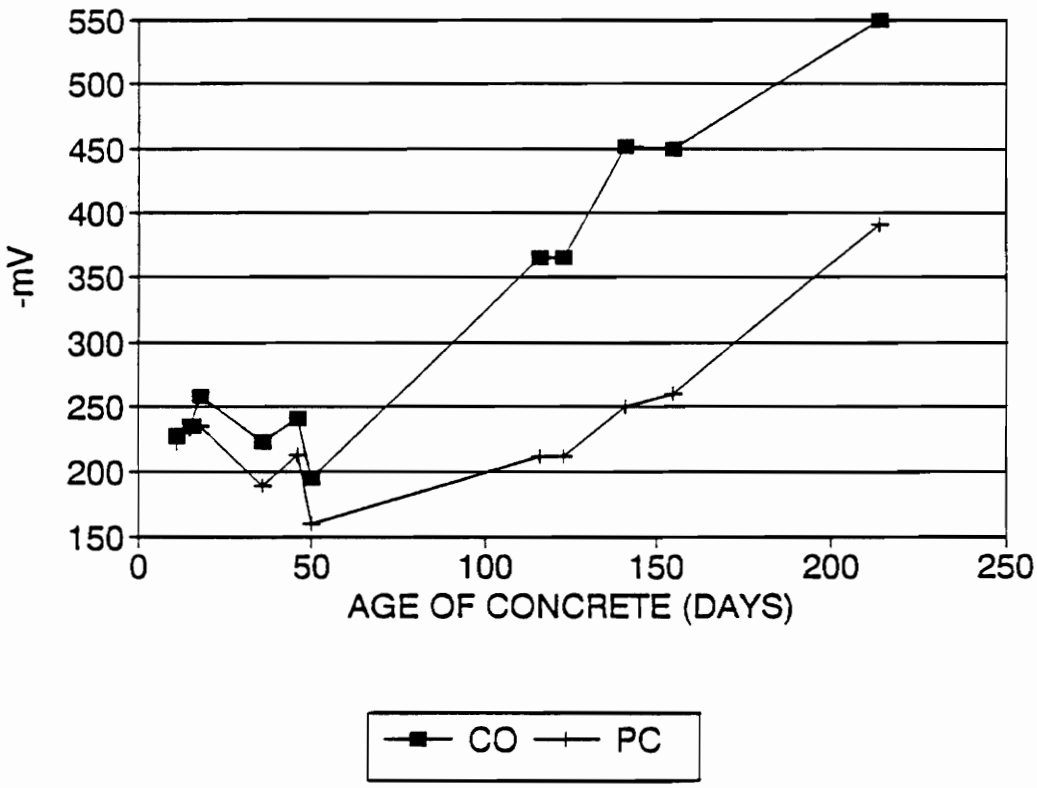

Figure 6C Pre-Treatment Mean Potential (1", 230 °F)

Polymer Impregnated Group

potential values, the mean of six readings were used for evaluation. The individual readings are presented in Appendix C. The mean I_{corr} value at day 214 was over 2 mA/sq ft for all the six series of specimens excepting the latex modified concrete overlay specimens. The low value for this series was a result of several rebars having lower than usual values at that point in time.

The specimens were prepared for the different treatment methods after day 214. Since it took about 33 days for the entire process of treatments to be completed, it can be safely assumed that at the actual time of treatments the corrosion levels were higher than what was indicated at day 214.

For reasons cited, the post-treatment potentials were not used for evaluation. The mean post-treatment potential values are presented in Figures 7A, 7B and 7C.

The mean values of the corrosion current (see Figures 8A, 8B and 8C) indicated that the control specimens progressively corroded to extremely high levels with the passage of time, while in all the treated specimens the corrosion levels dropped and then did not show appreciable fluctuation over time.

Since the last pre-treatment values had a significant range for the different series of specimens, the absolute mean post-treatment values is not a good measure for comparing the effectiveness of the five treatment methods with each other

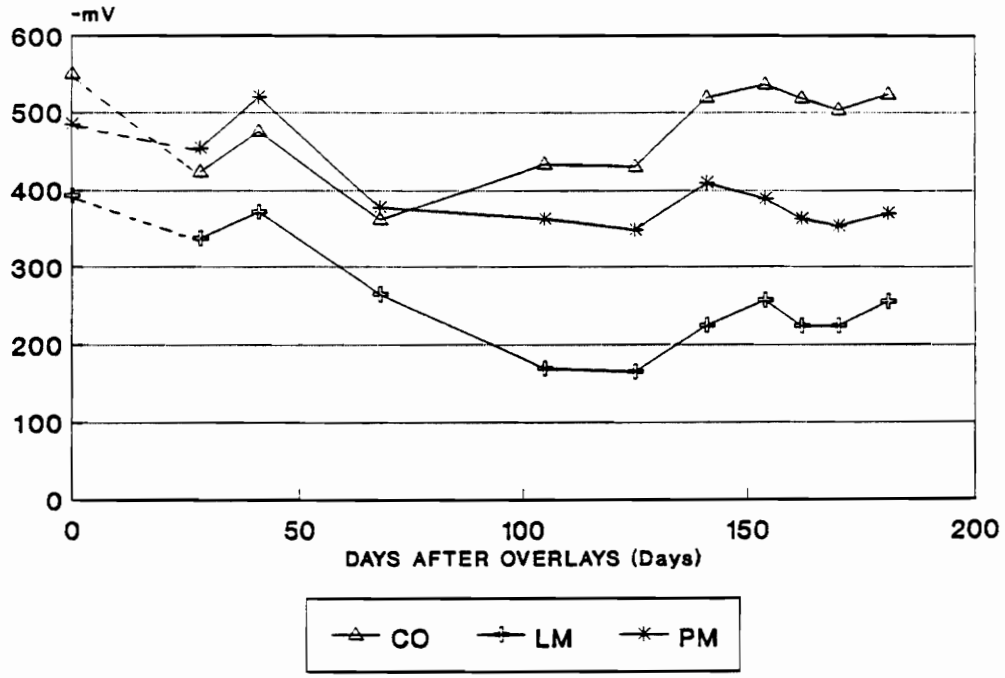

Figure 7A Post-Treatment Mean Potential (1", 230 °F)

Latex Group

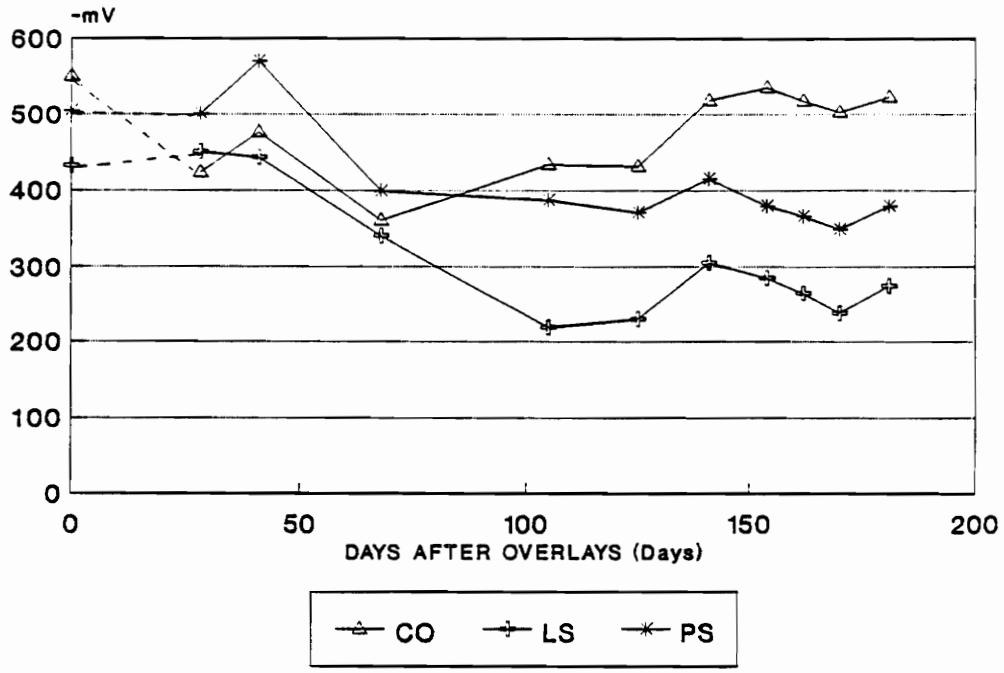

Figure 7B Post-Treatment Mean Potential (1", 230 °F)

Low Slump Group

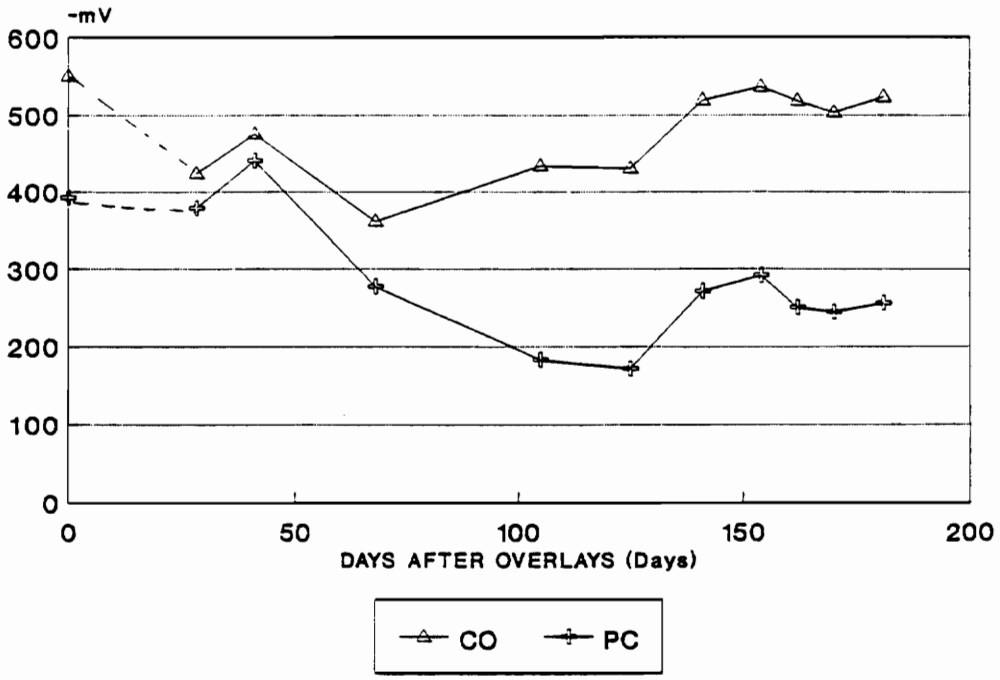

Figure 7C Post-Treatment Mean Potential (1", 230 °F)

Polymer Impregnated Group

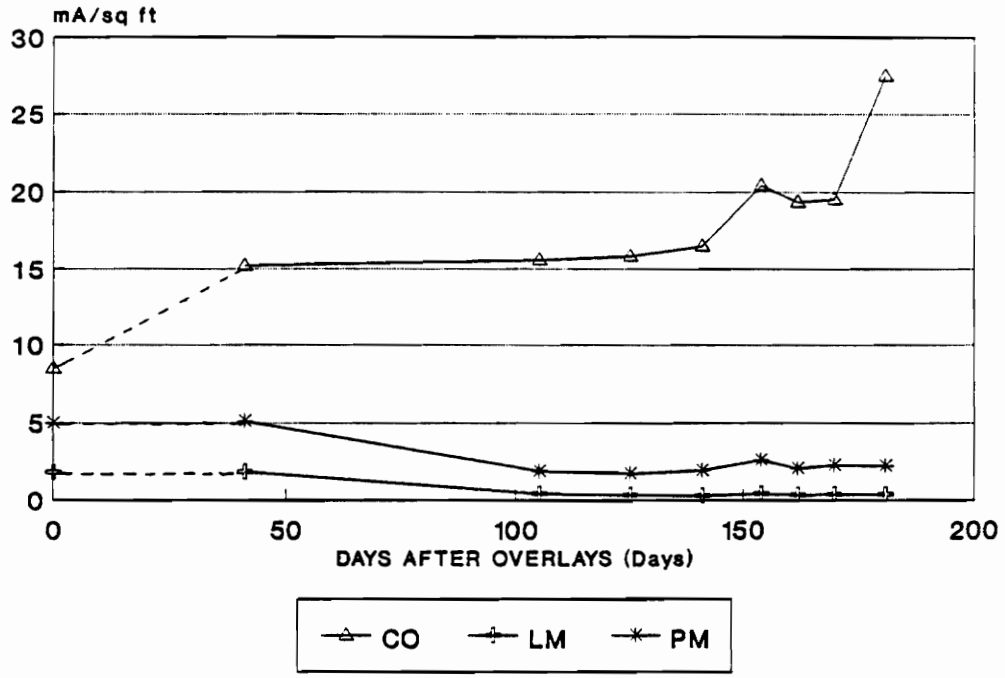

Figure 8A Post-Treatment Mean I_{corr} (1", 230 °F)

Latex Group

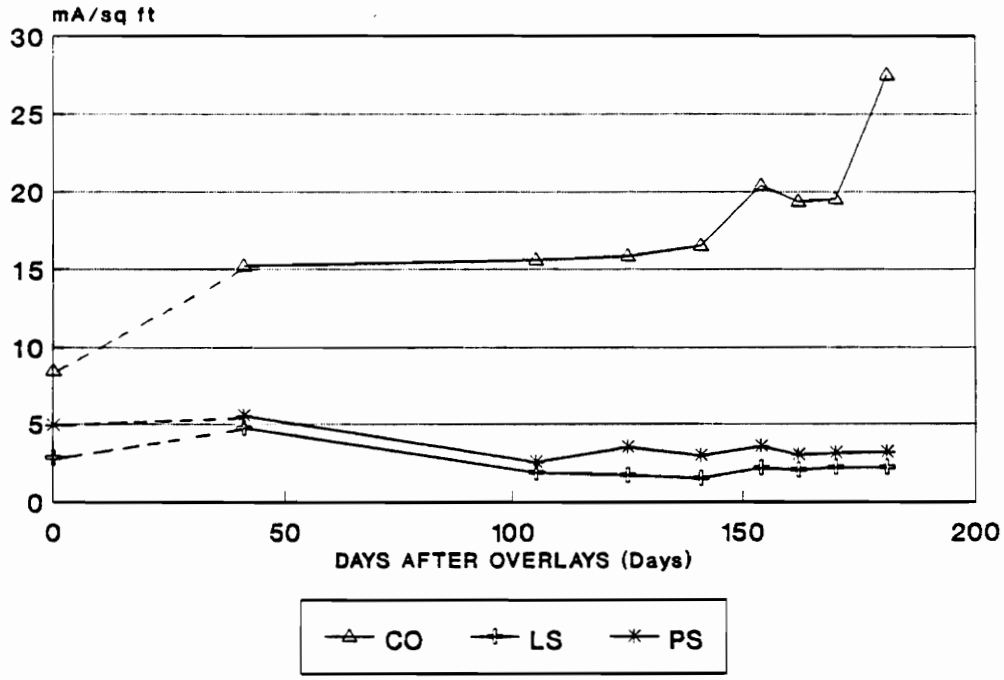

Figure 8B Post-Treatment Mean I_{corr} (1", 230 °F)

Low Slump Group

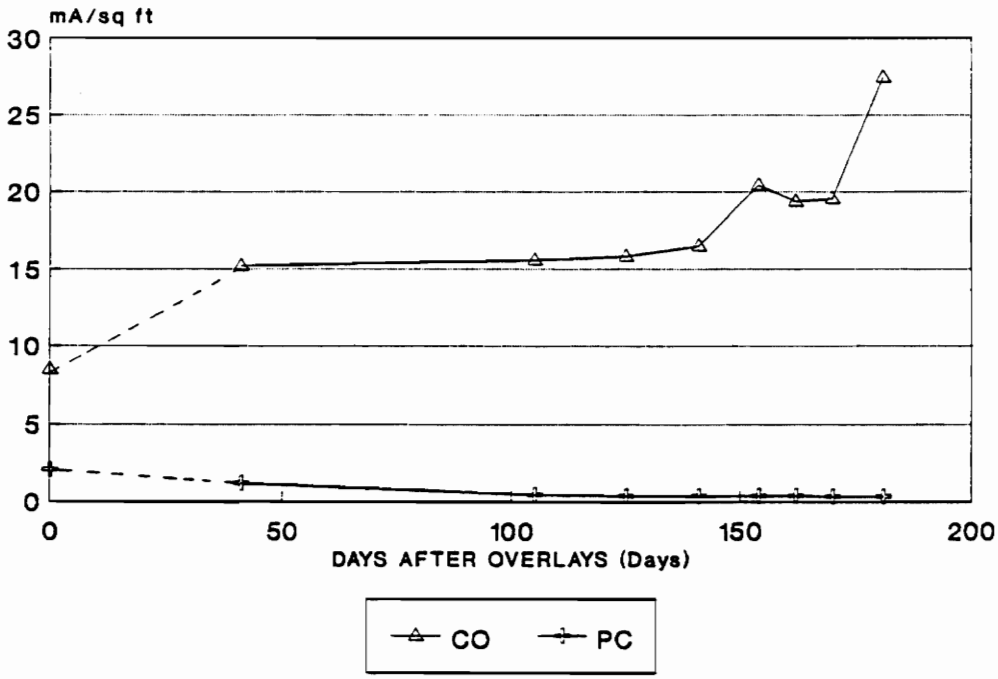

Figure 8C Post-Treatment Mean I_{corr} (1", 230 °F)

Polymer Impregnated Group

and with the control specimens. Therefore the % change in each post-treatment value was computed on the basis of the last pre-treatment value as follows:

$$\% \text{ change} = \{(B - P)/B\} \times 100 \qquad (3)$$

where,

B = last pre-treatment I_{corr} in mA/sq ft, and

P = present I_{corr} in mA/sq ft.

Therefore, a positive value of "% change" indicates that corrosion rate has decreased from its pre-treatment level, while a negative value of "% change" signifies a higher corrosion level compared to its pre-treatment value.

At day 181 after the application of the overlays, the control specimens had % change as -223.4 demonstrating the extreme deteriorated condition of the untreated specimens. See Figure 9A, 9B and 9C. The latex group and polymer impregnated groups demonstrated values of over +50 % at day 181. The corresponding figures for the low slump group were well below +50 % improvement level. However, they remained in the positive range indicating that the treatments did have the desired effect of reducing corrosion levels. The low slump overlay specimens had a value of +22.7 % while the low slump overlay with polymer impregnation had a slightly higher value of +36.2 %.

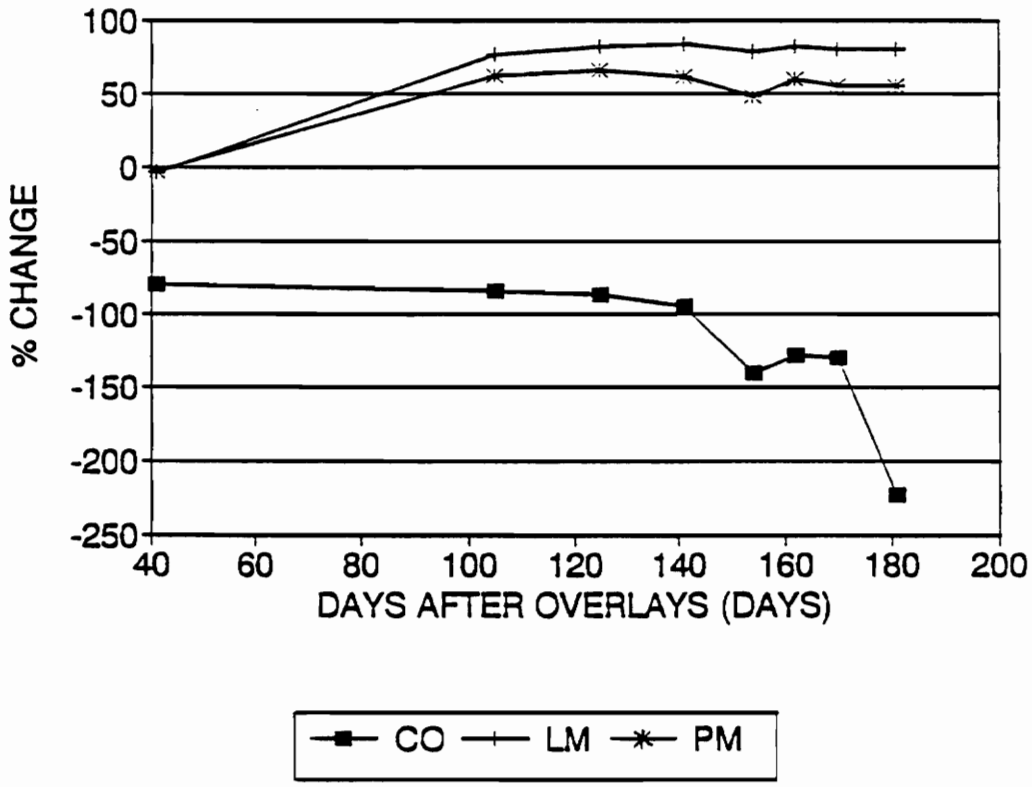

Figure 9A Percent Change in Mean I_{corr} (1", 230 °F)

Latex Group

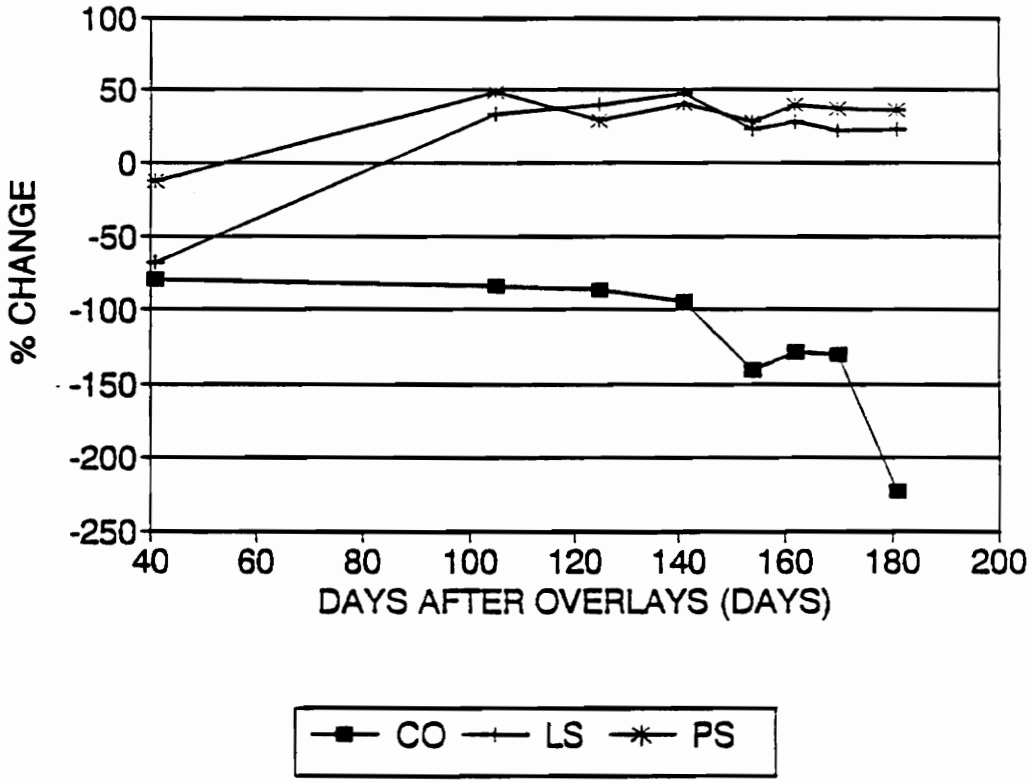

Figure 9B Percent Change in Mean I_{corr} (1", 230 °F)

Low Slump Group

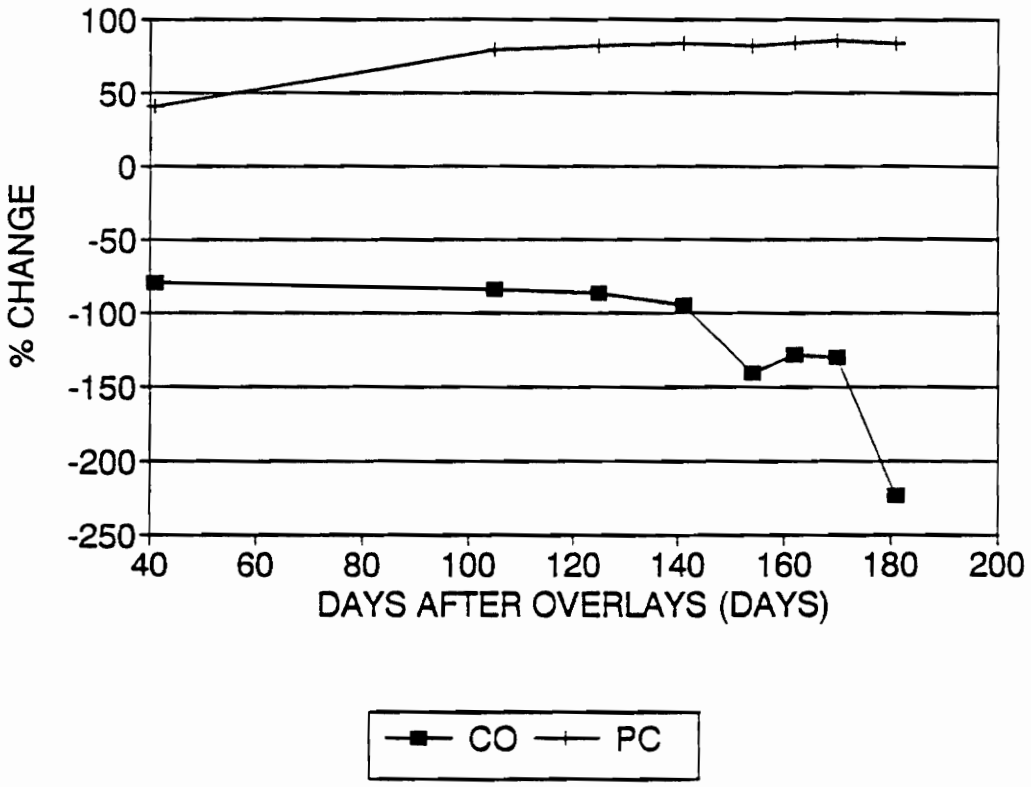

Figure 9C Percent Change in Mean I_{corr} (1", 230 °F)

Polymer Impregnated Group

At 41 days after overlays, all series of treated specimens, except for the polymer impregnated specimens had negative values of "% change". A possible explanation is that there is a time lag before the overlays cause a decrease in the corrosion rates.

The absolute difference in the "% change" between the last and first values may be a useful measure of the effectiveness of each treatment procedure. See Table 1.

The maximum value of this measure was 91.03 % for the LSDC specimens and the minimum value was 42.30 % for the polymer impregnated specimens. There seemed to be no well defined trend between the three groups. This indicated that there was no appreciable difference in the effectiveness of any treatment method. The specimens with only overlays demonstrated higher values than their counterparts which were polymer impregnated in addition to the overlays. This would seem to indicate that impregnation had *decreased* the effectiveness of the overlays in abating corrosion.

However, both the series with overlays and polymer impregnation, the PM series (LMC overlay-polymer-impregnation) and the PS series (LSDC overlay-polymer-impregnation) had the highest pre-treatment corrosion rates of 4.99 mA/sq ft and 4.92 mA/sq ft, respectively. It is conceivable that these higher corrosion rates had an effect on the "absolute difference in % change" values. It is reasonable to expect

Table 1 Measures for Evaluating Effectiveness of Treatments

SPECIMEN	LAST PRE-TREATMENT Icorr (mA/sq ft)	% CHANGE AT DAY 41	% CHANGE AT DAY 181	ABSOLUTE DIFFERENCE IN % CHANGE
Latex Group				
LM	1.76	-3.37	+79.85	83.22
PM	4.99	-2.89	+55.84	58.73
Low Slump Group				
LS	2.82	-68.35	+22.68	91.03
PS	4.92	-12.55	+36.19	48.74
Polymer Impregnated Group				
PC	2.07	+41.73	+84.03	42.30

that any treatment method would be more effective if the initial corrosion rate was low than the case where the initial corrosion rate was relatively higher. For a better analysis of the situation, the post-treatment corrosion rates should be monitored for a longer period of time than could be accommodated in the scope of this study.

From a comparison of the actual values of "% change", the low slump group appeared to have lower effectiveness as compared to the other two groups. As have been mentioned before, this measure might not be a very accurate representation of the situation, since it does not indicate the 'degree' of the "% change".

The values of the "% change" at day 41 (see Table 1) indicated that the low slump group also had been least effective in abating corrosion at this age. However, specimens which had been overlaid with LSDC (LS) had an unusually high negative value of "% change", viz. -68.35 % which was comparable to the "% change" of the control specimens at the same point in time, -79.47 %. The much lower negative value of "% change" (-12.55 %) in the specimens with LSDC overlay-polymer-impregnation (PS) could probably be attributed to the polymer impregnation. However, this value for the PS series was more negative than the other groups. The higher pre-treatment corrosion rates could not be forwarded as a possible cause, since the specimens with LMC overlay-polymer-impregnation (PM) also had

similar high pre-treatment corrosion rates. In the case of the PM series, the "% change" at day 41 was -2.89 % which was comparable to the -3.37 % value for the LMC overlay (LM) specimens.

A possible explanation for the apparently lower effectiveness of the low slump group is that the low design slump of LSDC overlay resulted in imperfect compaction after the overlay was placed. The LSDC overlay had a rough surface which suggests the presence of more void spaces resulting in increased permeability for more rapid ingress of chloride ions after treatment.

5.2 Influence of Cathode to Anode Area on Corrosion Rates

The standard electrical connections had a cathode to anode surface area (C/A) of 2. In order to study the influence of the C/A on corrosion rates, corrosion current readings were taken with different electrical connections such that the C/A were 1, 2, 3 and 4 as shown in Figures 10A and 10B. In each case, the anode involved was the right anode of each specimen. The left anode was kept isolated in order to obtain the micro-cell corrosion values. After each C/A connection type was completed, the specimen-system was allowed to stabilize for at least one day before readings were taken.

When I_{corr} readings were taken with the cathode and anode being separated by a distance, the obtained values were a mixture of micro-cell and macro-cell corrosion current, or mixed-cell corrosion current.

Effect of C/A on Mixed I_{corr}

Change in C/A did not have appreciable effect on the corrosion current for the five treatment methods. See Figures 11A, 11B and 11C. The corrosion abatement techniques had substantially decreased the corrosion rates, and increased cathode area had little influence in changing the corrosion rate. Thus, some

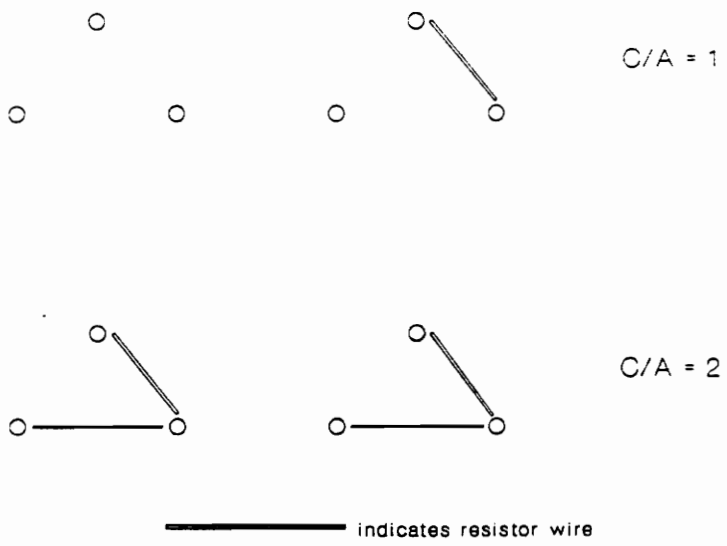

Figure 10A Different Electrical Connections Used

C/A = 1, 2

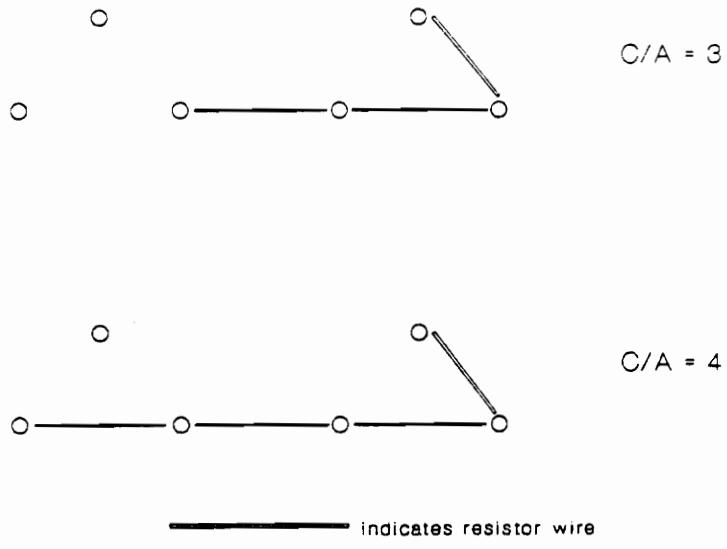

Figure 10B Different Electrical Connections Used

C/A = 3, 4

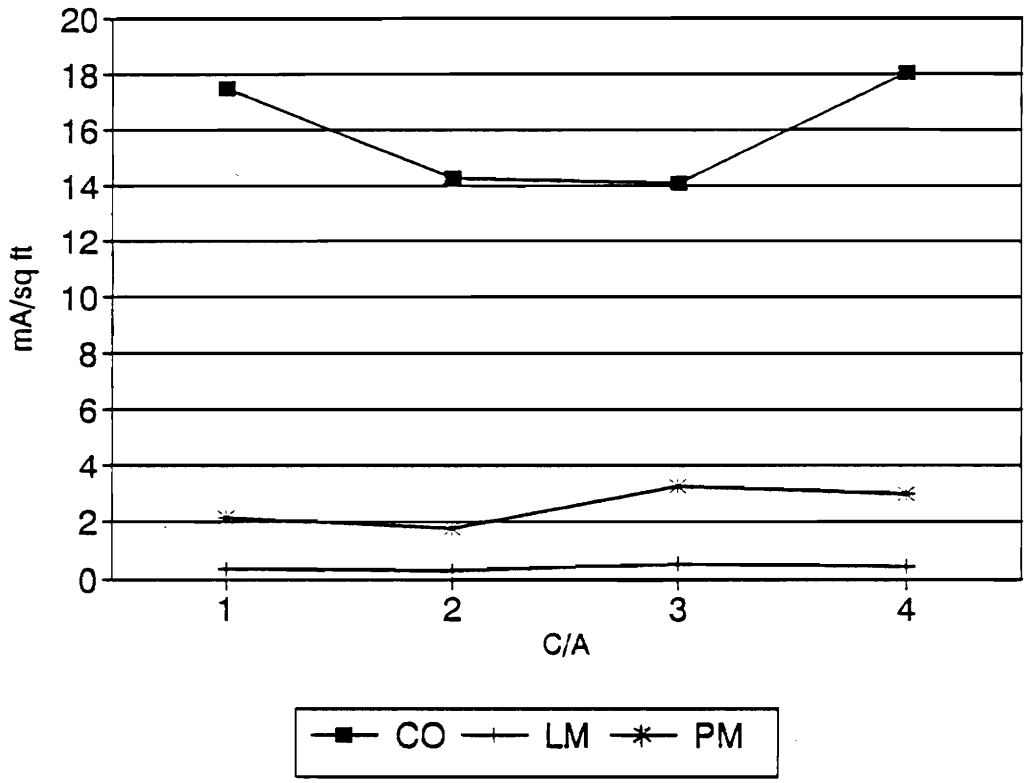

Figure 11A Mixed I_{corr} vs C/A (1", 230 °F)

Latex Group

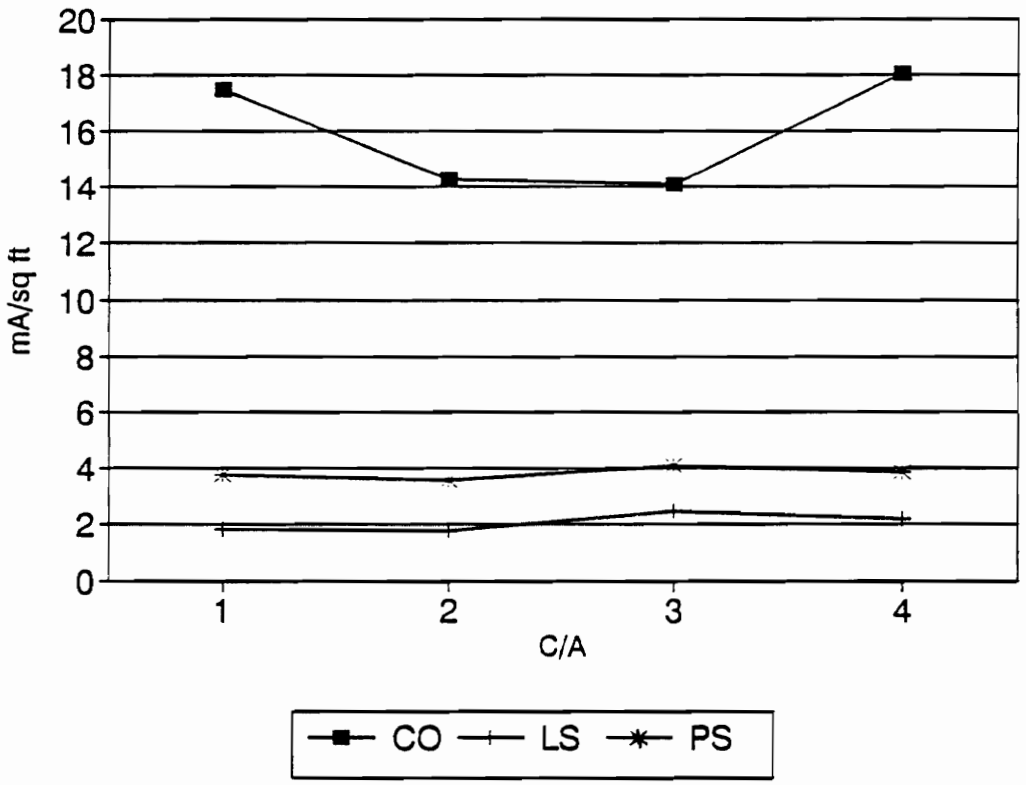

Figure 11B Mixed I_{corr} vs C/A (1", 230 °F)

Low Slump Group

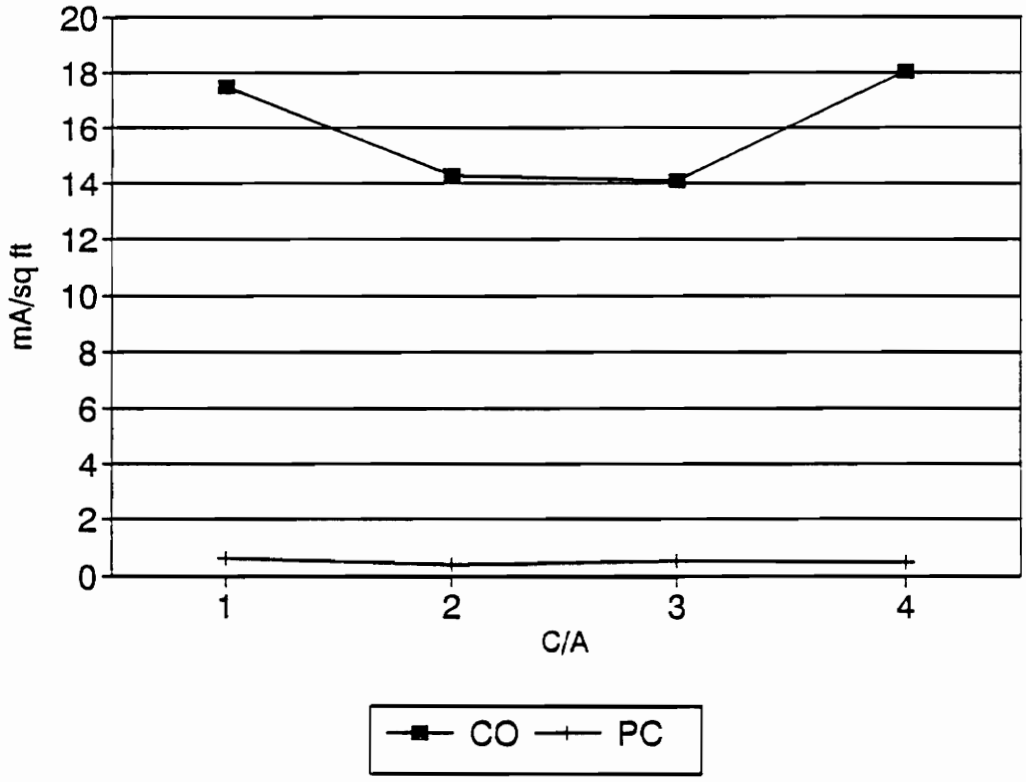

Figure 11C Mixed I_{corr} vs C/A (1", 230 °F)

Polymer Impregnated Group

other factor is controlling the corrosion rate of the treated specimens. Possible factors are chloride content, temperature, moisture content, available oxygen and resistance between the cathode and anode. Of these factors, the temperature, moisture content and available oxygen were more or less constant for the different C/A ratios. The chloride content could not have changed much, as all the readings with different C/A ratio were taken in a time span of nine days. However, resistance increases with increasing C/A ratio. Therefore, the inherent increment in I_{corr} with increase of C/A ratio was neutralized by the corresponding increase in resistance. Consequently, there was insignificant net change in the corrosion current. For the case of the control specimens, the corrosion rate (I_{corr}) was much higher and thus it was more sensitive to changes in C/A ratios. For C/A ratio between 1 and 2 and between 2 and 3, the I_{corr} showed decrements; a sharp drop followed by a more gradual decrease. In this region of the graph, the higher resistance not only negated the effect of the increase in C/A ratio but actually caused the I_{corr} to decrease. However between C/A ratio 3 to 4, the larger cathode area appears to have had an influence resulting in an increase in the corrosion current which returned to approximately the same rate as the C/A ratio of 1.

Effect of C/A on Macro-cell Corrosion

The macro-cell corrosion current were measured in mA for the corroding system. Individual readings are presented in Appendix C. For comparison purposes with the micro-cell and mixed-cell corrosion rates, the macro-cell current was converted to mA/sq ft for the corroding systems.

The corroding surface area was the uncovered portion of the anode which was 6.5" long. Therefore, the requisite surface area is given by: $\{\pi(d/2)^2 \times 6.5\}$ square inches; where, d = diameter of rebar in inch. Substituting ½" for 'd', the area is 10.21 sq.in. or 0.0709 sq.ft. Hence, to convert values from mA to mA/sq ft, the multiplicative factor is 1/0.0709 = 14.10382 was used.

As shown in Figures 12A, 12B and 12C, the changes in macro-cell corrosion current with increasing C/A ratio were similar to that of the trends observed in mixed-cell corrosion. For the specimens which underwent the five treatment methods, there were no significant difference in the macro-cell current with changing C/A ratio. However, for the control specimens the macro-cell current increased significantly with increase in C/A ratio.

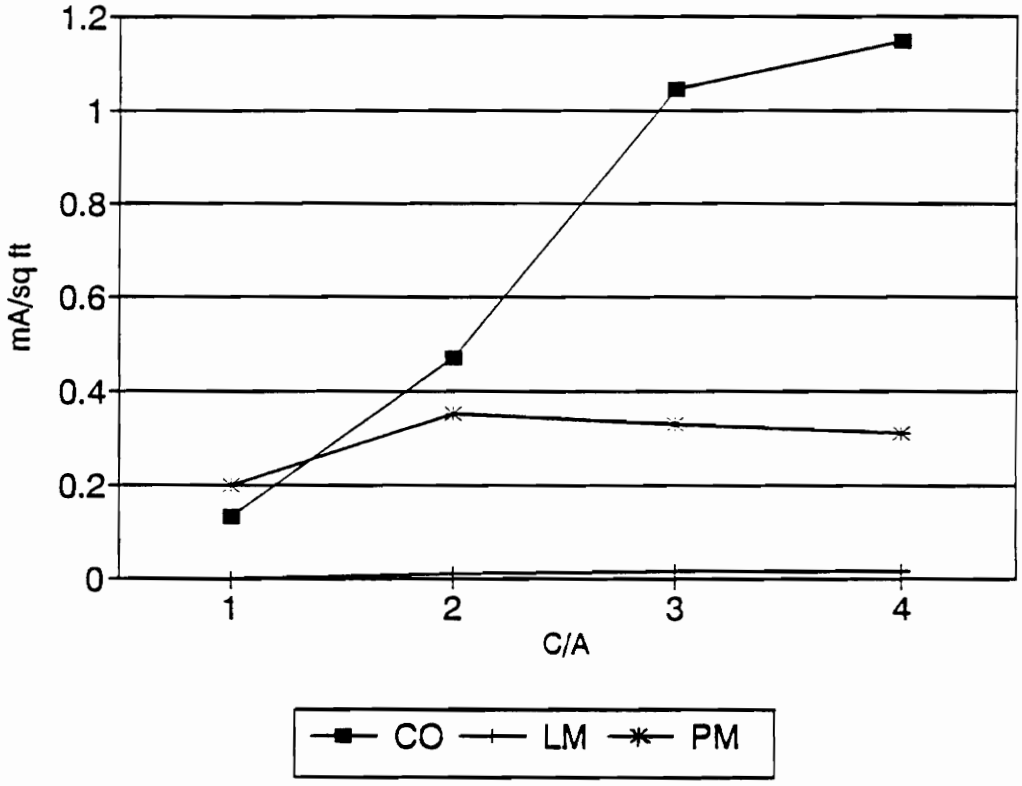

Figure 12A Macro I_{corr} vs C/A (1", 230 °F)

Latex Group

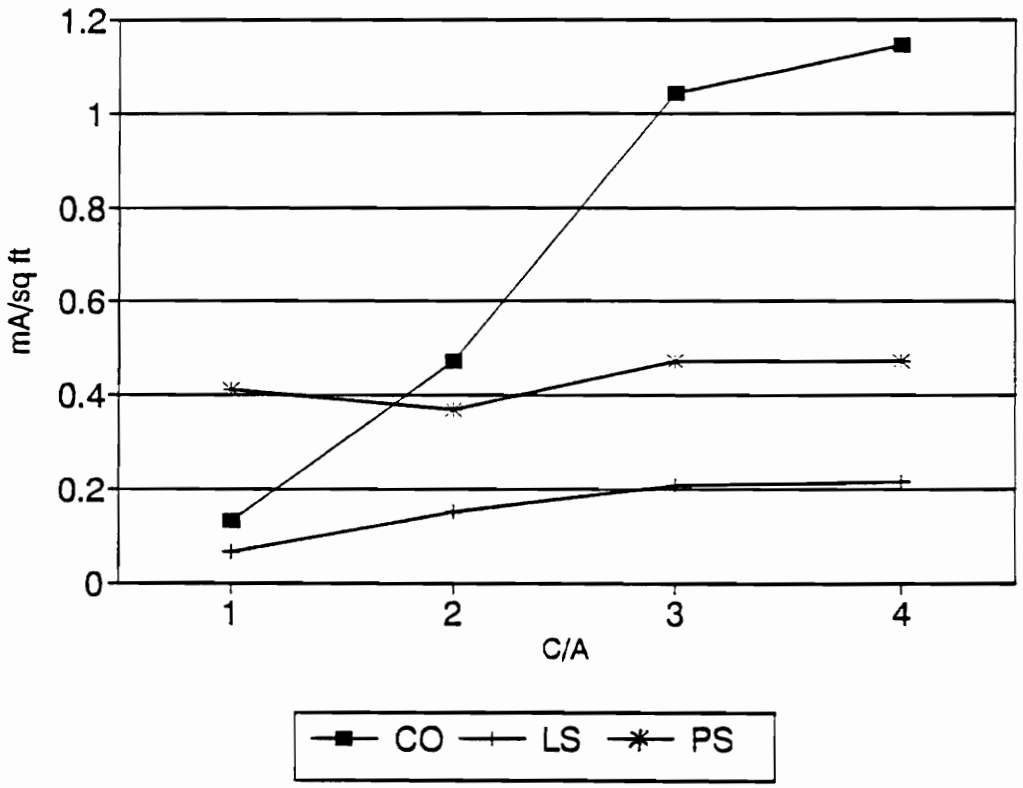

Figure 12B Macro I_{corr} vs C/A (1", 230 °F)

Low Slump Group

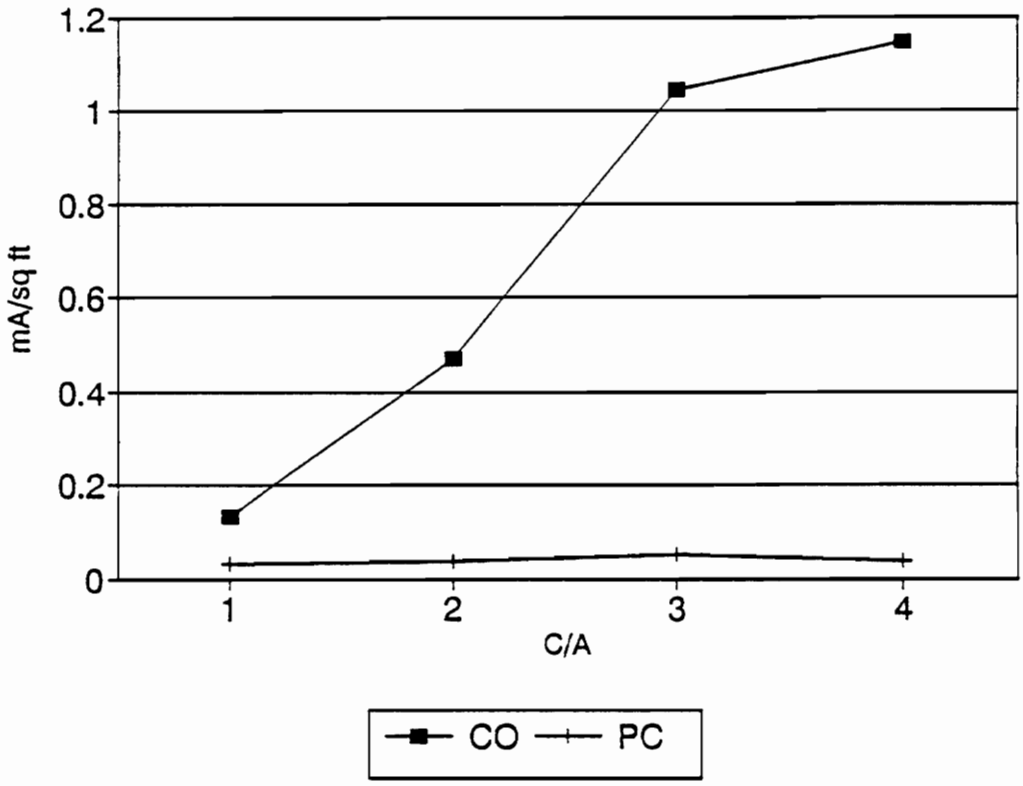

Figure 12C Macro I_{corr} vs C/A (1", 230 °F)

Polymer Impregnated Group

Change of Micro-cell I_{corr} over time

The treated specimens showed little change in the micro-cell current over a period of six days. See Figures 13A, 13B and 13C. As the corrosion level had been reduced, there were very little corrosion activity to reflect any change in their values over time.

In the control specimen, on the other hand, the micro-cell I_{corr} increased with time as expected, since the active corrosion of these specimens increased with time.

Comparison Between Micro-cell and Mixed-cell Corrosion

There was little difference between the micro-cell and mixed-cell corrosion for the treated specimens for the same reasons stated previously. For the control specimens, which were actively corroding the difference was apparent. See Figures 14A, 14B and 14C.

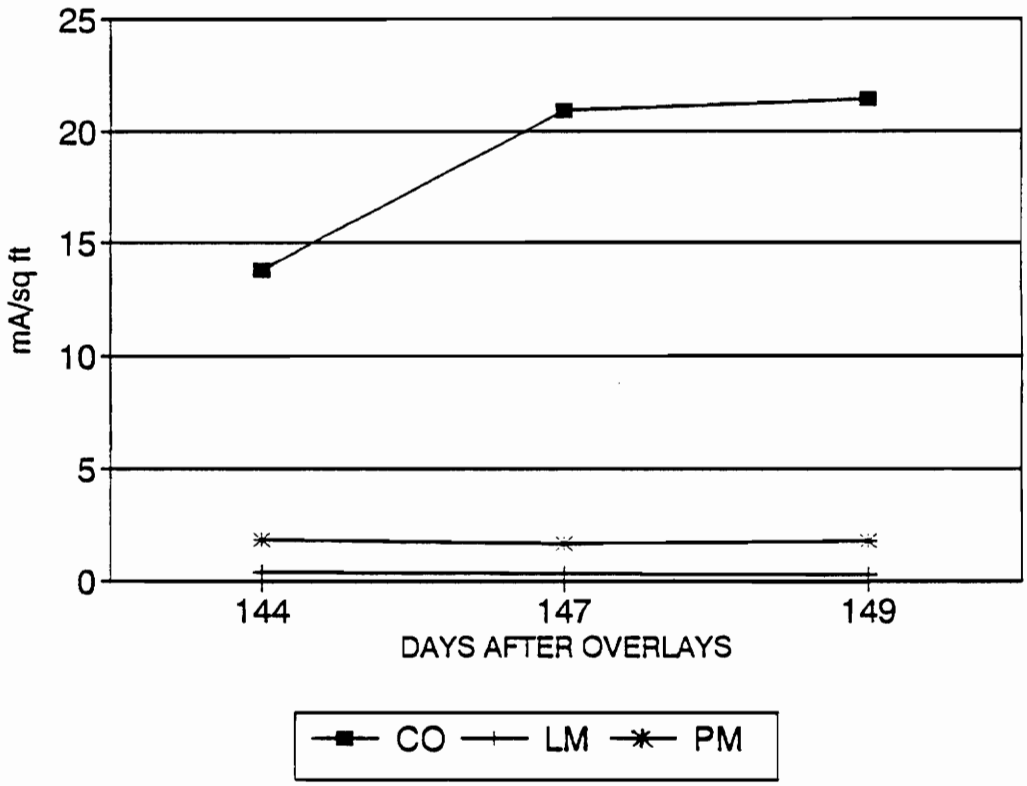

Figure 13A Micro I_{corr} vs Time (1", 230 °F)

Latex Group

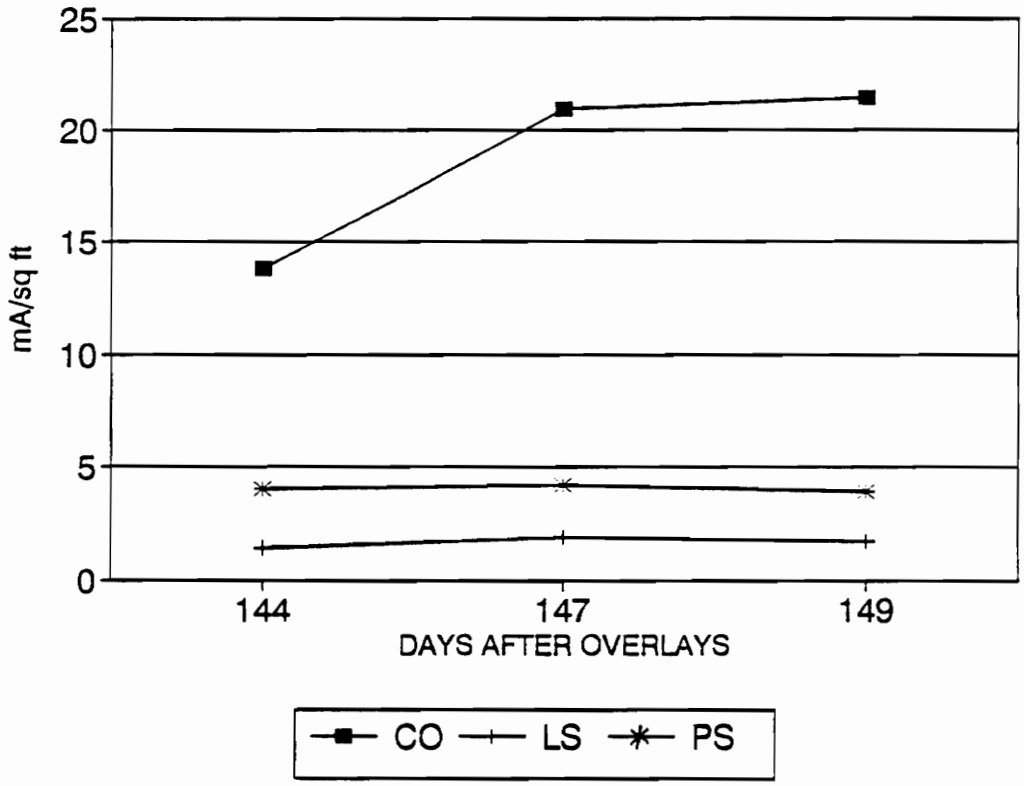

Figure 13B Micro I_{corr} vs Time (1", 230 °F)

Low Slump Group

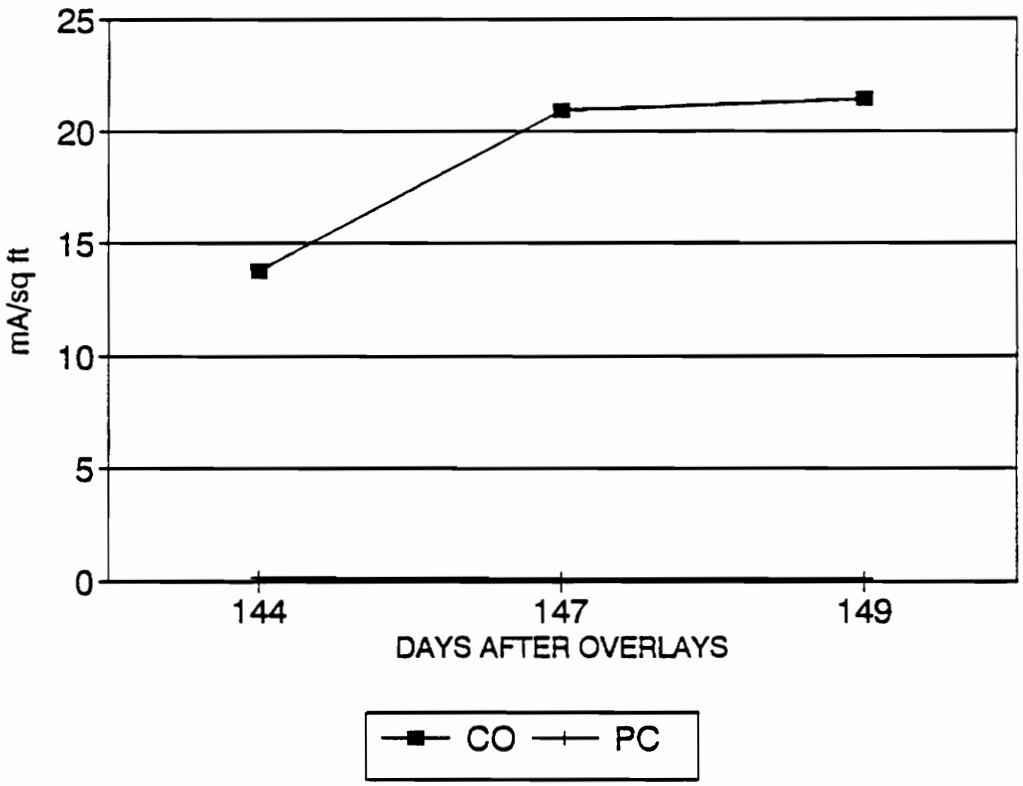

Figure 13C Micro I_{corr} vs Time (1", 230 °F)

Polymer Impregnated Group

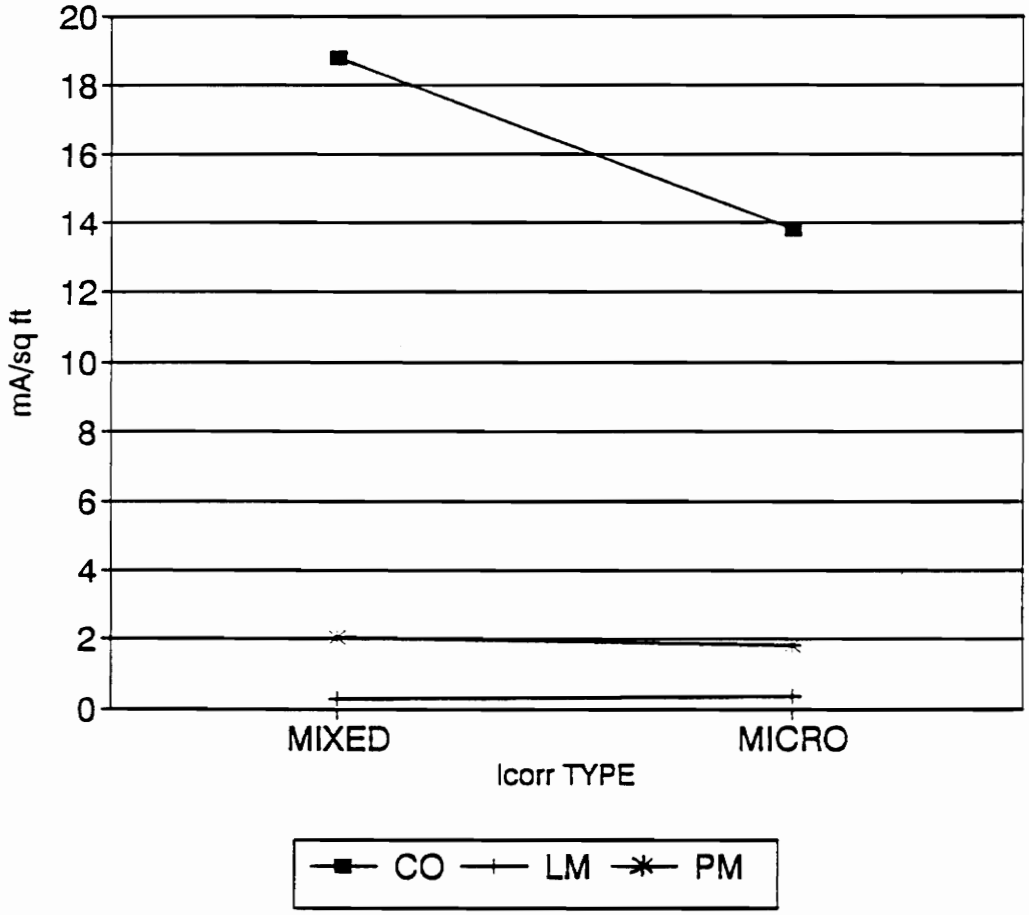

Figure 14A Mixed and Micro I_{corr} (1", 230 °F)

Latex Group

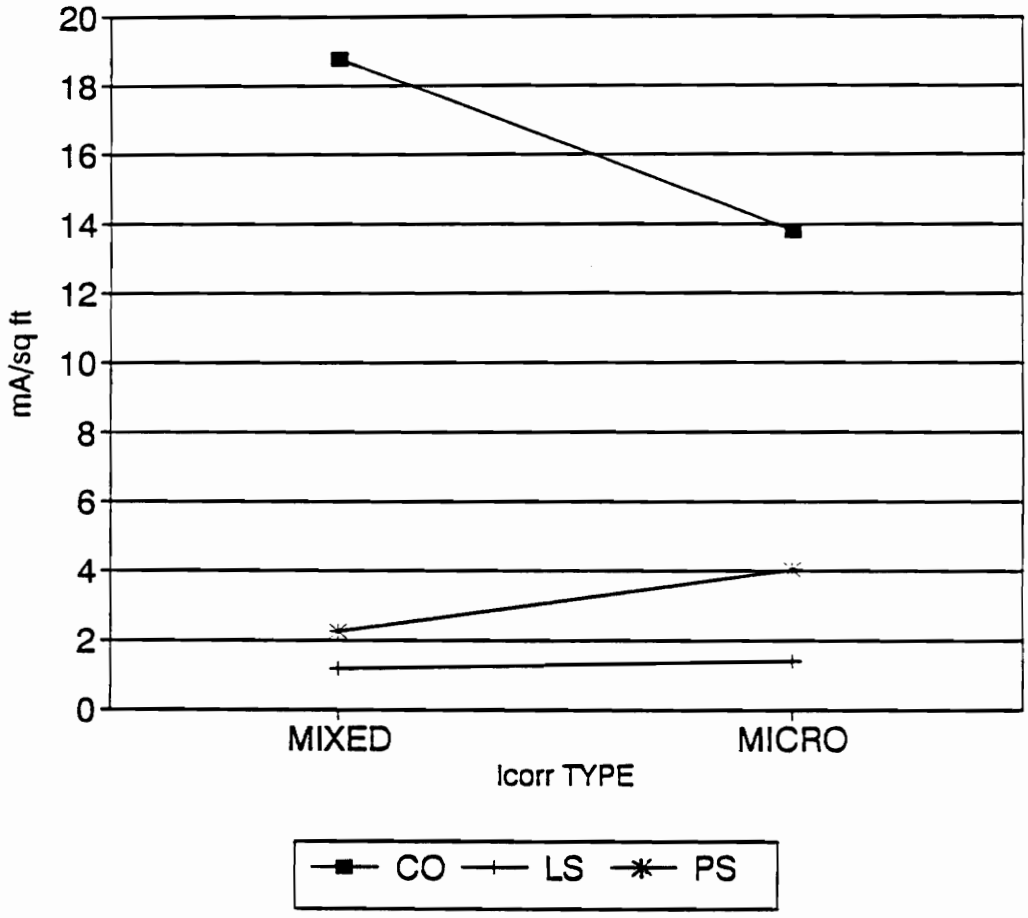

Figure 14B Mixed and Micro I_{corr} (1", 230 °F)

Low Slump Group

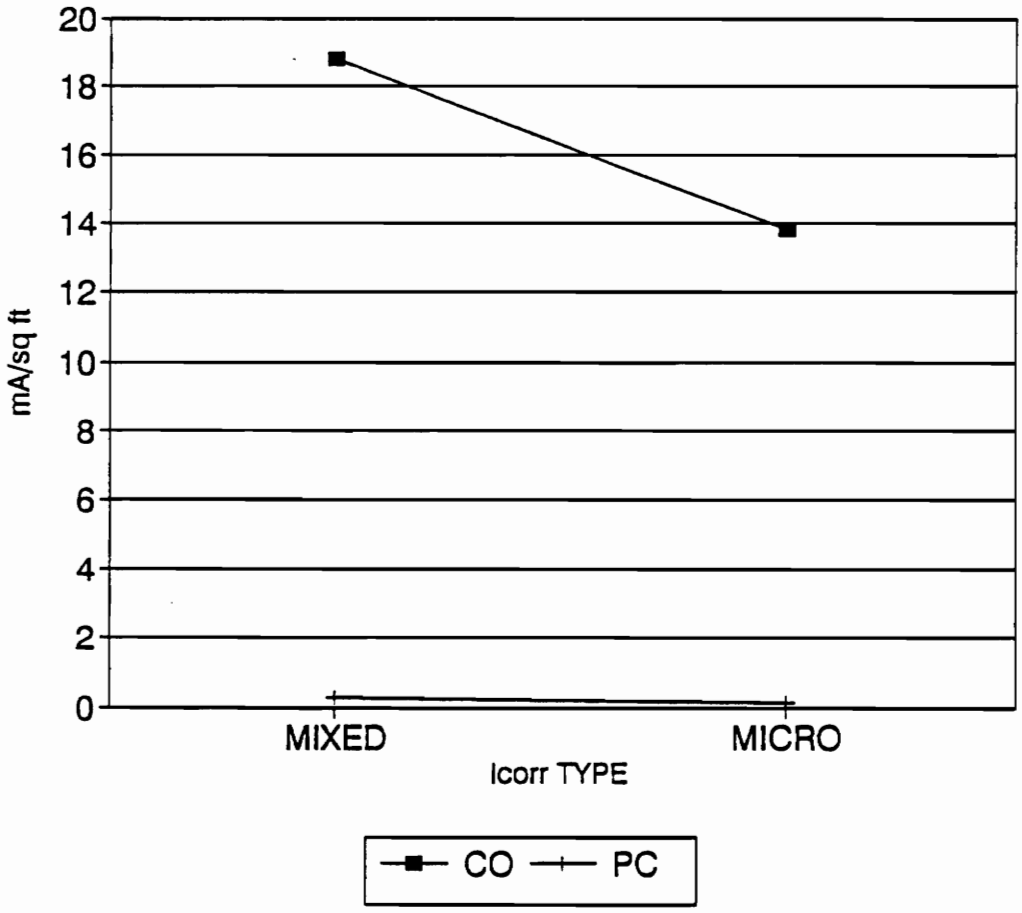

Figure 14C Mixed and Micro I_{corr} (1", 230 °F)

Polymer Impregnated Group

Comparison Between Micro-cell and Macro-cell Corrosion

As shown in figures 15A, 15B and 15C, the differences between the micro-cell corrosion and macro-cell corrosion were more pronounced for all the specimens than their corresponding differences between micro-cell and mixed-cell corrosion. This was expected since a major portion of corrosion current is due to the micro-cell.

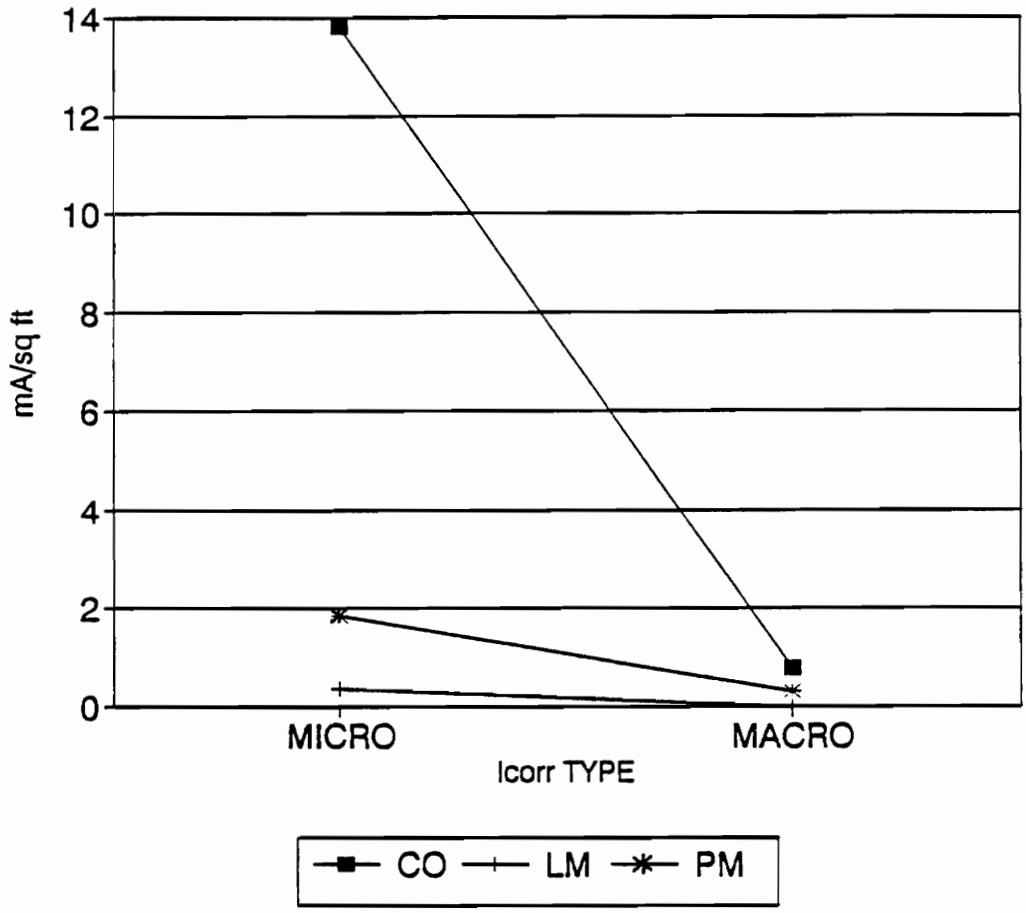

Figure 15A Micro and Macro I_{corr} (1", 230 °F)

Latex Group

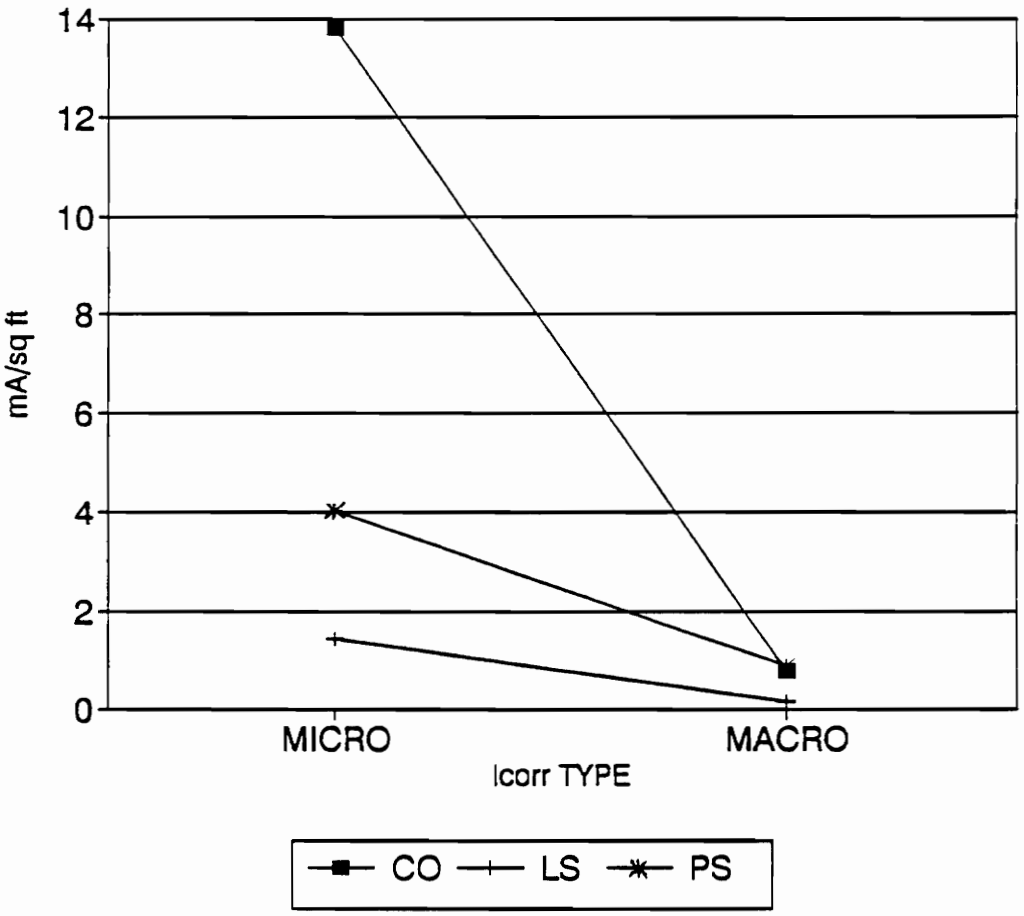

Figure 15B Micro and Macro I_{corr} (1", 230 °F)

Low Slump Group

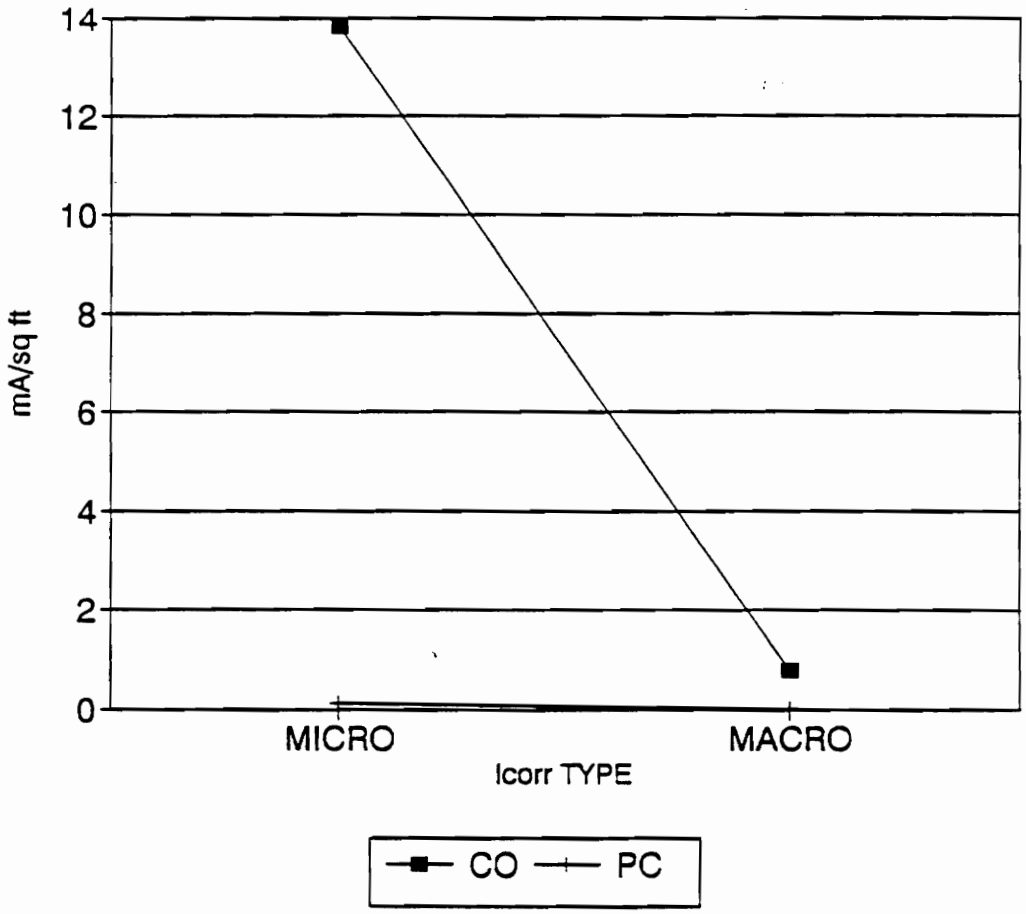

Figure 15C Micro and Macro I_{corr} (1", 230 °F)

Polymer Impregnated Group

5.3 Pre-impregnation Drying of Specimens

Three drying temperatures were used in this study: 150 °F, 180 °F and 230 °F. The drying temperatures refer to the temperature at ½" below the top rebar level at the time the heaters were turned off.

Drying Temperature 230 °F : Cover Depth 3" (2" overlay plus 1" cast)

Of the nine specimens that were dried to this temperature, the polymer impregnated (PC) series without an overlay and thus with a cover depth of only 1" attained the requisite temperature before the other specimens (see Figure 16). To minimize further increase in temperature while the other specimens were being dried to the requisite temperature, the PC specimens were covered with metal sheet. In spite of this, the temperature of the PC series continued to increase
The mean temperature of the LSDC overlay-polymer-impregnation (PS) series five minutes before heaters were shut off was less than 230 °F due to the fact that one of the three PS specimens had an unusually low temperature. It can be safely assumed that at the time the three heaters were shut off, eight of the nine specimens had temperatures close to 230 °F

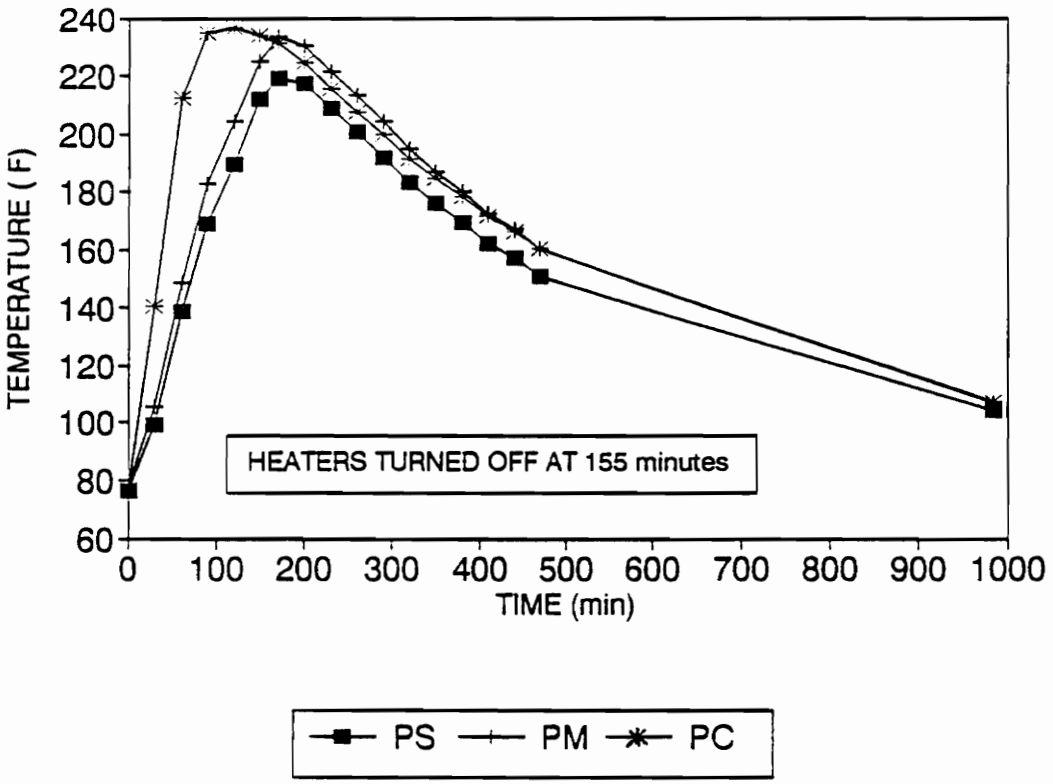

Figure 16 Temperature at ½" Below Top Rebar vs Time

(1", 230 °F)

or above at ½" below the top rebar level. The only specimen (PS2) which may have had a lower temperature could have had a faulty TC or connection which would cause a discrepancy in the temperature readings.

After the heaters were turned off, the internal temperature of most of the overlaid specimens continued to rise. This was not the case for the PC series which did not have an overlay. Concrete being a heat sink, the heat energy from the surface continued to be absorbed by the concrete below thereby increasing the internal temperature for a period of time after the heaters were turned off. Predictably, this phenomenon would be more pronounced with increased concrete depth as shown in Figure 16. After the heaters were turned off, the internal temperatures of the overlaid specimens increased between about 5 °F to 10 °F. The drying time was about 2½ hours.

During the cooling period, the surface and internal temperature approached each other and at about 1000 minutes (from the beginning) the surface and internal temperatures were nearly equal. Concrete retains heat for a long period of time and this was evident from the fact that even after 850 minutes from the time the heaters were turned off (1000 minutes from the beginning) the internal temperature was over 100 °F with an ambient temperature of about 50 °F (see Figure 17).

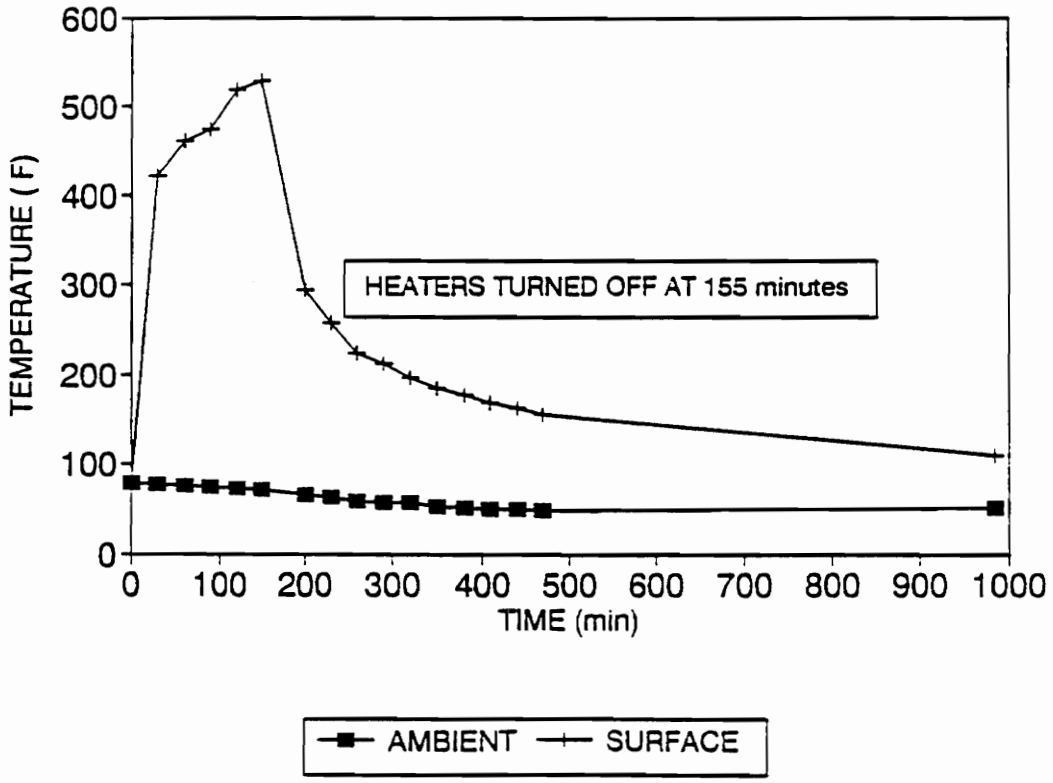

Figure 17 Surface and Ambient Temperature vs Time

(1", 230 °F)

During the heating, the surface temperature reached a maximum of 529 °F (see Figure 17) and then decreased sharply after the heaters were turned off. After which, for a period of about two hours, the rate of cooling was more gradual.

Drying Temperature 150 °F and 180 °F (Cover Depths: ¾" and 2")

Cover depth: 2"

After the heaters were turned off, the temperature increase at ½" below top rebar for the four specimens were between 8 °F and 18 °F (see Figures 18A and 18B). Two of these specimens (PM2 & PC3) were covered with sheet metal before the heaters were turned off. As a result, the temperature rise may have been somewhat less than what would have normally occurred if they were covered with insulation immediately after the heaters were turned off.
The drying time was approximately one hour.

Cover depth: ¾"

Increases in temperature after the heaters were turned off were between 20 °F and 24 °F (see Figures 18C and 18D).
The drying time was about ½ hour.

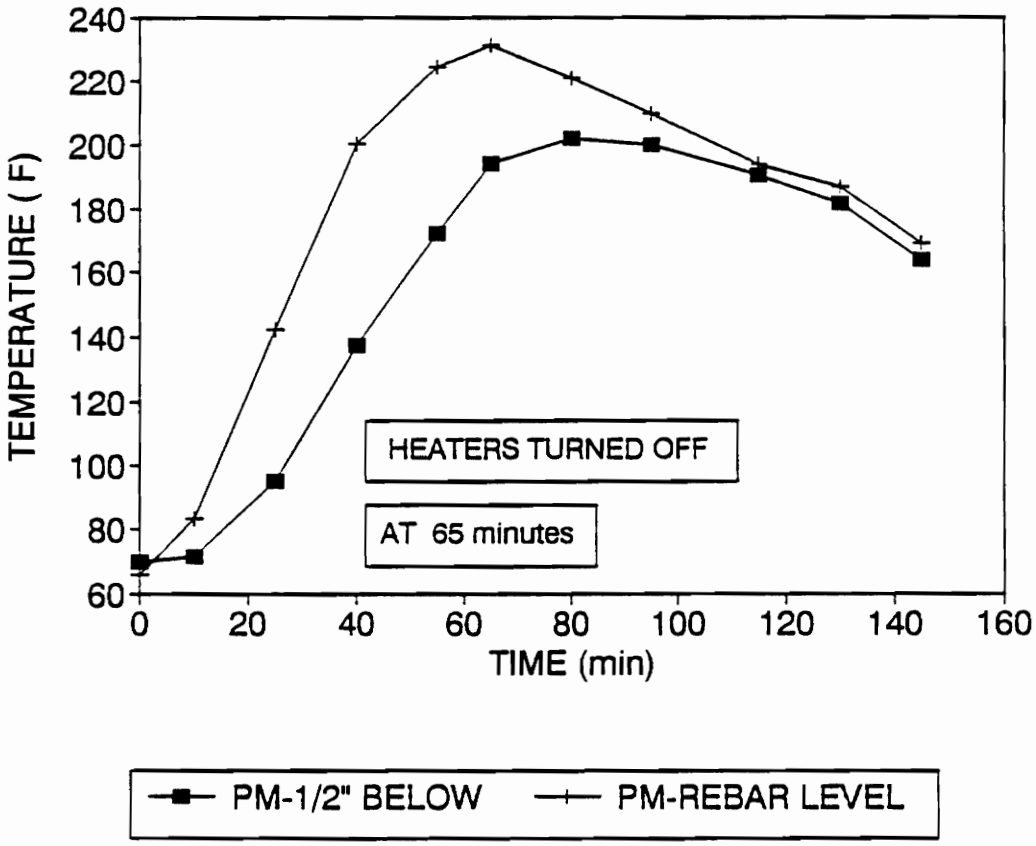

Figure 18A Internal Temperature vs Time (2", 180 °F)

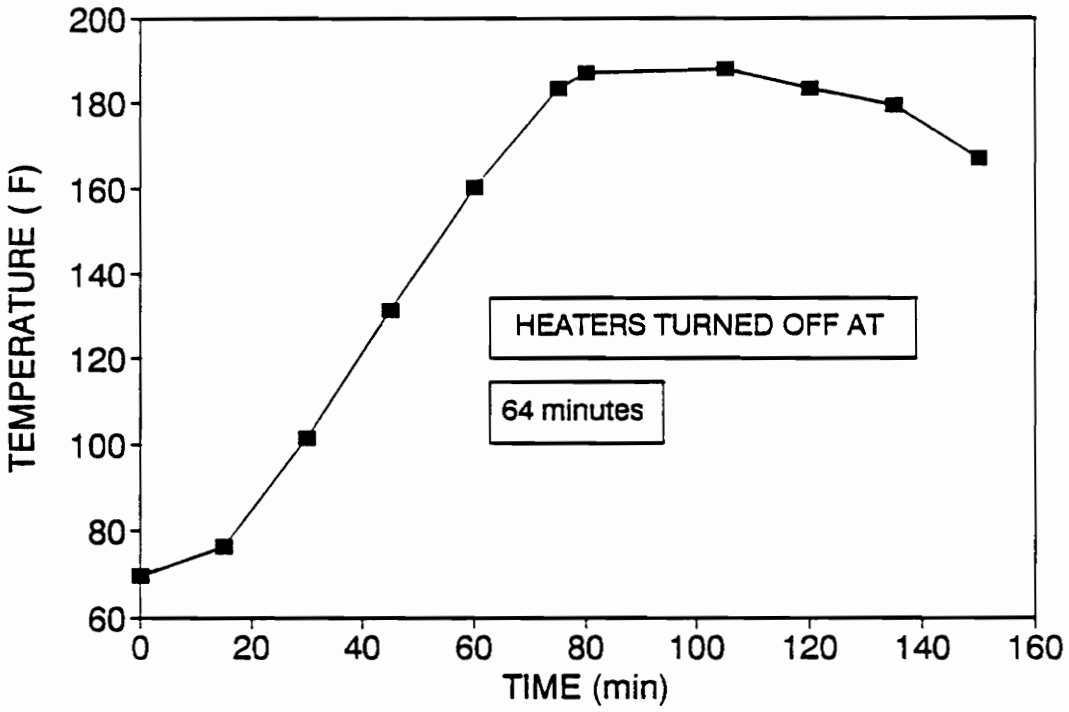

Figure 18B Temperature at ½" Below Top Rebar vs Time

(2", 150 °F)

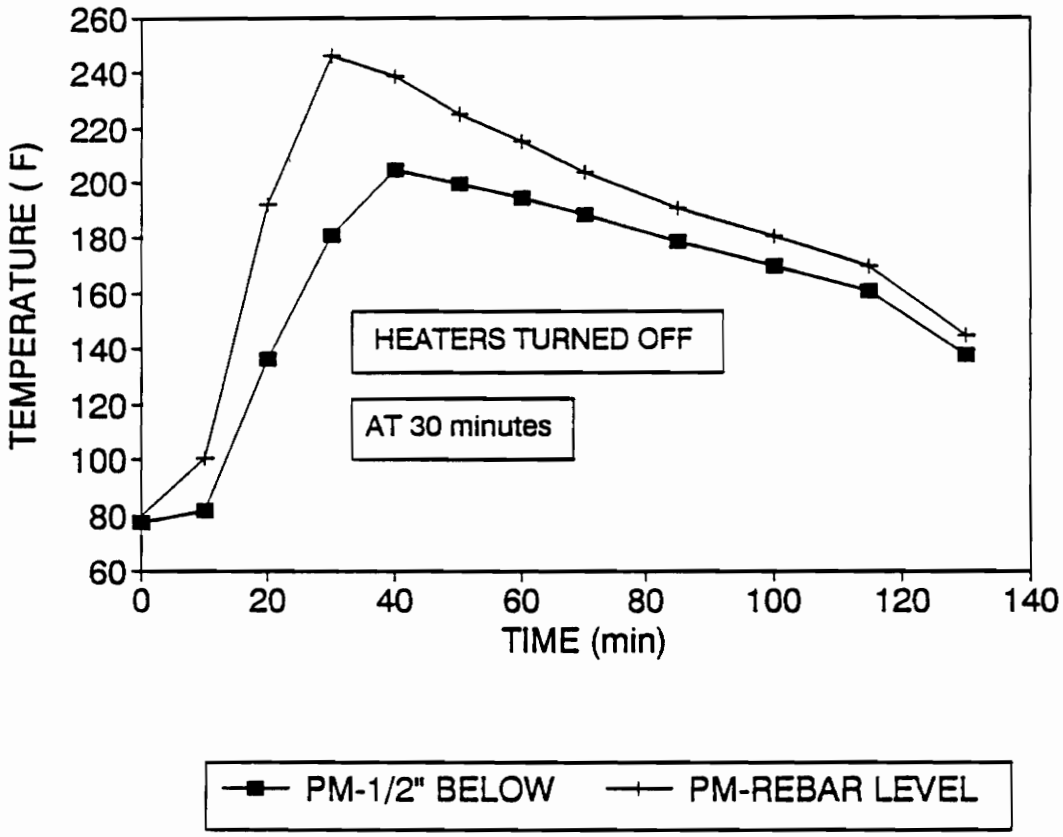

Figure 18C Internal Temperature vs Time (¾", 180 °F)

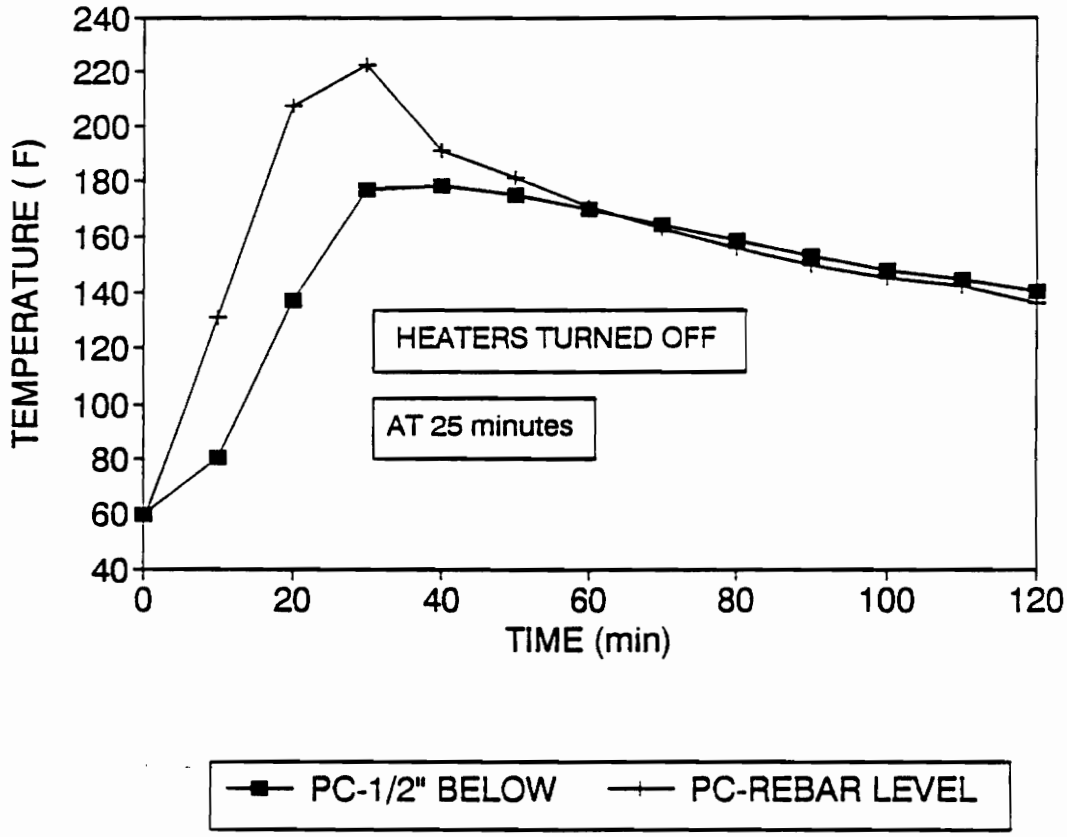

Figure 18D Internal Temperature vs Time (¾", 150 °F)

5.4 Optimization of Drying Temperature

The following analysis is with reference to Table 2.

With the increase in drying temperature, % volume of water lost increased, as more water was driven out of the cubes. At 75 °F, % volume monomer gained was 20 % and the value at 100 °F was 10.5 %. At 125 °F, % volume monomer gained was 8.8 %. At higher drying temperatures, % volume monomer gained increased with increasing drying temperatures up to 400 °F and remained constant afterwards at 10.3 % (see Figure 19). The cubes at 75 °F were visibly cracked after the impregnation stage and the high monomer content was probably due to direct physical entry of some monomer into the cracked cubes rather than entry only by diffusion. Although the cubes at 100 °F were not visibly cracked the anomaly in the monomer content might be due to direct entry of monomer via micro-cracks invisible to the unaided eye.

The difference in volume between water lost and monomer gained increased with drying temperature. Thus, at higher drying temperatures, water accessible voids were not being refilled with monomer. A possible explanation is that, monomer molecules being large organic molecules, were filling voids to a certain limiting size. Voids smaller than this limit could not be filled with the large monomer molecules.

The moisture content values following vacuum saturation of the

Table 2 Results from Impregnated Cubes

DRYING TEMP (F)	VOLUME OF WATER LOST DURING DRYING (%)	VOLUME OF POLYMER GAINED (%)	DIFFERENCE (%)	MOISTURE CONTENT AFTER VACUUM SATURATION (%)
75	-	20.0*	-	-
100	13.2	10.5**	2.7	0.75
125	14.0	8.8	5.2	0.70
150	15.5	9.3	6.2	0.85
175	15.3	9.7	5.6	0.70
200	16.0	9.7	6.3	0.37
225	16.5	9.5	7.0	0.58
250	16.6	9.0	7.6	0.52
300	17.1	10.0	7.1	0.44
400	18.3	10.3	8.0	0.59
500	19.2	10.3	8.9	0.68
600	20.2	10.3	9.9	0.92
CONTROL	-	-	-	2.67

* CUBES FRACTURED DURING IMPREGNATION

** POSSIBLE MICRO CRACKS DURING IMPREGNATION INVISIBLE TO THE UNAIDED EYE

Table 2 Results from Impregnated Cubes (Contd.)

DRYING TEMP (F)	RESISTIVITY BEFORE SALT APPLICATION (1000 ohm-cm)	RESISTIVITY AFTER SALT APPLICATION (1000 ohm-cm)	DIFFERENCE IN RESISTIVITY (1000 ohm-cm)	CHLORIDE CONTENT (lb/cu yd)
75	-	-	-	-
100	406	13.2	392.8	0.61
125	401	12.5	388.5	0.66
150	350	13.2	336.8	0.65
175	654	20.7	633.3	0.65
200	793+	20.5	772.5	0.61
225	490	26.0	464.0	0.62
250	513	16.8	496.2	0.60
300	849	34.3	814.7	0.60
400	487	57.8	429.2	0.55
500	267	35.5	231.5	0.57
600	200	27.3	172.7	0.54
CONTROL	4.8	2.8	2.0	14.38

+ MEAN FROM TWO CUBES; THIRD CUBE HAD VERY HIGH VALUES

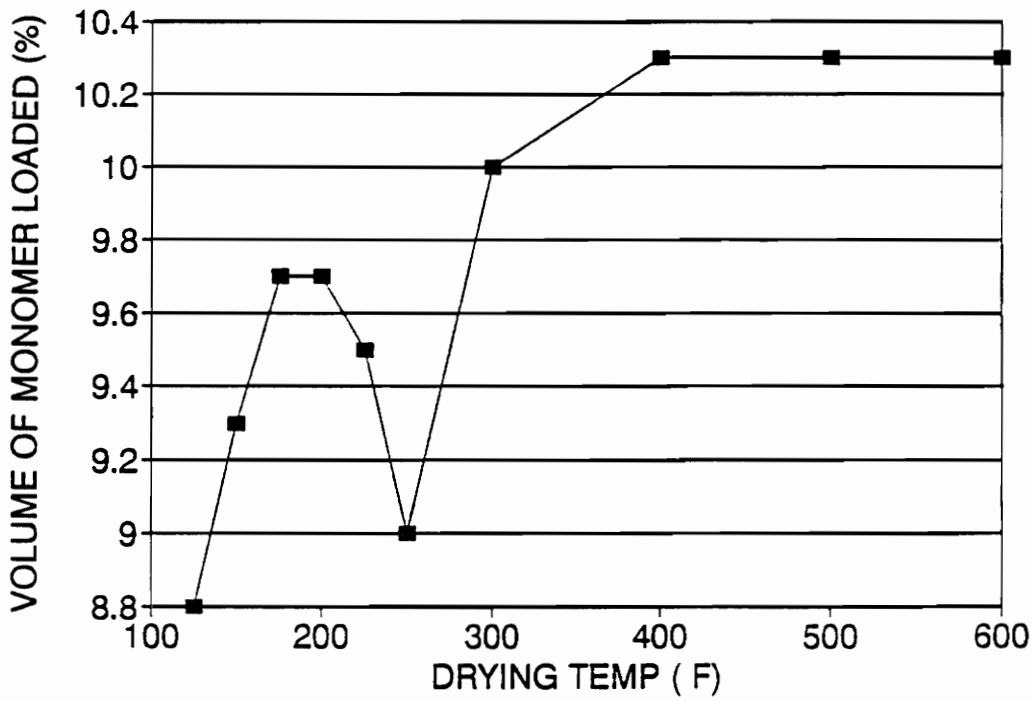

Figure 19 Volume of Monomer Loaded vs Temperature

cubes are presented in Figure 20. The lowest value of moisture content was at 200 °F. After this, the moisture content increased with increasing temperatures. At temperatures below the boiling point of water, the higher moisture contents are the result of water remaining after drying. At higher temperatures, more water could fill the smaller voids which the monomer could not fill. At 200 °F, most of the available void spaces had been filled by the monomer molecules, resulting in the low moisture content. The moisture content of the control cubes (unimpregnated) was much higher (2.67 %) than any of the impregnated cubes. Thus, even at low drying temperatures, some degree of monomer impregnation is possible. With reference to Figure 21, the resistivity values before salt application showed peak values at 200 °F and 300 °F and then decreased at higher temperatures. The lowest resistivity value was 200,000 Ω-cm. Previous studies [23, 24, 25, 26] suggested different resistivity values above which corrosion will not occur. The smallest value is 12,000 Ω-cm [23, 24] while the highest is 60,000 Ω-cm [25]. Thus, even if the most conservative value was to be adopted, it would result in the lowest obtained resistivity value being in the no-corrosion region.

The resistivity values followed a trend which supported the corresponding values of moisture content. Around 200 °F, the moisture content was the lowest and the resistivity was near

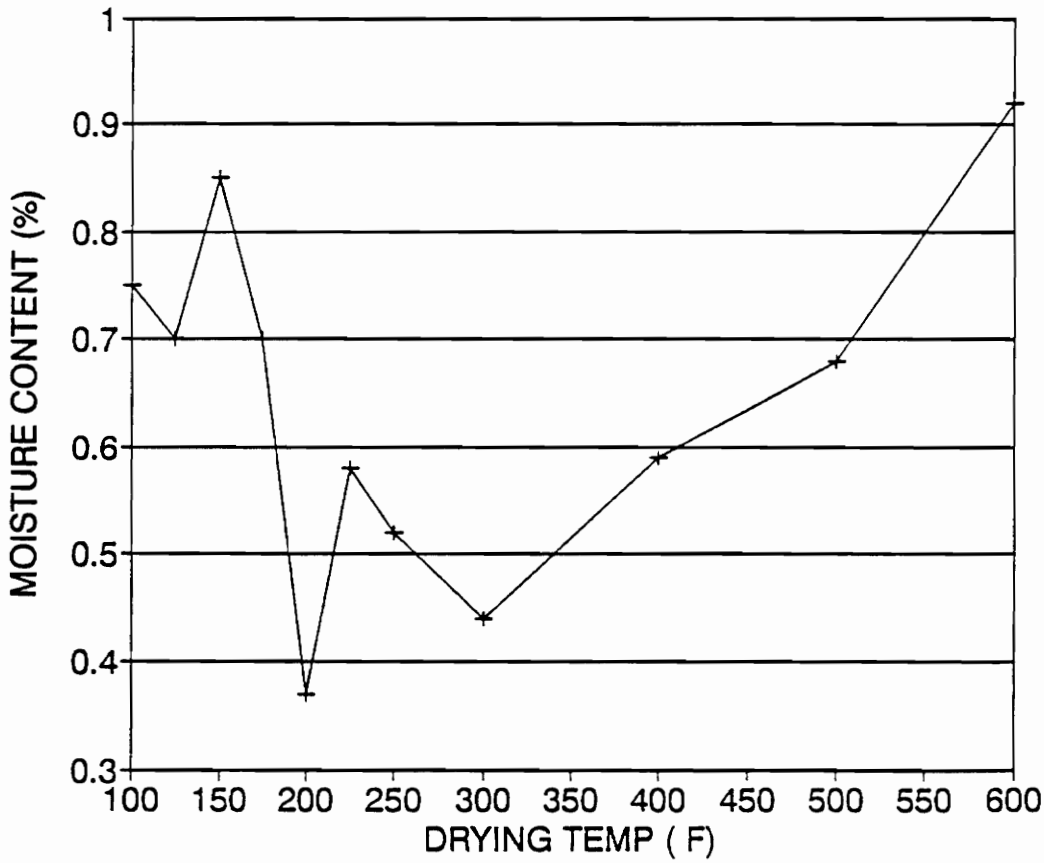

Figure 20 Moisture Content vs Temperature

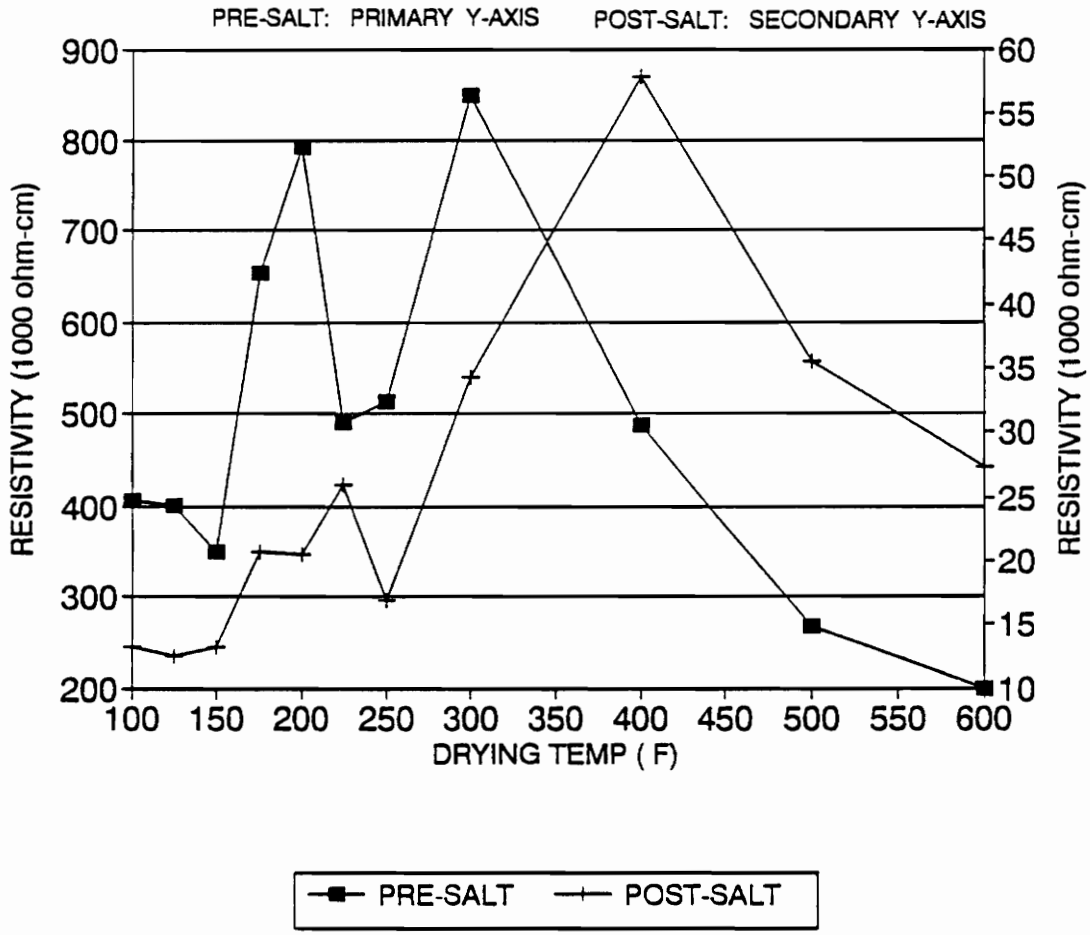

Figure 21 Resistivity vs Temperature

its peak. Since, the ionic pore solution is the conducting agent, the resistivity of concrete increases with decreasing moisture content. Predictably, at 600 °F when the moisture content was high, the resistivity was low.

The resistivity values after salt application were much lower than their pre-salt application values (see Figure 21). The trend of the post-salt application resistivity values was similar to that of the pre-salt application ones, with respect to drying temperatures. Apart from the large shift downwards, there was apparently a slight shift to the right.

The values of the post-salt application resistivity were low due to the Cl^- ions being present in the mortar pore water. The value corresponding to 200 °F was 20,500 Ω-cm which is greater than the lowest suggested no-corrosion value of 12,000 Ω-cm, but less than the highest suggested value of 60,000 Ω-cm. However, the possibility remained that the cubes were not fully surface dry when the post-salt application resistivity values were taken, which could have resulted in lower values than actual.

Acid Etching and Chloride Content of the Cubes

Application of the acid had no discernible effect on the impregnated cubes, as the polymer molecules prevented the dissolving of cementitious particles. However, in the non-impregnated cubes the cement portion was attacked by the acid. For a more visual demonstration of this phenomenon, both impregnated and unimpregnated cubes were colored with a permanent marker and then etched with the acid. In the impregnated cubes, almost all the color remained while for the non-impregnated cubes the color started to fade after repeated applications of the acid.

The relationship between chloride content and drying temperature (see Figure 22) indicated that with higher drying temperatures there was a lowering of the chloride content as higher volume of the polymer resisted the Cl^- ingress into the cubes. The maximum value at a drying temperature of 125 °F was 0.66 lb/yd^3.

For the control cubes, the chloride content was much higher (14.38 lb/yd^3) than in the impregnated cubes. With the absence of polymer molecules, the chloride ions readily diffused into the mortar cubes.

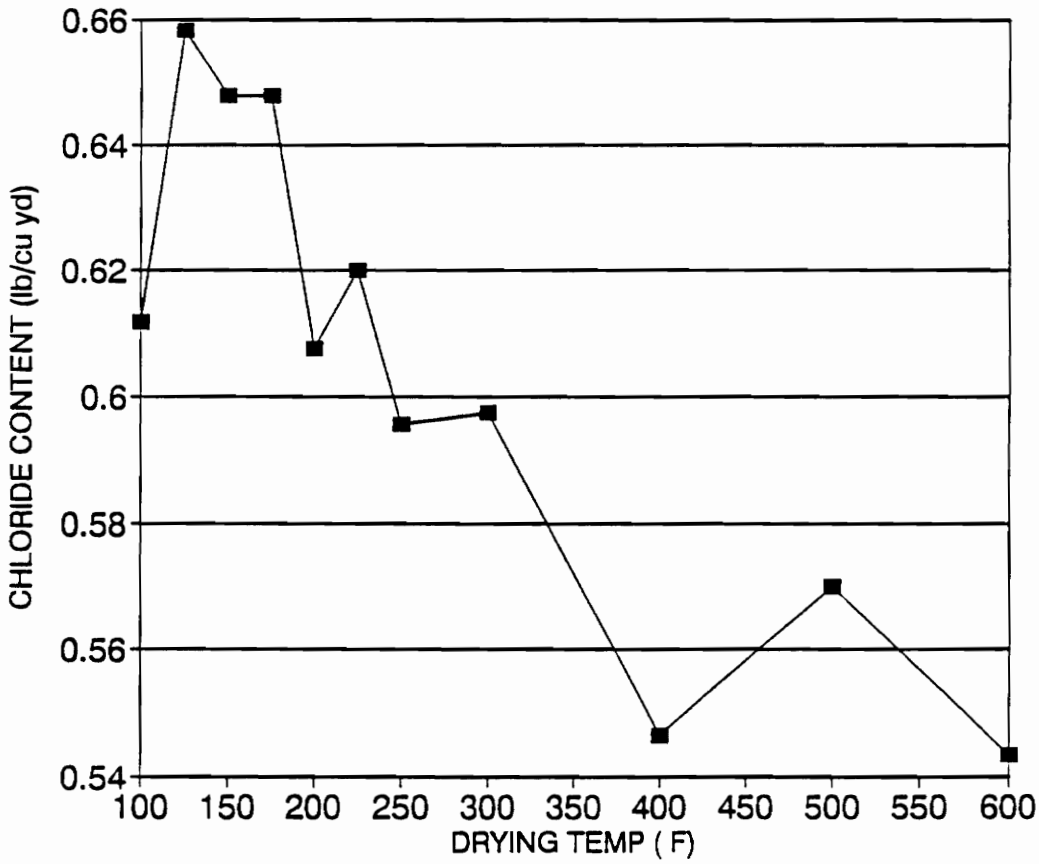

Figure 22 Chloride Content vs Temperature

Results from Mercury Porosimeter Test

The following analysis is with reference to Table 3.

The total intrusion volume was the volume of mercury which could be forced into the samples per gram of the sample weight under the maximum pressure of about 50,000 psi.

At lower drying temperatures, this volume was high, as fewer voids were filled with polymer (see Figure 23). As a reminder, prior to the test, the cubes were dried at 220 °F. At pre-impregnation drying temperatures of 200 °F and 225 °F, there were abrupt decrements in the total intrusion volume. Thus, it appears that most of the available voids at these temperatures were filled with polymer. At higher temperatures the total intrusion volume increased. More void spaces were present which were too small for the polymer molecules to occupy. As expected, the control cubes had more intrusion volume (0.0606 cc/g) than any of the impregnated cubes excepting for the cubes dried to 175 °F. (This aberration might be due to experimental error).

The above conclusion was further supported by the total pore area of the cubes at different temperatures. At lower temperatures, the total pore area was high; at 200 °F and 225 °F the total pore area was the least and at higher drying temperatures the total pore area increased (see Figure 23). The total pore area of the control cubes was higher than any

Table 3 Data from Porosimeter Test

DRYING TEMP (F)	TL INTRUSION VOLUME (cc/g)	TOTAL PORE AREA (sq m/g)	AVERAGE PORE DIA (micrometers)	% CAPILLARY
100	0.0518	5.2038	0.0398	7.5823
125	0.0435	5.7887	0.0300	7.0170
150	0.0520	6.0464	0.0344	7.7263
175	0.0693	7.1469	0.0388	9.2071
200	0.0080	1.0022	0.0319	0.9541
225	0.0042	0.2114	0.0795	0.9501
250	0.0185	1.0314	0.0716	2.9150
300	0.0544	5.8839	0.0370	6.7780
400	0.0426	5.7121	0.0298	6.4912
500	0.0419	6.1251	0.0273	7.0573
600	0.0367	5.3034	0.0277	5.1400
CONTROL	0.0606	7.9242	0.0306	7.0250

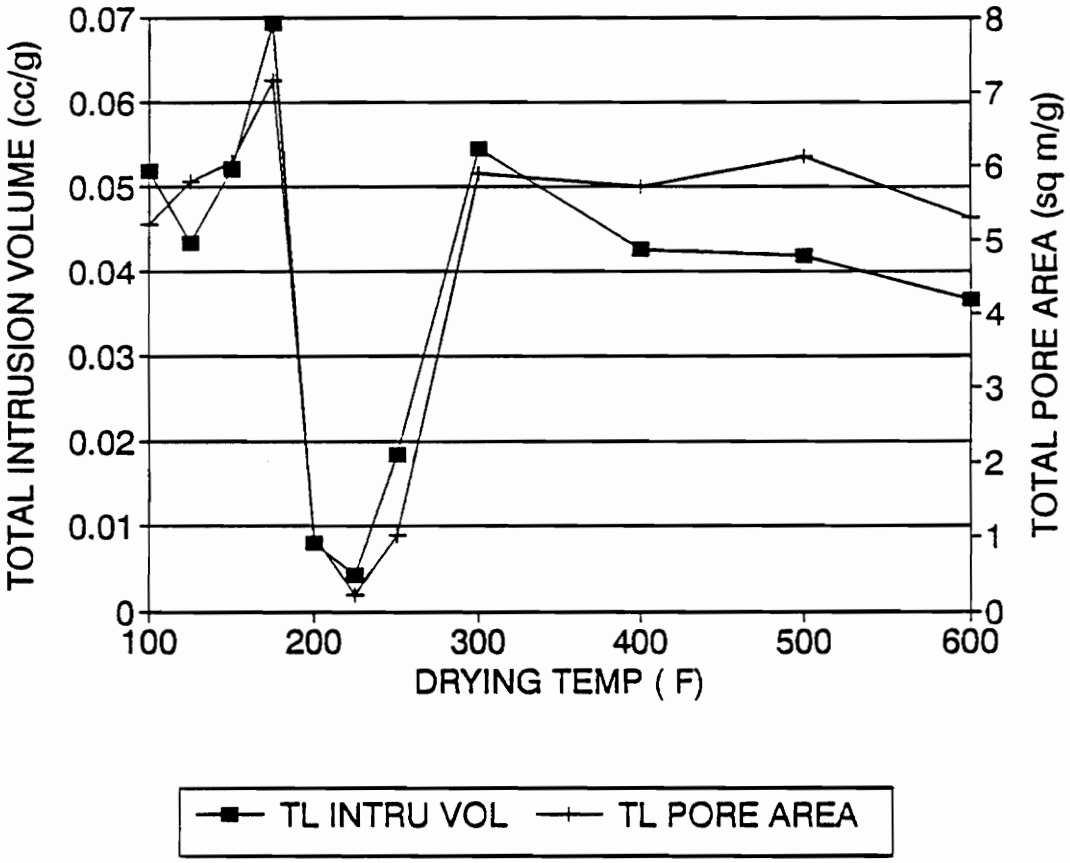

Figure 23 Intrusion Volume & Pore Area vs Temperature

of the impregnated cubes (see Table 3).

The average pore diameter showed a decrease at temperatures over 250 °F. This indicated that in spite of larger total pore area at higher temperatures, the average pore diameter of accessible pores is smaller. This supports the hypothesis of selective filling up of pores by the monomer. The high value of average pore diameter at 225 °F and 250 °F may be due to the ink-well effect.

The % capillary results further supported the hypothesis regarding the nature of monomer impregnation at different drying temperatures. The lowest % capillaries were at 200 °F and 225 °F where the monomer molecules had filled most of the available pore spaces.

Results from the Scanning Electron Microscope-Energy Dispersive X-Ray Spectroscope System (SEM-EDS)

The following analysis is with reference to Table 4.

The SEM identifies the elements in the sample and their relative quantities. Since little conclusion could be drawn from the absolute values of the amounts of each element identified, the ratios of carbon to other elements were calculated. Carbon does not normally occur in regular concrete. Carbon is a major component of the polymer. On the other hand, calcium (Ca) occurs only in the cement and not in the polymer. The values of C/Ca had abrupt increases at 225 °F and 250 °F indicating the presence of larger quantities of polymer (see Figure 24). The C/O had no pronounced trends over temperature probably due to the fact that oxygen is present both in the cement and the monomer. The absolute quantity of silicon (Si) at 225 °F was very low. This might be due to there being little cementitious particles or it being masked by the polymer in the spot the SEM scanned. This would explain the abnormally high value of C/Si at this temperature.

Although the SEM results could be interpreted as supporting previous conclusions, very definite inferences should not be drawn from this test due to the following reasons:

1. The SEM scans a small area of the sample. As the sample is non-homogeneous, the relative ratios of elements in one spot

might be a biased representation of the sample as a whole.

2. The SEM scans only the surface and certain elements which might be present in significant quantities below the surface would not be represented in the results.

Table 4 Data from SEM-EDS Test

DRYING TEMP (F)	C/O	C/Ca	C/Si
100	0.4210	0.0413	0.0282
125	0.5709	0.0256	0.0219
150	0.4853	0.0118	0.0283
175	0.2072	0.0136	0.0127
200	0.5116	0.0199	0.0148
225	0.4081	0.2584	10.2799
250	1.7015	0.2327	0.0309
300	0.0351	0.0344	0.0015
400	0.1077	0.0257	0.0033
500	0.2538	0.1393	0.0074
600	1.1697	0.0456	0.1427
CONTROL	0.0195	0.0034	0.0066

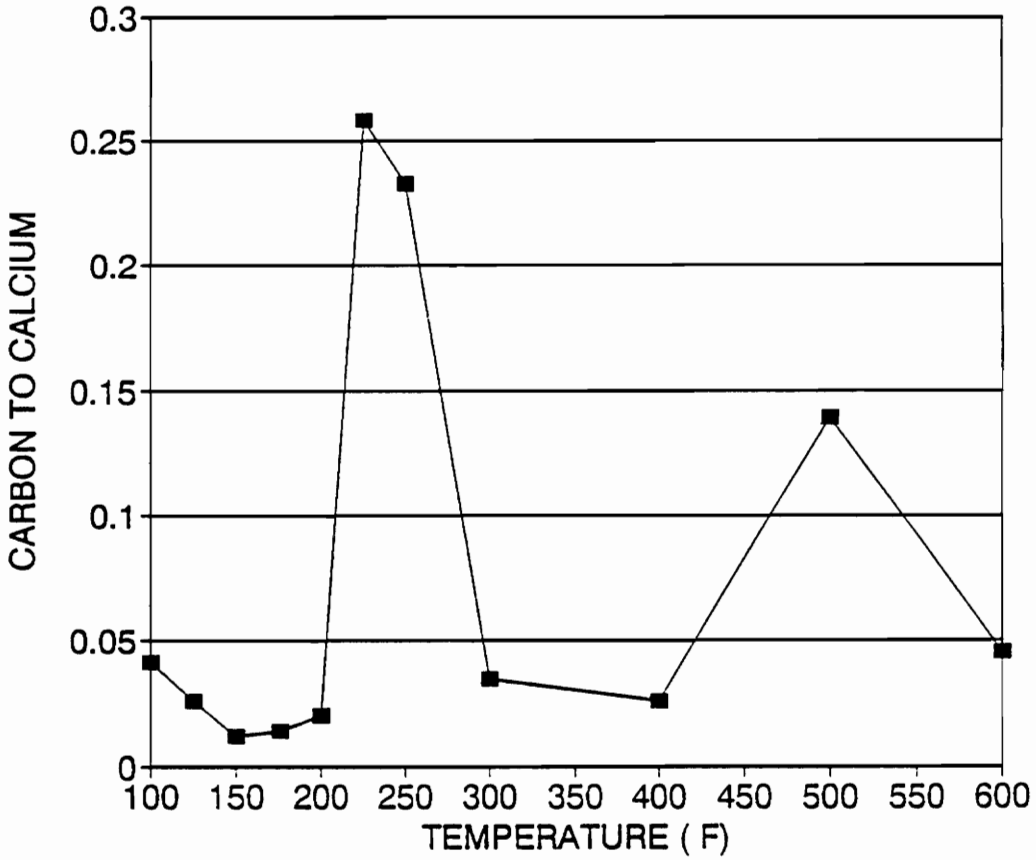

Figure 24 Carbon/Calcium vs Temperature

5.5 Comparison of Corrosion Activity of Specimens Dried at Different Temperatures

As stated before, laboratory specimens were dried to three different drying temperatures before polymer impregnation: 150 °F, 180 °F and 230 °F. The corrosion current data from this study was organized into two groups for more lucid presentation. In the first group, the 1" cover depth impregnated specimens dried at 230 °F were compared with the ¾" cover depth specimens dried to the lower drying temperatures. In the second group the same 1" cover depth specimens were compared to the 2" cover depth specimens dried at the lower temperatures.

First Group

At the time of impregnation, the ¾" cover depth specimens had very high rates of corrosion (see Figure 25). One of the specimens (PC3) had a visible crack running on the surface vertically over the left rebar. PC2 had corrosion products on the top but did not have any visible cracks. There were other specimens with the same cover depth (which were not treated) that had visible signs of active corrosion. It is likely that, at that point in time, most if not all of the ¾" cover depth

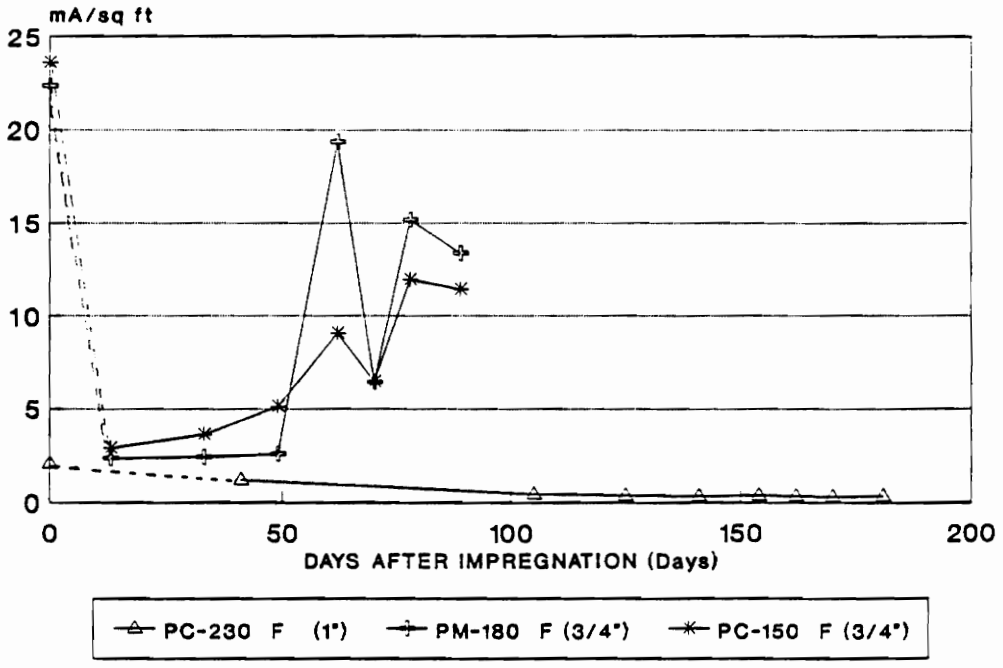

Figure 25 Post-Treatment Mean I_{corr}

(1", ¾"; 150 °F, 180 °F, 230 °F)

specimens had some structural damage due to high corrosion rates even though they were not visible in all specimens. After impregnation, the corrosion rates in all the specimens decreased. However, after a period of time, the corrosion rates in the ¾" cover depth specimens started to rise. Even then, at day 89 after impregnation the " % change" was still positive (see Figure 26). After drying and subsequent impregnation, cracking above the rebar was visually evident in these specimens. Most displayed hair line cracks. The cracks were responsible for allowing large quantities of chloride ions to enter the impregnated specimens resulting in some corrosion despite the presence of polymer in the concrete. The unusually low value of "% change" for the PM specimens dried to 180 °F at day 62 might be due to experimental error (see Figure 26).

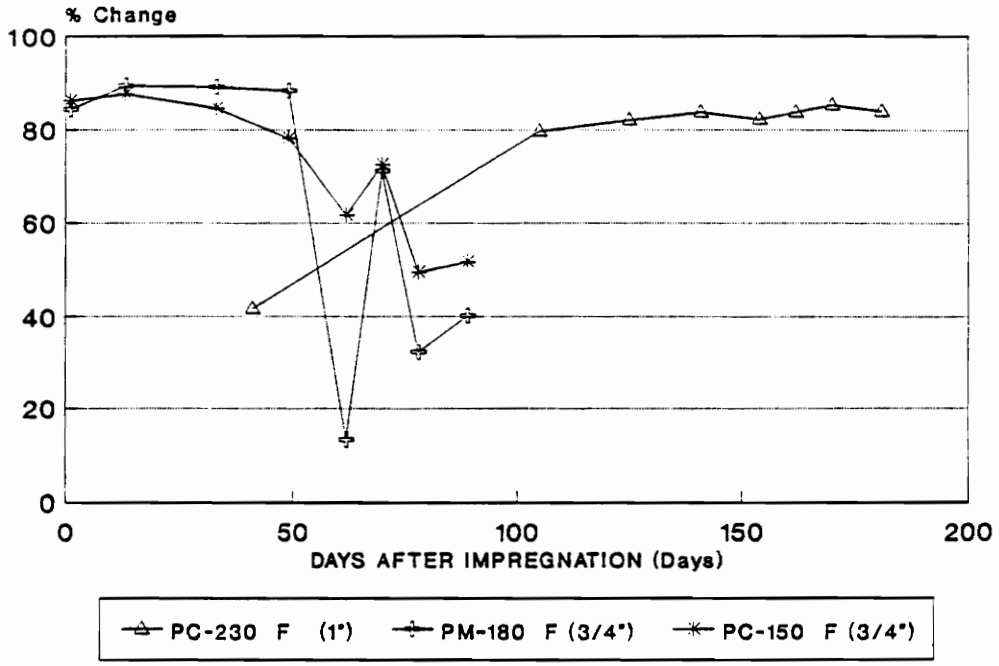

Figure 26 Percent Change in Mean I_{corr}

(1", ¾"; 150 °F, 180 °F, 230 °F)

Second Group

At the time of impregnation, the mean corrosion rates in the 2" cover depth specimens were very low and not in the active corrosion region (see Table 5). The corrosion current at day 89 after impregnation for these specimens were actually higher than their pre-impregnation values. However, the corrosion current was still low and not in the active corrosion region. Definite conclusions regarding these specimens could not be reached. The corrosion rates of these specimens need to be monitored for an extended period to observe the nature of changes, if any.

Table 5 Mean I_{corr} (1", 2"; 150 °F, 180 °F, 230 °F) (mA/sq ft)

SPECIMEN	DRYING TEMP (F)	COVER DEPTH (")	LAST PRE-TREATMENT	AFTER IMPREGNATION DAY 1	DAY 13	DAY 33	DAY 41
PC	230	1	2.0664				1.2040
PM	180	2	0.5800	0.9203	1.9020	1.7082	
PC	150	2	0.9058	1.2682	2.6342	1.9678	

SPECIMEN	DRYING TEMP (F)	COVER DEPTH (")	AFTER IMPREGNATION DAY 49	DAY 62	DAY 70	DAY 78	DAY 89
PC	230	1					
PM	180	2	1.8375	2.8790	1.4879	1.5358	2.2069
PC	150	2	2.2730	2.6421	1.6429	1.5994	2.4018

Table 5 Mean I_{corr} (1", 2"; 150 °F, 180 °F, 230 °F) (mA/sq ft)

(Contd.)

SPECIMEN	DRYING TEMP (F)	COVER DEPTH (")	AFTER IMPREGNATION DAY 105	DAY 125	DAY 141
PC	230	1	0.4195	0.3690	0.3352
PM	180	2			
PC	150	2			

SPECIMEN	DRYING TEMP (F)	COVER DEPTH (")	AFTER IMPREGNATION DAY 154	DAY 162	DAY 170	DAY 181
PC	230	1	0.3671	0.3347	0.3050	0.3300
PM	180	2				
PC	150	2				

6.0 FINDINGS AND CONCLUSIONS

6.1 Findings

1. The Cu-$CuSO_4$ Half-Cell proved to be an unreliable instrument after active corrosion cells had been successfully abated by the various treatment methods.
2. The three-electrode linear polarization device (3LP) manufactured by Kenneth C. Clear, Inc. was sensitive to ambient temperature.
3. It was confirmed that the major portion of the corrosion cell is micro-cell in nature.
4. Reducing concrete drying temperature from 230 °F to 180 °F resulted in drying time reduction by a factor of 2.5.
5. Concrete with structural damage impairs the effectiveness of polymer impregnation as a corrosion abatement technique.
6. Polymer molecules, being large organic molecules fill voids in concrete selectively and there exists a lower limit of void size which can be filled by the monomer.
7. Polymer impregnation of mortar cubes provided good resistance against the ingress of chloride ions.

6.2 Conclusions

1. There was little difference in the effectiveness of the five treatment methods used in this study. However, there remained a possibility that treatments involving low slump dense concrete overlay might be less effective as a corrosion abatement technique.
2. For low corrosion rates of treated specimens, the cathode to anode area in the corrosion cell have little influence on the corrosion activity.
3. Pre-impregnation drying temperatures can be lowered to 180 °F at ½" below top rebar level at the time heaters are turned off. Due to the thermal gradient, the temperature at that depth would continue to rise to about 200 °F. The study on the mortar cubes yielded the conclusion that optimum impregnation is achieved at a drying temperature of about 200 °F.

7.0 RECOMMENDATIONS FOR FUTURE RESEARCH

The following are suggested areas for future studies. Some of the recommendations stemmed from this research while others were studies which could not be accommodated within the scope of this project.

If a modified version of the 3LP device incorporating temperature correction is not available in the market in the near future, an experimental study could perhaps be undertaken to develop an empirical temperature correction factor such that all 3LP data taken at different temperatures could be transformed to a base temperature. This would expand the use of the 3LP device to all weather conditions.

A study on operator variability in the 3LP device could easily be undertaken. Several operators would take readings with the same instrument on the same specimens. The differences in instrument readings would be tested for statistical significance.

The exact cause of the failure of the Cu-$CuSO_4$ half-cell to interpret corrosion rates after corrosion activity is stopped should be investigated. This may lead to suitable modifications so that the half-cell would be a more useful tool.

Long term studies should be performed to investigate the

nature of corrosion activities long after treatment methods had been applied. This would lead to the development of life-cycle models for different bridge deck rehabilitation techniques covered in the present study.

Other practical factors could be added to the study of effectiveness of the treatment methods used in this study. Two suggested factors are the influence of traffic volume and major classes of vehicle loadings on the bridge decks.

APPENDIX A

DESIGN PARAMETERS

Table A1 Mix Design - Specimens

Quantities per batch of specimens (SSD) in lb

Cement:	42.64
Water:	16.96
Coarse aggregate:	72.54
Fine aggregate:	109.54

BATCH #	SLUMP (")	AIR (%)	TEMP (F)
1	2 1/4	6 3/4	59
2	1 3/4	6 1/2	58
3	3 1/4	8 1/2	56
4	2 1/2	7 1/2	57

Table A2 Compressive Strength - Specimens (psi)

BATCH #	7 DAY	28 DAY
1	2390	4850
2	4697	5917
3	3827	5556
4	3800	5376

Table A3 Mix Design - Overlays

Quantities are in lb (OD)

	LSDC	LMC
Cement:	54.43	43.56
Water:	19.29	7.96
Latex:	-	13.77
Coarse aggregate:	87.70	86.70
Fine aggregate:	87.96	97.07
AEA (Microair):	11.40 ml	-
Total:	249.38	249.06
Slump:	0.25"	5.5" (after 5 min)
Air:	6.5 %	4 %
Bonding agent:	Cement paste	Latex paste

Table A4 Compressive Strength - Overlays (psi)

Overlay	7 DAY	14 DAY
LMC	6068	6700
LSDC	5988	6562

Table A5 Mix Design - Latex Modified Mortar

Cement:	33.42 lb
Sand:	96.92 lb
Water:	7.17 lb
Latex:	1.25 gal

Table A6 Mix Design - Mortar Cubes

Quantities for six cubes in g

Portland cement (Type I):	500
Water (w/c=0.47):	235
Sand:	1380

Table A7 Compressive Strength of Air Dried Mortar Cubes (psi)

Cube #	Strength
1A	5125
1B	4625
1C	3625

Table A8 Properties of Materials Used in the Specimens

(A) Coarse Aggregates

Unit weight:	96.5 lb/cu ft
Voids in dry rodded aggregate:	44.18 %
Bulk Specific Gravity (Dry):	2.77 g/cc
Bulk Specific Gravity (SSD):	2.78 g/cc
Apparent Specific Gravity:	2.81 g/cc
Absorption:	0.57 %

(B) Fine Aggregates

Bulk Specific Gravity (Dry):	2.61 g/cc
Bulk Specific Gravity (SSD):	2.66 g/cc
Apparent Specific Gravity:	2.66 g/cc
Absorption:	0.36 %
Fineness Modulus:	3.39

Table A9 Properties of # 7 Stone Used as CA in the Overlays

Unit Weight:	95.22 lb/cu ft
Voids in dry rodded aggregate:	43.06 %
Bulk Specific Gravity (Dry):	2.68 g/cc
Bulk Specific Gravity (SSD):	2.71 g/cc
Apparent Specific Gravity:	2.77 g/cc
Absorption:	1.26 %

APPENDIX B

INSTRUMENT USE

(1) Copper-Copper Sulfate Half-Cell

The half cell was used in accordance with the American Society for Testing and Materials Standard C-876-87 [16].

The main components in this test are a Copper-Copper Sulfate Half-Cell, two lengths of cables with alligator clips at one end, a voltmeter, pieces of sponge and wetting agent. The wetting agent used was common soap solution.

The cable connected to the positive terminal of the voltmeter was hooked to the anode. The negative terminal was attached to the half-cell. The voltmeter was adjusted such that it read millivolts.

Three readings were taken per anode. Thus, a total of six readings were taken for each specimen. The sponge pieces were so cut that they were only a little bigger in size than the half-cell cross section area. The sponge were moistened with the wetting agent and placed on the concrete surface directly over the anode. The three positions were the front, middle and rear. The wetting of the concrete was for ensuring good conductivity in the electrical circuit formed by placing the half-cell on top of the wet sponge. The voltage readings were taken after the display had stabilized within a few millivolts. Normally this occurred within three minutes of placing the half-cell on the sponge.

In taking half-cell readings as in the 3LP measurements, the

concrete was kept sufficiently wet throughout the length of the measurement were taken.

(B) The Three Electrode Linear Polarization Device

The 3LP device (Model 3LP NBSI) is manufactured by Kenneth C. Clear, Inc. The three electrodes are the corroding rebar (anode), the counter electrode through which the counter-potential is applied and a standard Cu-$CuSO_4$ half-cell.
The instrument imposes a known value of potential in a direction contrary to that of the current in the corrosion cell thereby polarizing the normal cell. The corresponding value of the current is noted. This operation is repeated for four values of potential. The counter potential used were 0, 4, 8 and 12 mV. The corresponding values of current (I_{appl}) were recorded in mA.
The Stern-Geary equation was employed which is:

$$I_{corr} = I_{appl} \ (\beta_a \times \beta_c)/\{2.3 \ \Delta\phi \ (\beta_a + \beta_c)\} \qquad (4)$$

where,

I_{corr} = corrosion current in mA,

I_{appl} = current corresponding to the counter potential in mA,

$\Delta\phi$ = the counter potential in mV,

β_a = anodic tafel slope = 150 mV/decade, and

β_c = cathodic tafel slope = 250 mV/decade.

The values of the tafel slopes given above were obtained from a large number of experimental data and were provided in the 3LP manual [17].

The corrosion current in mA/sq ft is given by the following relation:

$$I_{corr} = 14953.95 \times S/(K.B) \qquad (5)$$

where,

I_{corr} = corrosion current in mA/sq ft,

$S = I_{appl}/\Delta\phi$, obtained from above,

K = corroding bar length in inches, and

B = bar number, as per ASTM specifications A-615.

In this study, K was 6.5" and B was 4.

In practice, the I_{corr} values in mA/sq ft were computed using an IBM-PC compatible software which is supplied with the 3LP package. The current values corresponding to the four imposed potential values and values of K and B were the input parameters.

(C) The Specific Ion Probe

The ion probe manufactured by James Instruments, Inc. [18] was used to obtain the chloride contents of selected specimens before treatments as well as for the mortar cubes.

The manufacturers provided three standard solutions marked 1, 2 and 3 of known chloride concentrations of 0.005 %, 0.05 % and 0.5 %, respectively. Before testing the powdered concrete samples (extraction procedure is described shortly), the probe had to be calibrated against the standard solutions. The meter was turned on and set in the "volt" mode. The meter displayed readings in mV. The probe was inserted in standard solution 1 and the meter reading was noted after a period of three minutes in which time the display had been allowed to stabilize. Similarly, the mV readings corresponding to solutions 2 and 3 were obtained.

James Instruments, Inc. recommends the use of a semi-log graph paper and plotting the mV readings against % Cl^- in order to get the calibration relation. In this study, however, a simple linear regression was run to obtain the calibration equation connecting mV with % Cl^-.

The calibration had to be performed each time the meter was turned on.

After the calibration was done, each sample was tested in the following manner.

3 g of sample - weighed in a triple beam balance - was introduced into a fixed volume of "chloride extraction solution" provided with the ion probe package and shaken vigorously for 15 seconds with the cap fixed tight. The probe was then immersed in it and the mV reading was taken after a period of three minutes. The reaction temperature was also recorded by inserting a TC wire into the solution of the extraction liquid and sample at the time the probe had been immersed in it.

The mV reading was substituted in the calibration equation to obtain the corresponding value of % Cl^-. Corrections for temperature and standardization to the standard potentiometric titration method (AASHTO T-260-78) were done. Finally, the chloride content in % Cl^- was converted to Cl^- in lb of chloride per cubic yard of concrete.

The extraction equipment consisted of a power drill with a hollow bit which had an orifice at the cutting edge, a tube that led from the drill to a standard wet-dry shop vacuum, a collection receptacle attached to the vacuum and ordinary coffee filter paper. The drill unit had a frame such that the depth of penetration could be adjusted.

The powdered sample was collected at the cutting edge of the bit and sucked by the vacuum via the tube and collected in a coffee filter placed in the collecting receptacle. The coffee filter was folded and stored in small plastic containers until

the ion probe test.

More details can be found in the thesis by Steve Herald [19].

(D) The Resistivity Meter

Resistivity of the mortar cubes were found with a modified soil resistivity meter. The two sets of cables in the meter was soldered onto two circular metal surfaces which served as the electrodes propagating the current through the cube. The contact diameter was 1 square inch. From Ohm's Law, $R = V/I$ where, R = resistance in Ω, V = potential in Volt and I = current in Ampere.

$R = \rho L/A$, where ρ = resistivity in Ω inch, L = length in inch, and A = cross section area in square inches. ρ, L and A can be any compatible units.

Transposing, $\rho = A.R/L$

In centimeters, the above translated into:

$$\rho = (\pi \times 2.54 \times 2.54 \times R)/(4 \times 2.54 \times 2)$$

Simplifying, $\rho = 0.997 \times R$

The meter read resistance values in Ω. However, since the values of resistivity and resistance were nearly equal in this particular experimental set up, the meter readings were approximated as resistivity values in Ω cm.

Two small circular pieces were moistened, placed over the contact area and the two contact areas were clamped tightly at

the center of two opposite sides of each cube. The dials were adjusted until the null point was reached and the dialed value was recorded. For each cube, three readings were taken across the three pairs of sides and the mean value of resistivity calculated.

APPENDIX C

EXPERIMENTAL DATA

Table C1 Potential (1", 230 °F) (-mV)

BEFORE TREATMENTS

SPECIMEN	DAY 11	DAY 15	DAY 18	DAY 36	DAY 46	DAY 50
CO1 L	240	260	400	370	350	340
CO1 R	220	230	230	190	230	160
CO2 L	230	240	230	190	220	160
CO2 R	230	230	230	190	220	160
CO3 L	220	220	230	200	220	170
CO3 R	230	230	230	200	210	180
LM1 L	220	230	230	200	230	350
LM1 R	230	230	230	200	230	160
LM2 L	230	230	230	200	210	160
LM2 R	230	230	230	190	210	170
LM3 L	230	230	240	200	220	170
LM3 R	230	230	240	190	220	160
LS1 L	230	220	230	200	220	160
LS1 R	230	230	230	190	220	170
LS2 L	210	230	230	190	210	170
LS2 R	220	240	240	190	210	170
LS3 L	220	230	240	190	210	170
LS3 R	230	230	240	190	210	170

Before treatments: days from time specimens were made
L = left rebar; R = right rebar

Table C1 Potential (1", 230 °F) (-mV) (Contd.)

BEFORE TREATMENTS

SPECIMEN	DAY 116	DAY 123	DAY 141	DAY 155	DAY 214
CO1 L	390	390	480	510	590
CO1 R	400	400	500	520	590
CO2 L	370	370	480	410	550
CO2 R	320	320	450	450	510
CO3 L	340	340	400	410	540
CO3 R	370	370	400	400	520
LM1 L	400	400	390	320	400
LM1 R	210	210	360	310	400
LM2 L	180	180	185	190	220
LM2 R	230	230	270	300	390
LM3 L	200	200	300	370	460
LM3 R	200	200	310	390	490
LS1 L	280	280	330	400	530
LS1 R	180	180	310	400	490
LS2 L	450	450	480	480	470
LS2 R	420	420	490	490	480
LS3 L	200	200	205	180	380
LS3 R	200	200	200	180	240

Before treatments: days from time specimens were made
L = left rebar; R = right rebar

Table C1 Potential (1", 230 °F) (-mV) (Contd.)

BEFORE TREATMENTS

SPECIMEN	DAY 11	DAY 15	DAY 18	DAY 36	DAY 46	DAY 50
PC1 L	220	240	230	200	210	180
PC1 R	220	230	240	180	210	160
PC2 L	220	230	230	190	220	150
PC2 R	220	230	240	180	220	150
PC3 L	230	230	240	190	210	160
PC3 R	220	240	230	190	210	160
PM1 L	230	230	240	190	210	160
PM1 R	220	240	230	190	220	160
PM2 L	220	220	240	190	210	170
PM2 R	220	230	230	190	210	160
PM3 L	230	240	240	200	210	180
PM3 R	230	230	230	190	210	170
PS1 L	230	230	230	190	210	160
PS1 R	240	230	230	190	210	160
PS2 L	230	240	230	190	220	160
PS2 R	230	240	240	200	220	170
PS3 L	230	230	230	190	210	170
PS3 R	230	240	240	190	210	170

Before treatments: days from time specimens were made
L = left rebar; R = right rebar

Table C1 Potential (1", 230 °F) (-mV) (Contd.)

BEFORE TREATMENTS

SPECIMEN	DAY 116	DAY 123	DAY 141	DAY 155	DAY 214
PC1 L	180	180	270	320	400
PC1 R	360	360	350	340	410
PC2 L	180	180	340	370	390
PC2 R	180	180	180	180	450
PC3 L	190	190	190	180	350
PC3 R	180	180	170	170	350
PM1 L	190	190	330	430	540
PM1 R	400	400	380	340	500
PM2 L	340	340	390	420	500
PM2 R	310	310	480	490	500
PM3 L	180	180	300	410	450
PM3 R	180	180	260	330	420
PS1 L	360	360	410	420	420
PS1 R	290	290	340	400	460
PS2 L	240	240	380	430	540
PS2 R	320	320	370	500	600
PS3 L	320	320	400	430	490
PS3 R	430	430	460	480	520

Before treatments: days from time specimens were made
L = left rebar; R = right rebar

Table C1 Potential (1", 230 °F) (-mV) (Contd.)

AFTER TREATMENTS

SPECIMEN	DAY 28	DAY 41	DAY 68	DAY 105	DAY 125
CO1 L	458	508	365	424	428
CO1 R	461	493	350	422	419
CO2 L	441	527	387	458	465
CO2 R	432	474	333	440	420
CO3 L	410	488	372	451	454
CO3 R	344	368	357	407	398
LM1 L	244	330	224	188	195
LM1 R	361	397	274	167	156
LM2 L	299	367	236	142	155
LM2 R	313	324	282	199	173
LM3 L	421	419	304	178	175
LM3 R	383	391	269	148	144
LS1 L	467	478	329	227	220
LS1 R	441	353	349	245	219
LS2 L	449	496	312	198	225
LS2 R	474	518	346	215	246
LS3 L	450	401	374	226	249
LS3 R	422	414	330	203	221

After treatments: days from time overlays were applied

L = left rebar; R = right rebar

Table C1 Potential (1", 230 °F) (-mV) (Contd.)

AFTER TREATMENTS

SPECIMEN	DAY 141	DAY 154	DAY 162	DAY 170	DAY 181
CO1 L	501	525	496	486	500
CO1 R	500	532	500	491	505
CO2 L	555	570	552	531	556
CO2 R	526	535	524	511	528
CO3 L	528	537	527	506	538
CO3 R	503	517	506	495	512
LM1 L	248	277	249	242	263
LM1 R	206	217	177	159	193
LM2 L	194	296	232	264	281
LM2 R	223	211	192	205	210
LM3 L	239	306	282	273	306
LM3 R	240	239	212	201	281
LS1 L	300	284	268	210	251
LS1 R	314	296	277	249	289
LS2 L	291	276	237	213	266
LS2 R	317	293	278	227	314
LS3 L	314	279	270	256	268
LS3 R	293	281	257	264	263

After treatments: days from time overlays were applied

L = left rebar; R = right rebar

Table C1 Potential (1", 230 °F) (-mV) (Contd.)

AFTER TREATMENTS

SPECIMEN	DAY 28	DAY 41	DAY 68	DAY 105	DAY 125
PC1 L	431	446	306	231	223
PC1 R	313	495	348	234	228
PC2 L	415	491	323	172	161
PC2 R	451	425	252	147	138
PC3 L	256	321	140	142	112
PC3 R	406	470	297	171	167
PM1 L	460	522	379	365	343
PM1 R	445	484	373	332	377
PM2 L	455	531	377	373	368
PM2 R	378	533	379	359	319
PM3 L	488	516	396	396	358
PM3 R	499	535	355	349	325
PS1 L	520	549	415	388	370
PS1 R	515	551	412	369	340
PS2 L	509	480	344	437	441
PS2 R	452	568	402	390	373
PS3 L	527	536	423	361	347
PS3 R	481	738	397	379	353

After treatments: days from time overlays were applied

L = left rebar; R = right rebar

Table C1 Potential (1", 230 °F) (-mV) (Contd.)

	AFTER TREATMENTS				
SPECIMEN	DAY 141	DAY 154	DAY 162	DAY 170	DAY 181
PC1 L	292	329	310	241	275
PC1 R	306	327	290	250	281
PC2 L	318	261	214	303	283
PC2 R	235	234	216	209	226
PC3 L	206	288	221	215	223
PC3 R	275	312	255	249	251
PM1 L	395	378	349	338	352
PM1 R	426	358	329	347	362
PM2 L	410	391	368	358	369
PM2 R	376	378	361	355	359
PM3 L	468	451	420	394	420
PM3 R	385	377	346	328	355
PS1 L	394	385	361	349	363
PS1 R	378	370	350	329	355
PS2 L	466	351	354	320	367
PS2 R	468	434	413	395	436
PS3 L	381	361	354	348	383
PS3 R	400	374	366	350	371

After treatments: days from time overlays were applied

L = left rebar; R = right rebar

Table C2 I_{corr} (1", 230 °F) (mA/sq ft)

	BEFORE TREATMENTS		AFTER TREATMENTS		
SPECIMEN	DAY 179	DAY 214	DAY 41	DAY 105	DAY 125
CO1 L	9.1601	9.2421	27.1644	19.0621	18.8822
CO1 R	8.9877	9.7140	26.2183	25.2179	27.0637
CO2 L	8.1091	8.5654	12.7388	15.0019	14.2436
CO2 R	5.9987	6.1685	4.7665	6.2312	6.5437
CO3 L	8.2721	9.9156	13.8625	19.8912	20.2999
CO3 R	7.3167	7.3590	6.7148	8.3167	8.0161
LM1 L	1.8823	1.9104	0.9705	0.2167	0.2099
LM1 R	1.8767	1.9112	0.6873	0.1922	0.1811
LM2 L	0.5987	0.6122	1.3559	0.4167	0.2761
LM2 R	1.7169	1.7298	1.8419	0.3354	0.4097
LM3 L	2.0492	2.1415	2.8728	0.4267	0.4112
LM3 R	2.2328	2.2784	3.2122	0.9177	0.4543
LS1 L	5.8791	6.9107	3.1949	0.5767	0.4731
LS1 R	2.7654	2.8874	1.7729	0.8798	0.4601
LS2 L	2.0761	2.1528	7.1161	2.4875	2.8297
LS2 R	2.0692	2.2006	9.6711	4.3495	3.5803
LS3 L	1.6954	1.8769	3.8894	2.3624	2.3164
LS3 R	0.8226	0.8905	2.8383	0.5837	0.6182

Before treatments: days from time specimens were made
After treatments: days from time overlays were applied

L = left rebar; R = right rebar

Table C2 I_{corr} (1", 230 °F) (mA/sq ft) (Contd.)

AFTER TREATMENTS

SPECIMEN	DAY 141	DAY 154	DAY 162	DAY 170	DAY 181
CO1 L	20.0961	24.8868	22.5303	25.1961	32.7229
CO1 R	22.9245	30.4701	27.2562	26.9354	40.3721
CO2 L	17.5728	19.0949	18.9985	20.6054	32.1389
CO2 R	7.8017	12.0988	10.1365	11.4975	11.8097
CO3 L	18.7165	18.8431	22.7547	20.0012	27.3928
CO3 R	12.1319	16.9729	14.5331	12.5606	20.3824
LM1 L	0.1654	0.2072	0.2359	0.2705	0.2777
LM1 R	0.1482	0.1913	0.1771	0.2101	0.1913
LM2 L	0.2144	0.3093	0.2302	0.1913	0.2892
LM2 R	0.3913	0.3999	0.2892	0.3999	0.3971
LM3 L	0.4359	0.5942	0.4258	0.5193	0.4661
LM3 R	0.4057	0.5956	0.5913	0.4934	0.5107
LS1 L	0.9121	0.7279	0.9308	0.6833	0.7136
LS1 R	0.9826	1.0473	0.8718	0.8028	0.7625
LS2 L	0.6831	3.5836	3.3851	3.3549	3.5922
LS2 R	3.6929	5.2511	4.4079	5.3618	5.1719
LS3 L	1.9206	1.7666	1.8515	2.2529	2.0991
LS3 R	0.6833	0.6042	0.7021	0.7279	0.7423

After treatments: days from time overlays were applied

L = left rebar; R = right rebar

Table C2 I_{corr} (1", 230 °F) (mA/sq ft) (Contd.)

	BEFORE TREATMENTS		AFTER TREATMENTS		
SPECIMEN	DAY 179	DAY 214	DAY 41	DAY 105	DAY 125
PC1 L	2.0006	2.0241	1.7657	0.3806	0.4687
PC1 R	1.7762	1.8803	2.4372	0.7791	0.6182
PC2 L	1.9762	1.9986	0.5924	0.1987	0.2559
PC2 R	2.5793	2.7761	0.4687	0.3688	0.3767
PC3 L	1.0292	1.8768	0.8066	0.4207	0.2847
PC3 R	0.9981	1.8423	1.1531	0.3692	0.2099
PM1 L	7.1792	8.4489	4.6501	1.8045	2.1395
PM1 R	2.0788	2.2847	3.9024	1.2523	0.4328
PM2 L	3.2791	3.7601	3.7988	1.3386	1.5284
PM2 R	10.0062	12.2651	5.7328	1.5931	1.4177
PM3 L	1.5421	1.7441	5.0009	1.9727	1.9037
PM3 R	1.4466	1.4479	7.7314	3.2741	2.6169
PS1 L	1.7654	1.9287	3.8075	1.3631	1.6191
PS1 R	1.9862	2.0671	3.6551	1.0482	1.4709
PS2 L	7.4293	7.6698	5.0584	4.3122	5.6594
PS2 R	9.7214	10.0161	6.4115	3.9455	5.2266
PS3 L	2.6609	2.6752	6.5308	1.6881	3.0569
PS3 R	4.9781	5.1917	7.7933	2.8887	3.9699

Before treatments: days from time specimens were made
After treatments: days from time overlays were applied

L = left rebar; R = right rebar

Table C2 I_{corr} (1", 230 °F) (mA/sq ft) (Contd.)

	AFTER TREATMENTS				
SPECIMEN	DAY 141	DAY 154	DAY 162	DAY 170	DAY 181
PC1 L	0.3871	0.4244	0.4776	0.3856	0.3323
PC1 R	0.5999	0.7668	0.5697	0.5611	0.6488
PC2 L	0.2633	0.1281	0.2388	0.2316	0.2676
PC2 R	0.4287	0.3985	0.3654	0.2287	0.3871
PC3 L	0.1755	0.2187	0.1654	0.1539	0.1511
PC3 R	0.1568	0.2661	0.1913	0.2691	0.1928
PM1 L	1.8055	2.0745	1.7121	1.9004	1.8918
PM1 R	0.5467	0.9768	1.3264	0.5352	0.4776
PM2 L	1.6832	1.9393	1.4631	1.9047	1.9321
PM2 R	0.9251	2.4385	1.9968	1.9695	2.2903
PM3 L	2.6183	2.9218	2.5349	2.7781	2.4284
PM3 R	3.8124	5.0107	3.0873	4.2857	4.2051
PS1 L	1.8271	2.1392	2.4428	1.8213	1.2201
PS1 R	1.5163	1.6645	1.3739	1.9637	1.7163
PS2 L	1.9134	1.9206	1.8645	2.7463	1.6127
PS2 R	4.9575	5.6826	4.3188	5.5459	5.2726
PS3 L	3.1103	4.5576	3.3045	3.4931	4.6295
PS3 R	4.2756	5.3056	4.5086	3.0197	4.4036

After treatments: days from time overlays were applied

L = left rebar; R = right rebar

Table C3 Macro I_{corr} (1", 230 °F) (mA)

	BEFORE TREATMENTS		AFTER TREATMENTS	
	DAY	DAY	DAY	DAY
SPECIMEN	141	155	28	76
CO1 L	-0.0371	-0.041	0.05	-0.009
CO1 R	-0.0683	-0.076	0.07	-0.019
CO2 L	0.0071	0.071	0.09	NA
CO2 R	-0.0581	-0.055	0.06	-0.019
CO3 L	-0.0542	-0.057	0.09	0
CO3 R	-0.0251	-0.021	0.08	-0.023
LM1 L	0.0201	0.011	-0.01	-0.001
LM1 R	0.0071	0.003	0.03	0
LM2 L	NA	0	-0.03	-0.001
LM2 R	NA	0.001	0.01	-0.002
LM3 L	NA	-0.006	0.06	-0.002
LM3 R	NA	0.015	0.11	-0.006
LS1 L	NA	-0.025	0.22	-0.011
LS1 R	NA	-0.017	0.11	0
LS2 L	0.0501	0.041	0.15	-0.037
LS2 R	0.0102	0.099	0.16	-0.035
LS3 L	NA	0	0.18	-0.001
LS3 R	NA	0	0.04	-0.003

Before treatments: days from time specimens were made
After treatments: days from time overlays were applied

L = left rebar; R = right rebar

Table C3 Macro I_{corr} (1", 230 °F) (mA) (Contd.)

	AFTER TREATMENTS				
	DAY	DAY	DAY	DAY	DAY
SPECIMEN	141	154	162	170	181
CO1 L	-0.025	-0.034	-0.032	-0.036	-0.043
CO1 R	-0.046	-0.065	-0.065	-0.071	-0.081
CO2 L	-0.097	-0.066	-0.131	-0.064	-0.152
CO2 R	-0.048	-0.058	-0.054	-0.056	-0.062
CO3 L	-0.041	-0.059	-0.069	-0.092	-0.128
CO3 R	-0.006	-0.061	-0.065	-0.068	-0.081
LM1 L	0	0	0.001	0.001	0.002
LM1 R	0	0	0	0	0
LM2 L	0	0.003	0.002	0.0001	0.009
LM2 R	0	0	0	0	0
LM3 L	0	0.006	0.012	0.011	0.016
LM3 R	-0.002	-0.002	-0.001	0.001	0.011
LS1 L	-0.007	-0.007	-0.005	-0.004	-0.004
LS1 R	-0.001	-0.001	-0.001	-0.001	-0.002
LS2 L	-0.023	-0.017	-0.011	-0.012	-0.003
LS2 R	-0.028	-0.023	-0.018	-0.015	0.026
LS3 L	-0.001	-0.001	0	-0.001	-0.001
LS3 R	-0.003	-0.002	-0.002	-0.002	-0.002

After treatments: days from time overlays were applied

L = left rebar; R = right rebar

Table C3 Macro I_{corr} (1", 230 °F) (mA) (Contd.)

	BEFORE TREATMENTS		AFTER TREATMENTS	
	DAY	DAY	DAY	DAY
SPECIMEN	141	155	28	76
PC1 L	NA	0.006	-0.03	-0.001
PC1 R	0.0101	0.007	0.04	0.002
PC2 L	NA	0.021	-0.01	-0.001
PC2 R	NA	0	-0.03	-0.021
PC3 L	NA	0	0.01	0
PC3 R	NA	0	-0.01	0.001
PM1 L	NA	-0.032	0.18	-0.042
PM1 R	0.0151	0	0.06	-0.007
PM2 L	-0.0291	-0.028	0.17	-0.031
PM2 R	-0.0351	-0.026	0.44	-0.041
PM3 L	NA	0.026	0.07	-0.009
PM3 R	NA	0.011	0.21	NA
PS1 L	-0.0281	-0.046	0.27	-0.054
PS1 R	NA	-0.024	0.15	-0.035
PS2 L	NA	-0.039	0.32	0
PS2 R	-0.0231	-0.024	0.31	0
PS3 L	-0.0392	-0.039	0.13	-0.032
PS3 R	-0.0582	-0.049	0.24	-0.058

Before treatments: days from time specimens were made
After treatments: days from time overlays were applied

L = left rebar; R = right rebar

Table C3 Macro I_{corr} (1", 230 °F) (mA) (Contd.)

	AFTER TREATMENTS				
	DAY	DAY	DAY	DAY	DAY
SPECIMEN	141	154	162	170	181
PC1 L	-0.004	-0.014	-0.007	-0.004	-0.004
PC1 R	-0.005	-0.008	-0.006	-0.008	-0.008
PC2 L	0	0.005	0	0	0
PC2 R	-0.003	-0.004	-0.002	-0.001	-0.002
PC3 L	0	-0.001	0	0	0
PC3 R	0	0	0	0	0
PM1 L	-0.031	-0.027	-0.019	-0.021	-0.019
PM1 R	0	-0.006	-0.003	0	-0.008
PM2 L	-0.024	-0.018	-0.013	-0.013	-0.012
PM2 R	-0.056	-0.027	-0.008	-0.011	-0.009
PM3 L	0.012	-0.003	-0.007	-0.011	-0.016
PM3 R	-0.019	-0.018	-0.015	-0.019	-0.019
PS1 L	-0.038	-0.021	-0.016	-0.016	-0.015
PS1 R	-0.032	-0.026	-0.021	-0.022	-0.021
PS2 L	-0.137	-0.141	-0.005	-0.096	-0.085
PS2 R	-0.009	-0.061	-0.036	-0.041	-0.052
PS3 L	-0.012	0.019	0.028	0.038	0.071
PS3 R	-0.037	-0.038	-0.024	-0.021	-0.017

After treatments: days from time overlays were applied

L = left rebar; R = right rebar

Table C4 Chloride Content of Selected Specimens (lb/yd^3)

(A) 1" cover, 230 F

SPECIMEN	DEPTH (")	BEFORE TREATMENTS DAY 71	DAY 190
CO1	0-1/2	17.01	19.38
	1/2-1	NA	12.91
	1-1 1/2	NA	8.03
	1-2	1.04	NA
	1 1/2-2	NA	1.74
CO3	0-1/2	12.21	19.07
	1/2-1	2.82	14.48
	1-1 1/2	0.69	3.38
	1 1/2-2	0.59	1.01
LS3	0-1/2	16.92	19.37
	1/2-1	11.97	14.17
	1-1 1/2	2.31	3.86
	1 1/2-2	0.79	1.15

Before treatments: days from time specimens were made

Table C4 Chloride Content of Selected Specimens (lb/yd^3)

(Contd.)

(B) 2" cover, 180 F

SPECIMEN	DEPTH (")	BEFORE TREATMENT DAY 154
PM1	0-1/2	19.71
	1/2-1	8.84
	1-1 1/2	1.74
	1 1/2-2	1.12
	2-2 1/2	0.97
	2 1/2-3	1.01
PM2	0-1/2	19.96
	1/2-1	7.34
	1-1 1/2	1.51
	1 1/2-2	1.44
	2-2 1/2	1.28
	2 1/2-3	1.23

Before treatment: days from time specimens were made

Table C5 Change in Micro I_{corr} over Time (1", 230 °F)

(mA/sq ft)

	POST-TREATMENT DAY 144	DAY 147	DAY 149
CO	13.7998	20.9234	21.4600
LM	0.3515	0.3194	0.2815
LS	1.4257	1.8659	1.6938
PC	0.1204	0.0949	0.0969
PM	1.8357	1.6357	1.7503
PS	4.0258	4.1931	3.9150

Table C6 Micro, Macro & Mixed I_{corr} (1", 230 °F) (mA/sq ft)

	MICRO	MACRO	MIXED
CO	13.7998	0.7663	18.7951
LM	0.3515	0.0000	0.2719
LS	1.4257	0.1457	1.1719
PC	0.1204	0.0188	0.2753
PM	1.8357	0.3150	2.0357
PS	4.0258	0.8791	2.2836

Table C7 Mixed I_{corr} for Different C/A (1", 230 °F) (mA/sq ft)

	C/A 1	C/A 2	C/A 3	C/A 4
CO	17.468	14.286	14.096	18.044
LM	0.369	0.315	0.527	0.454
LS	1.849	1.786	2.474	2.193
PC	0.627	0.395	0.531	0.486
PM	2.169	1.761	3.271	2.969
PS	3.761	3.583	4.114	3.852

Table C8 Macro I_{corr} for Different C/A (1", 230 °F) (mA/sq ft)

	C/A 1	C/A 2	C/A 3	C/A 4
CO	0.1316	0.4701	1.0437	1.1471
LM	0.0000	0.0094	0.0141	0.0141
LS	0.0658	0.1504	0.2069	0.2163
PC	0.0329	0.0376	0.0517	0.0376
PM	0.1975	0.3526	0.3291	0.3103
PS	0.4090	0.3667	0.4701	0.4701

Table C9 Potential (2", ¾"; 150 °F, 180 °F) (-mV)

SPECIMEN	COVER DEPTH (")	DRYING TEMP (F)	BEFORE IMPREGNATION DAY 10	DAY 28	DAY 98	DAY 186
PC2 L	2	150	150	160	160	
PC2 R	2	150	150	160	150	
PC3 L	2	150	150	160	160	
PC3 R	2	150	160	160	160	
PC2 L	3/4	150				454
PC2 R	3/4	150				418
PC3 L	3/4	150				481
PC3 R	3/4	150				452
PM1 L	2	180	150	160	160	
PM1 R	2	180	140	160	160	
PM2 L	2	180	160	170	150	
PM2 R	2	180	160	160	160	
PM1 L	3/4	180				460
PM1 R	3/4	180				476
PM2 L	3/4	180				466
PM2 R	3/4	180				335
CO1 L	2	-	160	150	160	
CO1 R	2	-	170	160	160	
CO2 L	2	-	150	160	160	
CO2 R	2	-	150	160	160	
CO1 L	3/4	-				447
CO1 R	3/4	-				427
CO2 L	3/4	-				417
CO2 R	3/4	-				418

Before impregnation: days from time specimens were made

L = left rebar; R = right rebar

Table C9 Potential (2", ¾"; 150 °F, 180 °F) (-mV) (Contd.)

SPECIMEN	COVER DEPTH (")	DRYING TEMP (F)	BEFORE IMPREGNATION DAY 199	BEFORE IMPREGNATION DAY 370	AFTER IMPREGNATION DAY 1	AFTER IMPREGNATION DAY 13	AFTER IMPREGNATION DAY 33
PC2 L	2	150	180	156	241	262	264
PC2 R	2	150	180	225	340	338	242
PC3 L	2	150	190	355	528	510	389
PC3 R	2	150	200	125	232	310	268
PC2 L	3/4	150			568	487	413
PC2 R	3/4	150			563	427	424
PC3 L	3/4	150			720	500	469
PC3 R	3/4	150			698	496	470
PM1 L	2	180	380	352	462	460	355
PM1 R	2	180	170	360	502	489	427
PM2 L	2	180	190	205	NA	327	318
PM2 R	2	180	190	180	NA	205	194
PM1 L	3/4	180			654	411	422
PM1 R	3/4	180			661	462	408
PM2 L	3/4	180			591	421	418
PM2 R	3/4	180			509	441	429
CO1 L	2	-	160	285	NA	290	171
CO1 R	2	-	170	301	NA	300	184
CO2 L	2	-	190	320	NA	205	189
CO2 R	2	-	180	318	NA	221	103
CO1 L	3/4	-			NA	397	407
CO1 R	3/4	-			NA	367	373
CO2 L	3/4	-			NA	380	388
CO2 R	3/4	-			NA	354	361

Before impregnation: days from time specimens were made
After impregnation: days from time of impregnation

L = left rebar; R = right rebar

Table C9 Potential (2", ¾"; 150 °F, 180 °F) (-mV) (Contd.)

SPECIMEN	COVER DEPTH (")	DRYING TEMP (F)	AFTER IMPREGNATION DAY 49	DAY 62	DAY 70	DAY 78	DAY 89
PC2 L	2	150	356	345	317	319	331
PC2 R	2	150	377	364	332	330	354
PC3 L	2	150	355	419	374	380	377
PC3 R	2	150	301	383	361	360	359
PC2 L	3/4	150	496	506	505	517	560
PC2 R	3/4	150	532	530	504	522	558
PC3 L	3/4	150	525	518	484	500	528
PC3 R	3/4	150	504	505	459	485	518
PM1 L	2	180	463	438	387	370	390
PM1 R	2	180	501	473	428	429	447
PM2 L	2	180	301	432	414	410	421
PM2 R	2	180	340	389	297	301	360
PM1 L	3/4	180	452	530	475	503	520
PM1 R	3/4	180	478	550	516	536	548
PM2 L	3/4	180	499	571	527	550	583
PM2 R	3/4	180	495	518	535	542	572
CO1 L	2	-	268	213	194	167	188
CO1 R	2	-	312	280	257	232	264
CO2 L	2	-	323	258	282	298	238
CO2 R	2	-	337	306	313	325	337
CO1 L	3/4	-	493	512	463	501	521
CO1 R	3/4	-	483	489	478	496	550
CO2 L	3/4	-	457	459	437	494	538
CO2 R	3/4	-	455	486	450	487	551

After impregnation: days from time of impregnation

L = left rebar; R = right rebar

Table C10 I_{corr} (2", ¾"; 150 °F, 180 °F) (mA/sq ft)

SPECIMEN	COVER DEPTH (")	DRYING TEMP (F)	BEFORE IMPREGNATION DAY 186	BEFORE IMPREGNATION DAY 370	AFTER IMPREGNATION DAY 1	AFTER IMPREGNATION DAY 13	AFTER IMPREGNATION DAY 33
PC2 L	2	150		0.6283	1.4551	1.9211	1.7197
PC2 R	2	150		0.9978	1.5615	3.1575	1.8161
PC3 L	2	150		1.5327	1.2221	4.0677	3.0368
PC3 R	2	150		0.4644	0.8339	1.3904	1.2984
PC2 L	3/4	150	24.0499		2.6715	3.9781	4.1094
PC2 R	3/4	150	19.0662		3.7571	4.0021	3.8867
PC3 L	3/4	150	28.0587		3.6435	2.1668	3.9742
PC3 R	3/4	150	23.1628		2.8585	1.5068	2.5392
PM1 L	2	180		0.2247	0.9964	1.9901	1.8591
PM1 R	2	180		0.2389	0.8441	1.8764	1.5557
PM2 L	2	180		0.9001	NA	1.7791	1.3602
PM2 R	2	180		0.9561	NA	1.9622	2.0576
PM1 L	3/4	180	25.7596		2.9505	1.2621	1.0762
PM1 R	3/4	180	27.1731		2.2804	1.2711	1.1057
PM2 L	3/4	180	32.6154		4.7119	3.8721	4.3511
PM2 R	3/4	180	3.7899		4.0505	2.9965	3.1302
CO1 L	2	-		0.9987	NA	0.9761	1.3803
CO1 R	2	-		1.0122	NA	1.2232	0.7103
CO2 L	2	-		2.0662	NA	1.0791	0.7807
CO2 R	2	-		1.9791	NA	0.8167	0.8095
CO1 L	3/4	-	32.4112		NA	35.7786	40.0406
CO1 R	3/4	-	22.3461		NA	22.3191	21.2432
CO2 L	3/4	-	11.9962		NA	34.2179	35.4969
CO2 R	3/4	-	11.4728		NA	22.5762	21.8399

Before impregnation: days from time specimens were made
After impregnation: days from time of impregnation

L = left rebar; R = right rebar

Table C10 I_{corr} (2", ¾"; 150 °F, 180 °F) (mA/sq ft) (Contd.)

SPECIMEN	COVER DEPTH (")	DRYING TEMP (F)	AFTER IMPREGNATION DAY 49	DAY 62	DAY 70	DAY 78	DAY 89
PC2 L	2	150	3.1837	2.1881	1.8127	1.8285	2.9549
PC2 R	2	150	2.7161	2.3911	1.9019	1.9954	2.5406
PC3 L	2	150	2.0846	3.6081	1.4444	1.3481	2.3565
PC3 R	2	150	1.1077	2.3809	1.4127	1.2257	1.7551
PC2 L	3/4	150	6.7529	9.1856	9.3626	15.4825	12.8699
PC2 R	3/4	150	8.3224	14.7819	9.6934	17.1973	13.2958
PC3 L	3/4	150	3.7534	6.7256	3.9663	8.3066	10.1121
PC3 R	3/4	150	1.7321	5.5401	2.8816	6.6393	9.2705
PM1 L	2	180	1.9263	2.7952	1.6041	1.5481	2.0385
PM1 R	2	180	2.3493	4.4741	2.2673	1.9652	3.2701
PM2 L	2	180	1.1381	1.5393	1.1092	1.3696	1.4343
PM2 R	2	180	1.9364	2.7075	0.9711	1.2602	2.0846
PM1 L	3/4	180	1.9896	14.3474	4.8956	8.7281	9.6114
PM1 R	3/4	180	1.7192	14.7387	4.3418	6.3731	4.9992
PM2 L	3/4	180	4.5374	30.5506	10.7422	27.7798	27.1396
PM2 R	3/4	180	2.1939	17.7901	5.9027	17.6908	11.6543
CO1 L	2	-	2.3637	1.2027	1.1883	1.4357	1.0804
CO1 R	2	-	1.7407	1.3711	1.1998	1.3178	1.0775
CO2 L	2	-	1.2891	1.0185	1.1711	1.2746	0.6301
CO2 R	2	-	1.7997	1.7781	1.8314	1.4789	1.9652
CO1 L	3/4	-	43.9543	54.2045	43.0393	50.6727	89.9644
CO1 R	3/4	-	31.6986	47.6242	36.2821	51.0295	72.6908
CO2 L	3/4	-	45.9583	47.1207	41.7604	50.0181	94.4514
CO2 R	3/4	-	40.9447	53.8002	41.0799	60.9214	99.3371

After impregnation: days from time of impregnation

L = left rebar; R = right rebar

Table C11 Macro I_{corr} (2", ¾"; 150 °F, 180 °F) (mA)

SPECIMEN	COVER DEPTH (")	DRYING TEMP (F)	AFTER IMPREGNATION DAY 49	DAY 62	DAY 70
PC2 L	2	150	0.029	0.045	0.038
PC2 R	2	150	-0.053	-0.054	-0.041
PC3 L	2	150	-0.053	0	0
PC3 R	2	150	0.044	0.041	0.032
PC2 L	3/4	150	0.038	0.033	0.017
PC2 R	3/4	150	-0.042	-0.059	-0.076
PC3 L	3/4	150	0.001	-0.016	-0.022
PC3 R	3/4	150	0.021	0.071	0.049
PM1 L	2	180	0.079	0.046	0.029
PM1 R	2	180	0.041	0.031	0.015
PM2 L	2	180	0	0	0
PM2 R	2	180	-0.034	0.296	0.097
PM1 L	3/4	180	0.054	0.041	0.041
PM1 R	3/4	180	0.031	-0.019	-0.033
PM2 L	3/4	180	0	-0.129	-0.006
PM2 R	3/4	180	0.025	-0.215	-0.222
CO1 L	2	-	0.149	0.002	0.001
CO1 R	2	-	-0.201	0.016	0.011
CO2 L	2	-	-0.006	0	0
CO2 R	2	-	-0.035	-0.025	-0.025
CO1 L	3/4	-	0.006	0.099	0.175
CO1 R	3/4	-	0.018	-0.232	-0.134
CO2 L	3/4	-	0	0.027	0.096
CO2 R	3/4	-	-0.018	-0.119	0.018

After impregnation: days from time of impregnation

L = left rebar; R = right rebar

Table C11 Macro I_{corr} (2", ¾"; 150 °F, 180 °F) (mA) (Contd.)

SPECIMEN	COVER DEPTH (")	DRYING TEMP (F)	AFTER IMPREGNATION DAY 78	DAY 89
PC2 L	2	150	0.036	0.037
PC2 R	2	150	-0.043	-0.043
PC3 L	2	150	0	0
PC3 R	2	150	0.033	0.029
PC2 L	3/4	150	-0.001	-0.028
PC2 R	3/4	150	-0.119	-0.125
PC3 L	3/4	150	-0.049	-0.077
PC3 R	3/4	150	0.031	0.001
PM1 L	2	180	0.031	0.027
PM1 R	2	180	0.021	0.021
PM2 L	2	180	0	0
PM2 R	2	180	0.098	0.037
PM1 L	3/4	180	0.057	0.056
PM1 R	3/4	180	-0.015	0.013
PM2 L	3/4	180	-0.108	-0.111
PM2 R	3/4	180	-0.083	-0.067
CO1 L	2	-	0.002	0
CO1 R	2	-	0.011	0.009
CO2 L	2	-	-0.001	0
CO2 R	2	-	-0.027	-0.035
CO1 L	3/4	-	0.111	0.141
CO1 R	3/4	-	-0.133	-0.081
CO2 L	3/4	-	0.039	0.058
CO2 R	3/4	-	0.011	-0.011

After impregnation: days from time of impregnation

L = left rebar; R = right rebar

Table C12 Results of SLR Between Potential & I_{corr}

Fobs = 219.845	Prob > Fobs = 0.0001
R-Square = 0.4065	Adjusted R-Square = 0.4046

Pearson Correlation Coefficient = 0.63756

Number of Observations = 323

Table C13 Drying of Specimens (1", 230 °F) (Temp in °F)

CLOCK TIME	TIME (min)	AMBIENT TEMP	SURFACE TEMP	TEMP @ 1/2" BELOW TOP REBAR PS3	PS2	PS1	PM3	PM2	REMARKS
1550	0	79.5	78.5	76.9	74.3	77.8	79.9	78.1	Heaters turned on height of heaters = 9"
1605	15	-	398.9	-	-	-	-	-	
1620	30	76.7	421.8	97.3	94.5	105.5	101.2	105.7	
1635	45	-	451.5	-	-	-	-	-	
1650	60	76.3	459.9	136.9	126.2	153.1	139.3	151.1	
1700	70	-	-	-	-	-	-	-	
1720	90	74.5	473.7	165.8	150.3	190.7	168.5	187.5	
1730	100	-	-	-	-	-	-	-	
1750	120	72.6	518.9	187.5	169.1	212.0	190.9	210.4	
1820	150	70.9	528.8	207.5	188.5	239.2	209.8	231.9	Heaters turned off at 1825
1840	170	69.1	NA	213.1	195.3	248.9	216	243.8	
1910	200	65.8	294.8	211.9	193.1	247.0	212.8	241.8	
1940	230	63.3	257.7	203.2	185.5	238.0	202.7	233.2	
2010	260	58.7	225.0	194.2	178.4	230.2	194.9	226.2	
2040	290	56.6	212.9	183.7	170.4	221.2	185.3	217.5	
2110	320	57.0	197.6	175.1	162.8	211.6	175.6	208.1	
2140	350	53.2	186.2	167.4	156.9	203.8	167.9	200.5	
2210	380	51.4	179.0	160.5	150.9	196.2	161.1	193.2	
2240	410	50.1	170.0	153.5	144.5	188.7	154.1	185.6	
2310	440	50.5	164.0	148.1	140.0	183.0	148.9	179.8	
2340	470	48.5	157.1	142.4	134.6	176.1	142.9	173.3	
0815	985	50.9	110.4	98.4	93.2	120.3	96.1	114.6	

Table C13 Drying of Specimens (1", 230 °F) (Temp in °F)

(Contd.)

CLOCK TIME	TIME (min)	AMBIENT TEMP	SURFACE TEMP	TEMP @ 1/2" BELOW TOP REBAR PM1	PC3	PC2	PC1	REMARKS
								Heaters turned on
1550	0	79.5	78.5	75.6	76.6	78.0	76.0	height of heaters = 9"
1605	15	-	398.9	-	-	-	-	
1620	30	76.7	421.8	109.2	154.6	119.0	147.9	
1635	45	-	451.5	-	-	-	-	
1650	60	76.3	459.9	154.9	235.0	187.3	214.3	PC1 & PC3 covered with
1700	70	-	-	-	253.1	-	230.7	metal sheet
1720	90	74.5	473.7	191.8	253.8	216.9	233.2	PC2 covered
1730	100	-	-	-	-	223.7	-	
1750	120	72.6	518.9	211.0	245.4	240.0	224.3	
1820	150	70.9	528.8	232.8	241.1	241.9	219.4	Heaters turned off at 1825
1840	170	69.1	NA	240.4	238.6	238.5	217.3	
1910	200	65.8	294.8	236.6	231.3	229.9	212.0	
1940	230	63.3	257.7	227.8	222.7	219.1	204.8	
2010	260	58.7	225.0	218.9	214.5	210.3	197.7	
2040	290	56.6	212.9	210.1	207.3	200.9	191.4	
2110	320	57.0	197.6	200.3	198.8	191.5	183.9	
2140	350	53.2	186.2	192.6	192.3	184.1	177.9	
2210	380	51.4	179.0	185.3	185.9	177.0	172.0	
2240	410	50.1	170.0	177.5	179.2	169.4	166.1	
2310	440	50.5	164.0	171.8	173.9	163.7	161.2	
2340	470	48.5	157.1	164.7	167.9	156.9	155.8	
0815	985	50.9	110.4	110.3	114.8	101.8	105.2	

Table C14A Drying of Specimens (2", 180 °F) (Temp in °F)

CLOCK TIME	TIME (min)	AMBIENT TEMP	SURFACE TEMP	TEMP @ 3" DEPTH PM1	TEMP @ 3" DEPTH PM2	TEMP @ 2" DEPTH PM1	TEMP @ 2" DEPTH PM2	REMARKS
1705	0	60	64.2	69.9	70.2	69.8	61.6	Heaters turned on
1715	10	57	322.4	70.9	71.8	82.0	84.7	height of heaters = 10"
1730	25	57	393.6	92.7	97.9	136.4	148.1	
1745	40	56	396.0	129.4	145.2	189.7	210.8	
1800	55	56	397.0	160.8	184.0	220.1	229.0	PM2 covered
1810	65	54	400.2	180.6	208.2	229.0	233.4	Heaters turned off
1825	80	53	312.1	196.0	208.1	219.2	222.0	
1840	95	53	211.7	195.2	204.5	207.6	211.7	
1900	115	52	162.7	184.8	196.5	190.5	197.2	
1915	130	52	145.3	174.0	189.6	185.1	188.7	
1930	145	50	134.1	156.9	171.1	169.7	168.6	

Table C14B Drying of Specimens (2", 150 °F) (Temp in °F)

CLOCK TIME	TIME (min)	AMBIENT TEMP	SURFACE TEMP @ 3" DEPTH			REMARKS
			TEMP	PC2	PC3	
1445	0	66	69.3	70.0	68.9	Heaters turned on
1500	15	67	236.5	75.5	76.8	height of heaters = 8 1/2"
1515	30	66	277.4	94.9	107.9	
1530	45	66	294.6	118.2	144.8	
1545	60	66	466.2	141.0	179.8	PC3 covered at 1536
						Heaters turned off at 1549
1600	75	65	300.2	175.3	191.6	
1605	80	65	272.1	182.0	192.1	
1630	105	60	219.0	189.3	186.8	
1645	120	56	197.5	186.6	180.4	
1700	135	52	189.2	183.2	175.6	
1715	150	50	184.1	172.5	161.7	

Table C14C Drying of Specimens (¾", 180 °F) (Temp in °F)

CLOCK TIME	TIME (min)	AMBIENT TEMP	SURFACE TEMP	TEMP @ 1 3/4" DEPTH PM1	TEMP @ 1 3/4" DEPTH PM2	TEMP @ 3/4" DEPTH PM1	TEMP @ 3/4" DEPTH PM2	REMARKS
1350	0	72	79.9	77.8	77.0	80.8	78.9	Heaters turned on
1400	10	72	235.1	80.6	82.9	98.6	102.3	height of heaters = 10"
1410	20	72	386.3	131.5	141.2	189.5	194.5	
1420	30	72	395.7	180.6	181.0	239.5	253.1	Heaters turned off
1430	40	72	205.7	205.1	204.7	237.3	239.6	
1440	50	70	144.8	199.2	199.8	223.4	226.7	
1450	60	70	133.6	193.9	195.1	213.8	216.7	
1500	70	70	120.1	188.2	188.4	202.4	205.6	
1515	85	68	108.7	178.6	178.7	189.3	191.9	
1530	100	68	111.9	169.9	169.8	179.3	181.6	
1545	115	68	110.4	160.9	160.2	169.1	170.3	
1600	130	66	89.3	137.7	138.0	144.0	145.4	

Table C14D Drying of Specimens (¾", 150 °F) (Temp in °F)

CLOCK TIME	TIME (min)	AMBIENT TEMP	SURFACE TEMP	TEMP @ 1 3/4" DEPTH PC2	TEMP @ 1 3/4" DEPTH PC3	TEMP @ 3/4" DEPTH PC2	TEMP @ 3/4" DEPTH PC3	REMARKS
1005	0	52	52.5	59.4	59.5	59.5	55.1	Heaters turned on
1015	10	54	267.6	83.6	77.3	139.5	122.3	height of heaters = 10"
1025	20	54	421.9	138.8	134.9	209.0	206.1	
								PC2 covered at 1028
								Heaters turned off at 1030
1035	30	55	243.3	177.4	176.1	213.6	231.0	
1045	40	56	179.5	175.4	181.1	176.8	205.0	
1055	50	57	152.6	171.8	178.0	166.7	195.6	
1105	60	58	139.8	166.5	173.3	157.5	184.2	
1115	70	60	118.3	160.8	167.9	150.6	174.7	
1125	80	61	109.5	155.3	161.9	144.6	166.8	
1135	90	63	100.4	149.9	155.6	140.0	159.7	
1145	100	63	111.6	145.5	150.4	136.3	153.2	
1155	110	64	110.1	142.5	146.7	134.3	149.6	
1205	120	64	111.3	138.4	142.3	130.9	141.5	

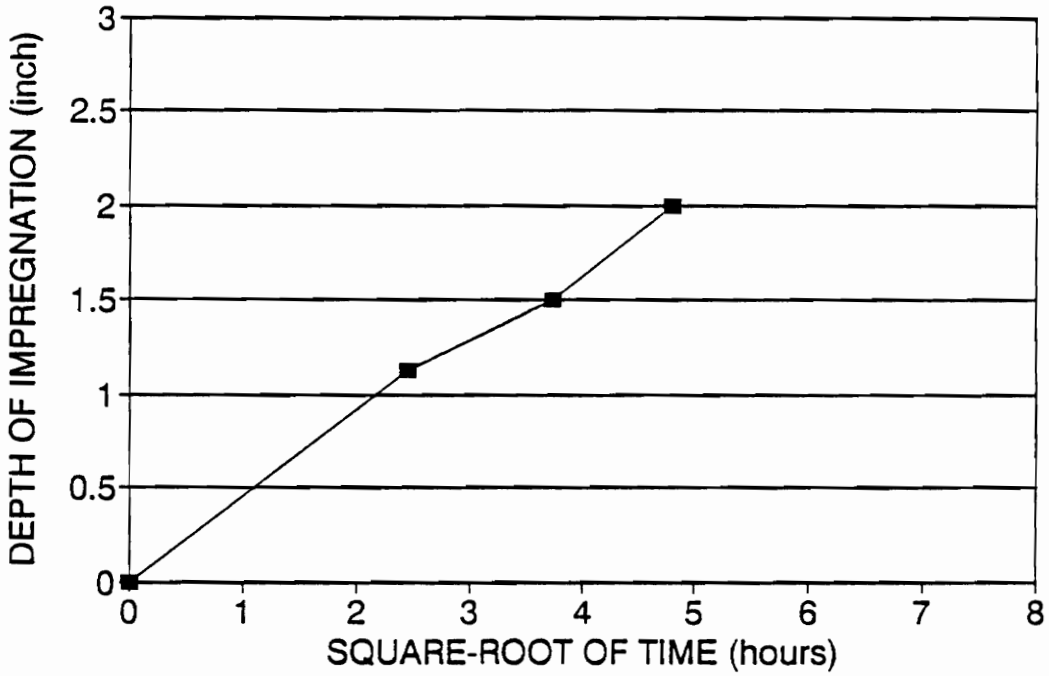

Figure C1 Depth of Impregnation vs Square-Root of Time

Figure C2 Non-Impregnated Sample under SEM (1 kX)

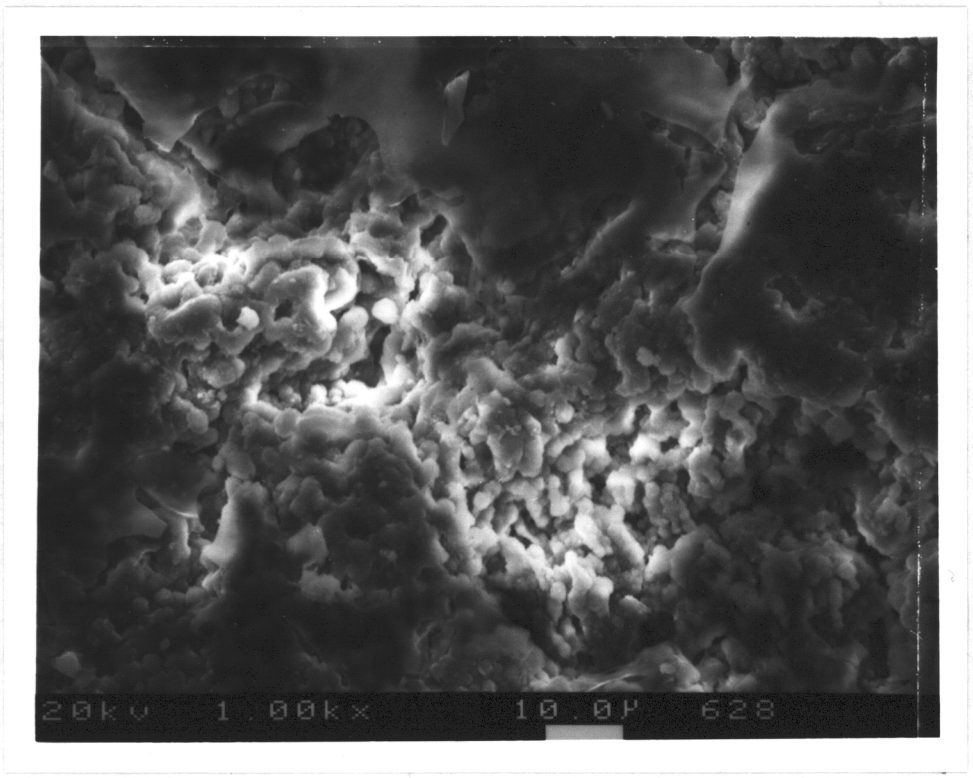

Figure C3 Impregnated Sample under SEM (1 kX)

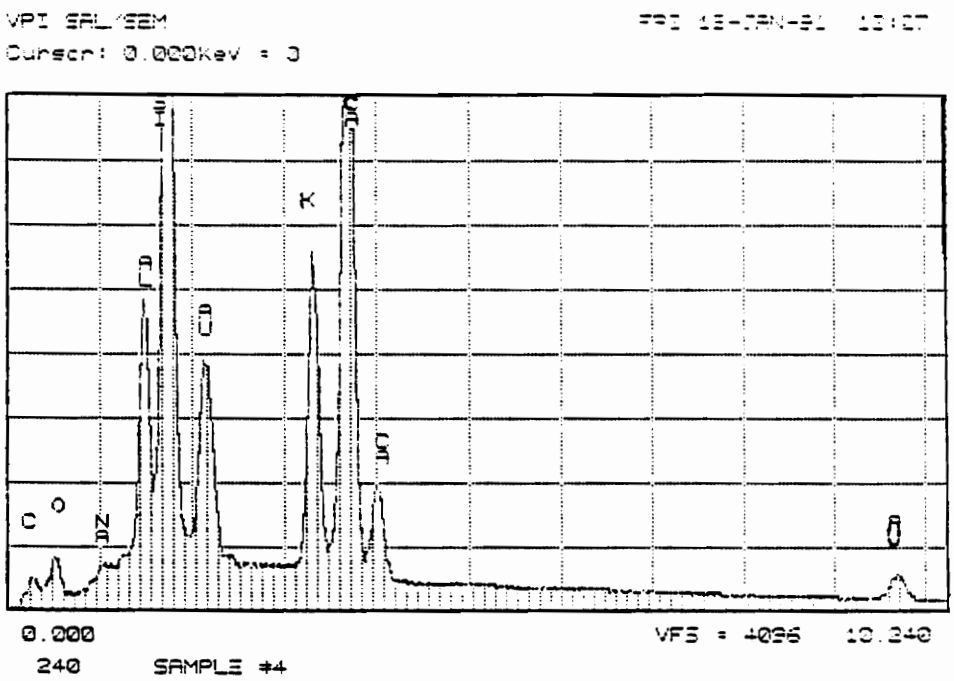

Figure C4 Illustrative Graph from the SEM-EDS

REFERENCES

[1] Durability of Concrete Bridge Decks, Report 5, Portland Cement Association, U.S. Bureau of Public Roads & Ten State Highway Agencies, 46pp (1969)

[2] Durability of Concrete Bridge Decks, Final Report, Portland Cement Association, U.S. Bureau of Public Roads & Ten State Highway Agencies, 35pp (1970)

[3] Slater, J.E.,"Corrosion of Metals in Association with Concrete", STP 818, ASTM, Philadelphia, PA, 83pp (1983)

[4] AASHTO, FHWA, TRB, NCHRP, Strategic Highway Research Program - Research Plans, Final Report, Technical Research Area 43, pp TRA 4-1 thru TRA 4-60 (May 1986)

[5] Morgan, John H., "Cathodic Protection", Leonard Hills Books Ltd, London (1959)

[6] Weyers, R.E. and Cady, P.D., "Development: Deep Grooving - A Method for Impregnating Concrete Bridge Decks", Transportation Research Record 962, pp 14-18 (1984)

[7] Weyers, R.E. and Cady, P.D., "Application: Deep Grooving - A Method for Impregnating Concrete Bridge Decks", Transportation Research Record 962, pp 19-21 (1984)

[8] Hall, Christopher, "Polymer Materials", John Wiley &

Sons, New York (1989)

[9] Manson, J.A.; Chen, W.F.; Vanderhoff, J.W.; Mehta, H.C.; Cady, P.D.; Kline, D.E. and Blankenhom, P.R., "Use of Polymers in Highway Concrete", National Cooperative Highway Research Program 190, TRB (1978)

[10] Uhlig, Herbert H. and Revie, R. Winston, "Corrosion and Corrosion Control", John Wiley & Sons (1985)

[11] Powers, T.C., "The Nature of Concrete", Significance of Tests and Properties of Concrete and Concrete Making Materials, STP 169B, ASTM, pp 59-73 (1978)

[12] Barneyback, R.S. Jr and Diamond, S., "Expression and Analysis of Pore Fluids from Hardened Cement Pastes and Mortars", Cement and Concrete Research, Vol 11, No. 2, pp 279-285 (1981)

[13] Fraczek, J, "A Review of Electrochemical Principles as Applied to Corrosion of Steel in Concrete or Grout Environment", Corrosion, Concrete and Chlorides - Steel Corrosion in Concrete: Causes and Restraints, SP-102, ACI (1987)

[14] Cady, P.D. and Weyers, R.E., "Chloride Penetration and Deterioration of Concrete Bridge Decks", Cement, Concrete and Aggregates, CCAGDP, Vol 5, No. 2, pp 81-82 (Winter 1983)

[15] Weyers, R.E., "Corrosion of Steel in Concrete", Third International Conference, Environmental Degradation of

Engineering Materials, Penn State, University Park, PA, pp 351-361 (1987)

[16] Annual Book of ASTM Standards, C-876-87, "Standard Test Method for Half-cell Potentials of Uncoated Reinforcing Steel in Concrete", ASTM, Philadelphia, PA

[17] K.C. Clear, Inc., 3LP Package - Test Procedure, Data Analysis, Procedure and General Information (June 1988)

[18] Test Model CL 500, Instruction Manual, James Instruments, Inc., Chicago

[19] Herald, S.E., "The Development of a Field Procedure for Determining the Chloride Content of Concrete and an Analysis in the Variability of the Effective Diffusion Constant", M.S. Thesis in Civil Engineering, Virginia Polytechnic Institute & State University, Blacksburg, VA (Sept 1989)

[20] Clear, K.C., "Reinforcing Bar Corrosion in Concrete: Effect of Special Treatments", SP-49, ACI, Detroit, MI, pp 71-82 (1975)

[21] Clear, K.C., "Time to Corrosion of Reinforcing Steel in Concrete Slab", Report # FHWA RD-76-70, FHWA, Washington, DC (April 1976)

[22] Nilsson Model 400 Solid State 4-Pin Soil Resistance Meter, Instruction Manual, Nilsson Electrical Laboratory, Inc., New York

[23] Manning, David G., "Detecting Defects and Deterioration

in Highway Structures", National Cooperative Highway Research Program, Synthesis of Highway Practice 118, TRB, National Research Council, Washington, DC (July 1985)

[24] Vassie, P. R., "A Survey of Site Tests for the Assessment of Corrosion in Reinforced Concrete", LR 953, Transport and Road Research Laboratory, England (1980)

[25] Tremper, B., Beaton, J. L. and Stratfull, R. F., " Causes and Repair of Deterioration to a California Bridge due to Corrosion of Reinforcing Steel in a Marine Environment Part II: Fundamental Factors Causing Corrosion", Highway Research Bulletin 182, TRB, National Research Council, pp 18-41, Washington, DC (1958)

[26] Browne, R. D., "Mechanisms of Corrosion of Steel in Concrete in Relation to Design, Inspection and Repair of Offshore and Coastal Structures", Performance of Concrete in a Marine Environment, SP-65, ACI, pp 169-204 (1980)

[27] Micromeritics Autopore 9200, Mercury Porosimeter, Instruction Manual

[28] Hearle, J. W. S., Sparrow, J. T. and Cross, P. M., " The Use of the Scanning Electron Microscope", Pergamon Press (1972)

[29] Gabriel, Barbra L., "SEM: A User's Manual for Materials Science", ASM, Metals Park, OH (1985)

VITA

Tapas Dutta was born in Calcutta, India on May 21, 1963. He completed his Bachelor of Civil Engineering at Jadavpur University, Calcutta, India in 1988. He started his graduate studies at Virginia Polytechnic Institute & State University in January 1989 on Transportation Materials in the Civil Engineering Department.